MASS SPECTROMETRY-BASED CHARACTERIZATION OF POSTTRANSLATIONAL MODIFICATIONS BY 4-HYDROXY-2-NONENAL

DISSERTATION

Presented to the Graduate Council of the
Graduate School of Biomedical Sciences
University of North Texas Health Science Center at Fort Worth

In Partial Fulfillment of the Requirements

For the Degree of

DOCTOR of PHILOSOPHY

By

Navin Rauniyar, M.S
Fort Worth, Texas
May 2010

ACKNOWLEDGEMENTS

First and foremost, my sincere gratitude goes to my advisor, Dr. Laszlo Prokai, for providing me with the opportunity to work in his lab and introducing me to the exciting field of mass spectrometry and proteomics. His continuous confidence and encouragement during the difficult times in research have motivated me and brought out the best of me. His expertise in various subjects, optimistic approach, creative thinking and enthusiasm for research have set an example and have inspired me for the rest of my life. I am especially grateful to Dr. Katalin Prokai-Tatrai for helping me with the abstruse chemistry involved in my work and assisting me in my endeavors with my project. I cannot imagine how I would have completed most part of my work without the motivation and feedback from her. Also, I was really fortunate to have the chance to work with Dr. Stanley M. Stevens, Jr. His expertise in instrument handling and conversant with different database search algorithms has provided me a different vision altogether. His suggestions and advice on certain problems in my project that at times were beyond my comprehension are greatly appreciated.

I would also like to share my gratefulness to my advisory committee members Drs. Andras Lacko, Michael Forster, Ladislav Dory, Katalin Prokai-Tatrai and Nathalie Sumien. I appreciate their readiness in taking time out for the occasional committee meetings and helpful comments and suggestions that were instrumental to the successful realization of this dissertation.

While working in the lab, I have had the opportunity to meet and work with several wonderful and affable people. I would especially like to thank Dr. Vien Nguyen for his help in isolating animal tissues and also for the scrumptious food he would occasionally bring for us to relish. Many thanks also go to Dr. Nilka and Jose for their help during my early days in the lab. In a likely manner, I wish to express my deepest appreciation to all other former and current lab members in Dr. Prokai's group, Drs. Peter Frycak, Rui Branca and Xiaoqian Liu, as well as Maciej Kukula, Tatjana Talamantes and Jia Guo, for providing a friendly and harmonic research environment in the lab and for giving me all the support I needed. Their motivation, ready-to-help attitude and team work have made the lab a place to look forward to come to every day.

I further wish to thank Dr. Alakananda Basu, former graduate advisor, for believing in me and giving me the opportunity to join the Molecular Biology and Biochemistry department. I am honored to be associated with this department and I am appreciative of its wonderful and friendly faculties, research and administrative staffs, and the students that have made my stay at this place a positive chapter in my life and career.

On a personal note, I thank my friends, Priya, Subhamoy, Mallika, Shashank and Pabak for being there whenever I needed them. The days of our late evening coffee get-togethers, parties and fun will always be memorable. A special thank goes to Vishwas Thorat, a dearest friend who encouraged and supported me to pursue a Ph.D. in the United States. I also thank my parents for supporting me throughout my studies and always wanting my best and praying for my well-being. Finally, I would like to thank everyone else who I may not have mentioned here but have added to my graduate school experience. I would not have accomplished this journey without all of your support and encouragement!

TABLE OF CONTENTS

ABBREVIATIONS

ROS Reactive oxygen species

HNE 4-Hydroxy-2-nonenal

MS Mass spectrometry

Da Dalton (molecular mass unit)

m/z Mass-to-charge

Th Thomson (mass-to-charge unit)

HPLC High performance liquid chromatography

LC Liquid chromatography

MS/MS Tandem mass spectrometry

LTQ-FTICR-MS Linear quadrupole ion trap-Fourier transform ion cyclotron resonance-Mass spectrometer

FT ICR Fourier transform ion cyclotron resonance

ESI MS Electrospray ionization mass spectrometry

MALDI-TOF MS Matrix-associated laser desorption ionization-time-of-flight mass spectrometry

LC–MS Liquid chromatography–mass spectrometry

LC–ESI-MS/MS Liquid chromatography–electrospray ionization tandem mass spectrometry

CID Collision induced dissociation

NL Neutral loss

LC–CID-MS/MS Liquid chromatography-Collision induced dissociation-Tandem mass spectrometry

ECD Electron capture Dissociation

LC–ECD-MS/MS Liquid chromatography-Electron capture dissociation-Tandem mass spectrometry

PUBLICATIONS INCLUDED IN THIS DISSERTATION

1. Rauniyar, N., Stevens, S. M.,Jr, and Prokai, L. (2007) *Fourier transform ion cyclotron resonance mass spectrometry of covalent adducts of proteins and 4-hydroxy-2-nonenal, a reactive end-product of lipid peroxidation.* Anal. Bioanal Chem. 389, 1421-1428

2. Rauniyar, N., Prokai-Tatrai, K., and Prokai, L. (2010) *Identification of carbonylation sites in apomyoglobin after exposure to 4-hydroxy-2-nonenal by solid-phase enrichment and liquid chromatography-electrospray ionization tandem mass spectrometry.* J Mass Spectrom. [Epub ahead of print]

3. Rauniyar, N., Stevens, S. M., Prokai-Tatrai, K., and Prokai, L. (2009) *Characterization of 4-hydroxy-2-nonenal-modified peptides by liquid chromatography-tandem mass spectrometry using data-dependent acquisition: Neutral loss-driven MS3 versus neutral loss-driven electron capture dissociation.* Anal. Chem. 81, 782-789

4. Rauniyar, N. and Prokai, L. (2009) *Detection and identification of 4-hydroxy-2-nonenal Schiff-base adducts along with products of Michael addition using data-dependent neutral loss-driven MS3 acquisition: Method evaluation through an in vitro study on cytochrome c oxidase modifications.* Proteomics 9, 5188-5193

LIST OF TABLES

CHAPTER III

CHAPTER V

LIST OF ILLUSTRATIONS

CHAPTER I

Figure

CHAPTER II

Figure

CHAPTER III

Figure

CHAPTER V

Figure

CHAPTER I

INTRODUCTION

Oxidative stress and generation of reactive oxygen species

Although several hypotheses concerning the nature of the mechanisms underlying the aging process have been postulated, there is an increasing body of relatively persuasive evidence that the oxidative stress is a major contributory factor in senescence.[1-3] Oxidative stress results in age-dependent increase in oxidatively modified proteins, lipids, and nucleic acids in the cells, and concomitantly to an enhancement in the development of one or more well-recognized, age-related impairments, including loss of physical acuity, cognitive function, and metabolic integrity.[4] Oxidative modifications of proteins and the subsequent accumulation of the modified proteins have also been found in various pathological states including atherosclerosis, diabetes, and Alzheimer's disease.[5,6] The generation of uncontrolled amounts of reactive oxygen species (ROS) is a major cause of oxidative stress.[7] The main endogenous source of ROS is mitochondrial respiration; however, ROS are also produced by peroxisomal β-oxidation of fatty

acids[8], glyoxylic acid cycle in glyoxysomes, microsomal cytochrome p450 metabolism of xenobiotic compounds, stimulation of phagocytosis by pathogens or lipopolysaccharides, as well as activities from a variety of cytosolic enzyme systems such as NADPH oxidases and xanthine oxidase. A number of exogenous sources (UV light, ionizing radiation and chemotherapeutics) can also trigger ROS production.[9] These mechanisms collectively lead to the generation of superoxide radicals ($O_2^{\cdot -}$), hydrogen peroxide (H_2O_2), and hydroxyl radicals (HO·). [9-11] The burden of ROS is counteracted by an intricate antioxidant system, which includes antioxidant enzymes, e.g., superoxide dismutase (SOD), catalase (CAT), and glutathione peroxidase (GPx), as well as nonenzymatic, low molecular weight antioxidant compounds such as glutathione and ascorbic acid. The antioxidants bind to and inactivate ROS and thus protect against oxidative stress and prevent damage to cells. SODs catalyze the dismutation of superoxide radicals to oxygen and H_2O_2, while catalase and glutathione peroxidase convert H_2O_2 to water. The low-molecular-weight antioxidant species offer protective effect against ROS either by directly scavenging the radicals by donating an electron to them or by chelating transition metals and, thereby, inhibiting the Haber-Weiss reaction that involves the formation of highly reactive hydroxyl radicals that can cause oxidation of macromolecules.[12] Glutathione (GSH), a thiol-containing tripeptide (γ-glutamyl-cysteinylglycine), is an important low-molecular-weight antioxidant and is often used as an indicator of the redox state of the cell.[12] It acts as a chelating agent for copper ions and prevents them from participating in the Haber-Weiss reaction. It is also a cofactor for the enzyme glutathione peroxidase, can scavenge ROS directly, and prevent oxidation of protein –SH groups.[12] Moreover, GSH also plays an important role in redox-sensitive cell signaling.[13] Homeostasis is maintained when the steady-state formation of ROS is normally balanced by a similar rate of their detoxification by aforementioned enzymatic/non-

enzymatic antioxidant cascade. However, oxidative stress results from an imbalance between production of ROS and antioxidant defenses and is influenced by one of three factors: 1) increased oxidants, 2) decreased antioxidants, and 3) failure to repair oxidative damage induced by ROS.[9]

Such reactive oxidants induce oxidative modifications of proteins. Generally, there are three types of amino acid oxidative modifications that can give rise to protein carbonyls: direct attack by ROS, conjugation with lipid peroxidation products, and reaction with reducing-sugars. Protein carbonylation caused by direct oxidation of amino acid residues by ROS often involves metal-containing proteins with the generation of HO· that cause site-specific modifications. Glutamic and aminoadipic semialdehydes formed from oxidative deamination of Lys and Arg side-chains are the main carbonyl products of metal-catalyzed oxidation of proteins.[14-16] Modification of proteins by cytotoxic, α,β-unsaturated aldehydes generated in lipid peroxidation are also a potential source of protein-bound carbonyls. Additionally, protein modifications by reducing sugars often lead to the formation of advanced glycation end products (AGEs), which also contribute to the protein carbonyl content. Physiologically and pathologically, all the above described modifications that contribute to protein carbonylation have been documented in aging and in neurodegenerative disorders.[17-18]

Lipid peroxidation and generation of 4-hydroxy-2-nonenal

The polyunsaturated fatty acids found in cell membranes and lipoproteins, especially low density lipoproteins, are susceptible to ROS-mediated oxidation. Lipid peroxidation and concomitant decreased mitochondrial membrane fluidity has been shown to increase with the age of the animals.[19-20] The formation of hydroperoxides in the unsaturated fatty acids of cholesterol

and phospholipid esters, as a result of ROS attack, causes formation of alkoxyl radical and subsequent scission to generate stable, relatively long-lived, diffusible bifunctional aldehydes that are generally considered to be cytotoxic because of their ability to covalently modify, among others, a variety of proteins.[16,21-24]

4-Hydroxy-2-nonenal (HNE) is a highly reactive *α,β*-unsaturated bifunctional aldehyde that is one of the major products of peroxidation of ω-6 polyunsaturated fatty acid (PUFAs, such as linoleic acid and arachidonic acid). HNE has been shown to react with His, Lys, and Cys residues in proteins preferentially via Michael addition, although Lys-Michael adducts are reversible.[21,25-26] In certain proteins, ε-NH_2 group of Lys are modified by Schiff- base formation.[27] A Michael addition to Lys or His residues results in a mass shift of 156 Da. In Schiff base condensation reactions with protein Lys residues, there is a concomitant loss of water resulting in a mass-addition of 138 Da (Figure 1).

At low levels, HNE acts as a signaling molecule;[28] moreover, moderate increase in its concentration can be detoxified by transporting it out of the cell, upon glutathionylation by glutathione-S-transferase, by the 76-kDa Ral-binding GTPase-activating protein RLIP76. HNE can also be eliminated by the activities of aldehyde dehydrogenase and alcohol dehydrogenase.[29] During oxidative stress, HNE is produced uncontrollably and saturates the pathways for metabolism allowing excess HNE to modify biological molecules.[30] HNE is a key mediator of oxidative stress and exerts numerous deleterious effects, including inhibition of protein and DNA synthesis and inhibition of catalytic activity of enzymes; and is also believed to play a major role in oxidative stress-induced cellular dysfunction. HNE is a relatively stable aldehyde that can migrate to regions other than its site of generation and can react with cellular biomolecules. The modification results in loss of protein function[31,32] and contributes to the enhanced accumulation

of oxidatively modified proteins via an impairment of ubiquitin/proteasome-dependent intracellular proteolysis.[33,34] Accumulation of potentially cytotoxic, proteolysis-resistant HNE cross-linked proteins can cause long term damage to cells.[34-37] Cross-linking occurs by coupling of Michael addition of amino acid nucleophiles (Cys, His, or Lys) at the C3 position with a Schiff base formation at the C1 carbonyl with ε-amino group of Lys.[27] In either case, the formation of carbonyl groups is a hallmark of severe oxidative stress.[34]

Methodological approach for detection of protein carbonylation

Several studies have reported the identification of carbonylated proteins in both gel-based and chromatography-based methods.[38-40] Initial studies identifying oxidized proteins in the brain have used gel electrophoresis with subsequent identification of protein spots by peptide-mass fingerprinting based on in-gel proteolytic digestion followed by matrix-assisted laser desorption ionization–time-of-flight (MALDI-TOF) mass spectrometry.[41-42] These studies have successfully identified carbonylated proteins and much has been learned using these techniques. Due to antigenicity of HNE adducts, specific antibodies have been generated and consequently several immunochemical techniques were developed.[43,44] These techniques, however, are often limited by incomplete specificity of the antibodies and quantitation of adducts can be complicated because antibody affinity can be modulated by the protein context of the epitope. Additionally, it should be pointed out that level of protein carbonyls can also be determined by the use of 2,4-dinitrophenyl hydrazine (DNPH), a carbonyl specific reagent. The addition of α,β-unsaturated aldehydes to nucleophilic amino acid side chains (imidazole group in His, amino group in Lys and thiol group in Cys), leaves the C1 carbonyl group available for reaction with DNPH. DNPH-treated proteins can be quantitated either spectrophotometrically, or immunochemically by the

use of anti-DNP antibodies.[45,46]

Identification of oxidized proteins provides very important information regarding the protein targets of oxidative damage; however, none of these studies identified sites of carbonylation or location of other oxidative stress-specific modifications in proteins. The protein identity provides the level of information needed for understanding the specific pathophysiological consequences of age-associated oxidative stress and their role in age-related loss of cognitive or psychomotor function. In addition, identification of the oxidation sites within a protein sequence can potentially provide information regarding how and why oxidative stress causes damage to living tissues and loss of functionality of specific proteins. The inherent limitation of the gel-based approach for protein identification is that this approach is constrained, for the most part, to abundant proteins in the samples[47], and very likely precludes the detection of oxidation-induced modification associated with low abundance proteins having important functions. The low abundant proteins cannot be resolved in the gels even if multiple narrow-range immobilized pH-gradient strips are run in parallel. Two-dimensional gel electrophoresis (2-DE) is also laborious and reproducible results are difficult to achieve.[48] Also, very basic/acidic proteins, transmembrane proteins, and very high molecular weight proteins are often excluded or unresolved using 2-DE gels. Therefore, there is a need for complementary methods for identification and characterization of these HNE-induced protein carbonyl modifications. Such drawbacks could potentially be overcome by using mass spectrometry (MS) as the detection means. MS-based approaches to characterize posttranslational HNE modification to proteins and peptides is promising because the peptide sequence and the protein identity with exact position of HNE modification can be directly determined through tandem mass spectrometry (MS/MS). Since MS is not dependent on crutches of antibodies; they are readily

applicable for finding novel HNE modification sites as well.

Mass Spectrometry (MS)

MS is the most comprehensive and versatile tool in protein chemistry and proteomics. The application of MS in proteomics involves studying protein complement of the cell, including their identification, posttranslational modification, quantification, subcellular localization and interacting partners. MS measurements are carried out in the gas phase and they typically measure the mass-to-charge ratio (*m/z)* of the ionized analytes. MS analysis of the sample can be performed in two ways: bottom-up and top-down. In the bottom-up approach, proteins are enzymatically digested into peptides prior to MS analysis, whereas in a top-down method an intact protein is analyzed.

(1) The bottom-up approach

Bottom-up approach is a popular method for protein identification based on peptide sequencing. In this method, proteins are digested into peptides by proteolytic enzymes (usually trypsin) and the resulting peptide mixtures are fractionated by reversed-phase liquid chromatography followed by mass spectrometry (RP-LC/MS) analysis. The tandem mass spectra of peptides are collected by inducing their dissociation, preferentially via collision induced dissociation (CID), which will be discussed in later segment in this chapter. The fragment ions, giving the primary sequence information of the peptides, are then usually searched in a database by appropriate algorithms (Figure 2). The bottom-up strategy is well suited for samples of high-complexity and identification of posttranslational modifications. The limitations of the bottom-up approach includes limited protein sequence coverage by identified peptides, loss of labile

posttranslational modifications, and uncertainty of the origin of the redundant peptide sequences.

(2) The top-down approach

This approach involves sequencing of proteins directly in the gas phase, without prior enzymatic digestion. In a top-down method, intact proteins are introduced into the MS and then subjected to "gas-phase proteolysis" by applying alternative fragmentation techniques such as electron capture dissociation (ECD) and electron transfer dissociation (ETD) for their successful identification. The benefit of these fragmentation techniques is that they yield a more complete fragmentation of the backbone and improved detection of posttranslational modifications. Higher sequence coverage of target proteins obtained in the top-down approach provides the advantage of identifying specific protein isoforms. The limitations of the top-down approach includes challenge in front-end separation of intact proteins, requirement of larger quantities of proteins and high-performance instruments that have the capacity, dynamic range, resolving power (to resolve overlapping isotopic distributions and identify the charge state) and mass accuracy (to improve identification confidence and limit search space for faster data processing) to analyze highly complex populations of proteins, their fragments and posttranslational modifications.

Separation technologies of proteins and peptides

The success of MS in proteomics is highly dependent on the separation technologies that simplify extremely complex biological samples into less-complex components that are more amenable to MS analysis. Front-end separation enhances the possibility of detection of weak ions that would otherwise be obscured by signals from coeluting high abundance species. The fractionation can be achieved either by one-dimensional gel electrophoresis or 2-DE, or by

chromatographic techniques. In gel-based approaches, a band or spot containing the protein is excised from the polyacrylamide matrix and digested *in situ* with a protease to create peptides and that, then, are extracted from the gel matrix for MS analysis. However, this method has a very limited dynamic range as described previously: only the most abundant proteins are observed, and several classes of proteins are known to be excluded or under-represented in 2-DE gels. These include very acidic or basic proteins, very large or small proteins and membrane proteins.[49] The standard gel-free method of front-end separation involves high-performance liquid chromatography (HPLC) coupled to MS. This methodology combines efficient separations of biological materials by liquid chromatography (LC) and sensitive identification of the individual components by MS. MS analysis of the components of the sample takes place on-line as they elute from the chromatography column. Even though various types of HPLC materials such as ion exchange, reverse phase, hydrophilic-interaction chromatography (HILIC), affinity, and hybrid materials can be used, reversed-phase (RP) chromatography is the workhorse in liquid chromatography–mass spectrometry (LC–MS) technique. Creating a peptide mixture sample for LC–MS is relatively straight-forward. A protein mixture is denatured by reduction with dithioreitol (DTT) and the Cys residues are then alkylated and subsequently digested overnight, preferentially with trypsin which generates peptides with an Arg or Lys residue at the C terminus. Digestion of the proteins can also be achieved by a two-step procedure that involves proteases, such as the endoprotease Lys-C followed by trypsin.

Reversed-phase liquid chromatography-mass spectrometry (RP-LC/MS)

In reversed-phase-liquid chromatography at pH ~ 3.0, peptide elution is primarily based on the peptide solution charge and its hydrophobicity. A single positive charge in a peptide is

sufficient to adsorb it to the column. With the same charge, the hydrophobic peptide is eluted later than the hydrophilic one. The charge number in a peptide is contributed by functional groups in the side chains of the basic amino acid residues (Lys, Arg and His), with one additional charge contributed by the N-terminus. Tryptic peptides are generally doubly charged because they terminate in Lys or Arg and have a free N-terminus.[50] The compatibility of buffers used during RP-LC with electrospray ionization (ESI) has made it the method of choice for separation of compounds prior to MS. The outlet of a RP column can be directly coupled to the ESI inlet of the MS to analyze complex peptide mixtures, a method known as LC–MS.[51] In a typical LC–MS experiment, the peptides are eluted from a RP column according to their hydrophobicity, are ionized via ESI and, then, transferred with high efficiency into the MS for analysis. Any individual peptide can be sequenced by isolating the ions of the eluting peptide in the collision cell of the mass analyzer, fragmenting them, and obtaining the tandem mass spectrum (MS/MS). In this manner, a large number of peptides can be sequenced in a single LC–MS analysis, even those that have the same molecular weight but differ in hydrophobicity. In practice, MS is often programmed to perform one scan to determine peptide masses, and three to ten data-dependent acquisitions on abundant peptide species for sequencing which takes less than 15 seconds to complete and generates hundreds of MS/MS spectra in a single run of an hour.[52] To achieve the best sensitivity and efficiency of separation, nanoLC columns (50-100 μm in internal diameter) packed with polymeric or silica-based, octadecylsilica-coated (C18) stationary phases with particle sizes in the 3- to 10-μm range are used routinely.[52] The smaller column inner diameter (i.d.), the lower the flow rate for the same chromatographic separation and, hence, the higher the sensitivity. However, 75 μm i.d. is a compromise between ultimate sensitivity and trouble-free separation.

Moreover, highly complex, large-scale proteomics samples can be fractionated by multidimensional separation that combines several separation techniques to improve the resolving power. During multidimensional separation, each dimension uses different molecular properties as a basis of separation. For example, in a two dimensional-liquid chromatography separation setup, the first dimension can be size exclusion chromatography or cation exchange chromatography coupled to a reverse phase column in a subsequent dimension that is inline with MS.[53-54] RPLC is usually the last dimension in multidimensional separation, prior to MS analysis. Multidimensional protein identification technology (MudPIT) is a popular separation approach in which samples of high complexity are subjected to strong cation-exchange (SCX) chromatography and eluted in a series of steps with increasing salt concentration. Each fraction is analyzed subsequently by MS following elution through RP column.

Instrumentation

There are three main components of a MS: an ionization source that converts analyte molecules into gas-phase ions, a mass analyzer (or mass analyzers in certain MS/MS instruments) that separates ionized analytes on the basis of *m/z* ratio, and a detector that records the number of ions at each *m/z* value (Figure 3).

Ionization techniques

A critical requirement for analyzing biomolecules by MS is the ability to transfer large and polar analytes of interest into gas-phase ions. The development of soft ionization methods, MALDI[55] and ESI[56], have revolutionized the field of MS. These ionization techniques have enabled the transfer of polar, nonvolatile, and thermally unstable proteins and peptides into the

gas phase without extensive degradation. The effort related to the development of MALDI and ESI was recognized by awarding the 2002 Nobel Prize in Chemistry to John Fenn and Koichi Tanaka.

(1) Matrix-assisted laser desorption ionization (MALDI)

MALDI-MS, first introduced in 1988 by Hillenkamp and Karas,[57] has become a widespread analytical tool for peptides, proteins, and most other biomolecules. In MALDI, samples are co-crystallized onto a sample plate with a low-molecular-weight organic matrix compound that usually has a conjugated aromatic ring structure (e.g., 2,5- dihydroxybenzoic acid [DHBA], sinapinic acid [SA], or α-cyano-4-hydroxycinnamic acid [CHSA]) that, thus, can absorb at the wavelength of a UV laser (e.g., 337 nm for the nitrogen laser). A laser irradiation of this analyte-matrix mixture causes desorption of matrix and $[M+H]^+$ ions of an analyte, into the gas phase.[58] The ions are then extracted into the MS for analysis (Figure 4). MALDI can measure compounds with high accuracy and subpicomole sensitivity which can be extremely useful for their identification and characterization. This is mainly due to the pulsed nature of most lasers where ions are formed in discrete events and, when mass analysis is synchronized with ion formation, very little sample is wasted.[59] Moreover, the generation of singly charged ions in MALDI makes it applicable to the top-down analysis of high molecular-weight proteins. Also, unlike ESI, MALDI has relatively high tolerance to salts and buffers.

(2) Electrospray ionization (ESI)

In contrast to MALDI, ESI is a technique used to produce gas-phase ions from solution-bound molecules. During ESI, the solubilized sample is passed through a high voltage needle at

atmospheric pressure. A voltage of 2-6 kV applied between the electrospray needle tip and the inlet of the mass spectrometer (MS) results in the formation of electrically charged droplets. Evaporation of solvent from the droplet decreases its radius and, as the droplet gets smaller, the repulsion between the charges at the surface increases. At the critical radius given by the Rayleigh equation (see below), the repulsive Columbic force overcomes the cohesive force of the surface tension resulting in disintegration of the droplets into a number of small parent droplets and progeny droplets. The process of repeated evaporation and fission events ultimately lead to the formation of very small, "final" droplets which are the precursors of the multiply protonated gas phase ions of proteins or peptides,[60,61] and eventually these ions make their way into the mass analyzer of the MS (Figure 5).

Rayleigh equation:

$$Q_{Ry} = 8\Pi(\varepsilon_0 \gamma R^3)^{1/2}$$

where, Q_{Ry} is the charge on the droplet, γ the surface tension of the solvent, R the radius of the droplet, and ε_0 the electrical permittivity.

A wide range of compounds can be analyzed by ESI-MS; the only requirement is that the molecule be sufficiently polar to allow attachment of a charge. Fenn and co-workers have demonstrated that ESI-MS could be used very effectively for the analysis of peptides and proteins with molecular mass in the kDa (kilo-Dalton) range.[62] Due to the propensity of ESI to produce multiply charged analytes, MS with modest mass-to-charge (*m/z*) ranges could be used to detect analytes with masses exceeding the nominal *m/z* range of the instrument. The formation

of series of peaks with differing *m/z* values, but corresponding to the same molecular mass in the ESI mass spectrum, is known as a charge state envelope. The actual mass of the compound can be deduced by solving a series of equations. Since ESI ionizes the analytes out of a solution, it is performed in either the infusion mode or coupled to LC. In the infusion mode, the sample is simply introduced into a continuous liquid stream (typically a mixture of an organic and aqueous liquid such as 50:50 methanol:H_2O) via an injection valve. Complex samples are preferentially analyzed by integrated LC–MS, whereas MALDI-MS is normally used to analyze relatively simple peptide mixtures.[63]

Mass analyzers

Mass analyzers are an integral part of each instrument because they can store ions and separate them on the basis of *m/z* ratios. There are five principal types of mass analyzers currently used in proteomic research, which mainly differ in how they determine the *m/z* ratios of the peptides.

(1) Time-of-flight (TOF) mass analyzers:

TOF analyzers accelerate the ions by using a short voltage gradient and measure the time taken to traverse a field-free flight tube. As all the ions with the same charge obtain the same kinetic energy after acceleration, the lower *m/z* ions achieve higher velocities than the higher *m/z* ions. The flight time is inversely proportional to the square root of the *m/z* of the ions. MS/MS with TOF analysis is most commonly practiced by placing a collision cell between the two TOF analyzers or by configuring a TOF analyzer as the second stage in hybrid instruments.

(2) Quadrupole (Q) mass analyzers:

Quadrupole analyzers resolve ions according to *m/z* by applying radio frequency (rf) and direct current (DC) voltages to four precisely parallel rods which are typically cylindrical or hyperbolic in geometry, allowing only a narrow *m/z* range to reach the detector in the electric field generated. By scanning the amplitude of this electric field and recording the ions at the detector, a mass spectrum is obtained. The *m/z* ratio of the ions that are allowed to pass through the quadrupole is proportional to the DC voltage applied to the rods; the higher the voltage, the higher the *m/z* value that is allowed to pass. For MS/MS analysis, three quadrupoles can be configured together (to form a "triple-quad"). The first and third quadrupoles are used for scanning whilst the middle quadrupole is used as a collision cell.[49]

(3) Ion trap (Quadrupole ion trap, QIT; linear ion trap, LIT or LTQ) mass analyzers:

QITs focus ions into a small volume with an oscillating electric field; the trapped ions are, then, resonantly activated and ejected by electronic manipulation of this field. They can rapidly shift between "MS scan" that involves scanning for masses of the analytes and "MS/MS scan" which induces fragmentation of the ions detected in the MS scan. Ions are selected for MS/MS analysis by using an rf voltage applied to the end caps to selectively eject all ions in the trap except for a chosen precursor ion. A resonating frequency that corresponds to the resonant frequency of the isolated ion is then applied to the end caps at amplitude of a few percent of that required to eject the ion. The precursor ion starts to oscillate and collide with the helium buffer gas, which eventually induces fragmentation of the precursor ion.[49] Owing to the operating principle of the trap, the lower end of the fragment mass range (below about a quarter of the

parent ion mass) cannot be observed.[52] LITs are a recent improvement of quadrupole ion traps, with higher scan ranges, larger electronic trap fields, and higher resolution.

(4) Fourier-transform ion cyclotron resonance (FTICR) mass analyzers:

FTICR-MS uses high magnetic fields to trap the ions and cyclotron resonance to excite and detect them.[64] Fourier transformation is used to obtain mass spectra from image current detected in receiver plates upon pulse excitation of the trapped ions. MS/MS analysis with FTMS is similar to that in the ion trap: ions are first isolated by ejecting all other ions in the cell using resonance excitation and, then, a pulse of gas is introduced into the cell and a small voltage is applied to the transmitter plate. By varying the amplitude of the resonating frequency, the precursor ion starts to oscillate and collide with the background gas, inducing dissociation and production of fragment ions. After a period of time, the ions are excited into higher cyclotron orbits and detected.[49]

(5) Orbitrap mass analyzers:

The Orbitrap MS neither uses rf nor a magnet to hold ions inside, but is based on new principles of physics that involves the separation of ions in an oscillating electric field.[65] In the Orbitrap, ions are trapped and they orbit around a central spindle-like electrode and oscillate harmonically along its axis with a frequency characteristic of their *m/z* values, inducing an image current in the outer electrodes that is Fourier transformed into the time domain producing mass spectra.[66]

The generation of short bursts of ions in the vacuum during MALDI and a continuous beam of ions in an atmosphere during ESI typically led to coupling MALDI with TOF mass

analyzers which measure the mass of intact peptides. ESI, however, has mostly been coupled to ion traps and triple quadrupole instruments and used to generate fragment ion spectra.

Protein identification by database searching

The widespread use of MS in biological studies has been made possible by the development of algorithms for the identification of proteins. The search algorithms compare the MS data to a database, originally using a set of peptide masses (peptide mass fingerprinting) and now increasingly using fragmentation of ions of the individual peptides (tandem mass spectrometry).

(1) Peptide mass fingerprinting

MALDI-TOF is used to identify proteins by a method known as peptide mapping or peptide-mass fingerprinting. Proteins, upon proteolysis with a specific protease, produce groups of peptides with masses that constitute mass fingerprints unique for a specific protein. Therefore, if a sequence database containing the specific protein sequence is searched using selected masses (i.e., the observed peptide mass fingerprint), then the protein is expected to be correctly identified within the database. This comparison is performed by an algorithm that matches a set of measured peptide masses with a list of theoretical masses generated following *in silico* digestion of proteins in the database and a score is assigned to each match. The peptide matches are eventually listed based on their ranks.[67] More sophisticated scoring algorithms take the mass accuracy and the percentage of the protein sequence covered into account and attempt to calculate a level of confidence for the match.[52] The technique requires a purified target protein and has been commonly used in conjunction with prior protein separation by 2-DE which is

followed by analysis in MALDI-TOF mass spectrometers. The single biggest disadvantage of peptide mass fingerprinting is ambiguity in protein identification due to peptide mass redundancy.

(2) Tandem mass spectrometry (MS/MS)

In this method, protein identification is based on the primary sequence information generated from fragmentation of the selected peptide ions in a tandem mass spectrometer. The process of acquiring tandem mass spectra consists of two steps. The first step (MS1) involves separation of mixture of charged peptides entering the MS according to their *m/z* ratios to create a list of the most intense peptide peaks. In the second MS analysis (i.e., MS/MS), the instrument is adjusted so that the peptide ion of interest is isolated in a collision cell according to its *m/z* value (i.e., by filtering away other ion species that have different *m/z* values). The selected peptide ion species is "activated" (e.g., by collisions with an inert gas such as helium that imparts internal energy into the ions) to undergo subsequent fragmentation. The *m/z* values of the fragment ions, which give primary sequence information of the precursor peptide, are recorded (Figure 2). The fragmentation upon CID, which is the most commonly used method, occurs predominantly at the peptide bonds such that a ladder of fragment ions, each of which differs by the mass of a single amino acid, is generated. The fragments are derived from the N- or C-terminus of the peptide and are designated as "b" or "y" ions, respectively. If the positive charge associated with the parent peptide ion remains on the amino-terminal side of the fragmented amide bond, then this fragment ion is referred to as a "b" ion and is assigned as a "y" ion if the charge remains on the carboxyl-terminal side of the cleaved amide bond (Figure 6). The subscripts designate the specific amide bond that was fragmented to generate the observed

fragment ions.[68] The MS/MS fragment ions contain sequence information that can be matched with peptide sequences from *in silico* "digested" protein sequence databases for peptide and subsequent protein identification. Because the tandem mass spectra contains structural information related to the sequence of the peptide, rather than only the peptide mass, these searches are generally more specific and discriminating.

Fragmentation methods (Peptide sequencing by tandem mass spectrometry)

Within an MS, individual proteins or peptides are separated and fragmented for sequencing and localization of posttranslational modification site(s). The fragment mass data can then be used to search the database for peptide identification. The two most popular methods of fragmentation are:

(1) Collision-induced dissociation (CID)

CID, also called collision-activated dissociation (CAD), is the most common ion-activation method used in the present day mass spectrometers for peptide cation dissociation. Peptide ion fragmentation is promoted by a "mobile" proton; i.e., the fragmentation of most protonated peptides requires the involvement of a proton at the cleavage site.[69] During CID, the addition of energy via collision activation with neutral and inert target gases (e.g., helium) mobilizes the proton to backbone heteroatoms (e.g., backbone carbonyl oxygen). These transfers are facilitated by the proton affinity to the heteroatom. Protonation at the backbone sites initiates cleavage of the backbone to produce b- and/or y-type fragments with charge retention on the N- or C-terminus, respectively.[49] The dissociation products provide the "structural fingerprint' of a particular peptide ion and thereby provide detailed structural information (e.g. amino acid

sequence) on the peptide. When trypsin is used for the digestion of proteins, the resulting peptides will have Arg or Lys residues as their C-termini. For example, the y-ion series of tryptic peptides will start with masses y_1=147 (Lys) or 175 (Arg). The next fragmentation peak in the y ion series, the y_2 ion, differs by the mass of an amino acid residue and, thus, "spells out" the next amino acid. Similarly the b-ion series starts with b_1 for the N-terminal amino acid and is traced upward in the molecular weight. In very high quality spectra, it is possible to interpret the fragmentation ladders (the b- and y-ion series) from the low mass end through to the highest mass ion; however, not all fragment ions are present at detectable levels. Therefore, it is often possible to interpret part but not all of the sequence with confidence.[52] Tandem mass spectra are usually interpreted with the aid of database search algorithms that help in correctly identifying the peptides.

(2) Electron capture dissociation (ECD)

While CID cleaves at the amide bonds in a peptide and produces b- and y-ion pairs, electron capture dissociation (ECD), used primarily with FTICR instrument, cleaves extensively along the N-Cα bond of the peptide/protein backbone, producing c- and z-ion pairs during the capture of a thermal electron by a multiply protonated peptide/protein cation. ECD is a favored technique for MS/MS of proteins in a top-down application because, unlike CID, it can cause dissociation in very large biomolecules at many sites providing more sequence information. It is also suited for sequencing posttranslationally modified peptides as it generally cleaves only the peptide backbone leaving the modified amino acid side-chains intact and, thus, allowing both peptide identification and precise determination of localization of the posttranslational modifications.[70] As a result, ECD enables efficient sequencing of phosphopeptides,

glycopeptides and other types of modified peptides as well as intact, modified proteins.[71,72] Electron transfer dissociation (ETD) is a fragmentation technique analogous to ECD. During ETD, singly-charged radical anions formed, e.g., from anthracene, transfer an electron to multiply protonated peptides and induce fragmentation of the peptide backbone producing c- and z-ion series.[73]

Computational algorithms for peptide identification

The profiling of proteins in a sample can be achieved by search programs that match the MS/MS spectra of peptides recorded during sample analysis with the theoretical spectra. A series of computational methods for the assignment of peptide sequences based on automated interpretation of the MS/MS spectra and protein sequence database searching have been developed.[74] The search programs calculate a similarity score that evaluates the degree of match between the experimental MS/MS spectrum and a theoretical spectrum (e.g., SEQUEST, Thermo Corp., **http://www.thermo.com/**) or uses a statistical approach to evaluate the probability of observing the MS/MS fragment ions (e.g., Mascot, Matrix Science, **http://www.matrixscience.com/**).[51] SEQUEST adopts a cross-correlation approach, in which peptide amino acid sequences from a protein database are used to construct theoretical mass spectra and the degree of overlap or cross-correlation between the theoretical and experimental mass spectra determines the best match.[49,67] Peptides are accepted as genuine hits, if they fulfill the criteria such as a score above a chosen significance cutoff, correct enzymatic cleavage, and absence of other peptides that match with a similar score.[67] In the probability-based matching of Mascot, the MS/MS fragment ion masses calculated from peptide sequences in the database are compared with the experimentally observed peaks, and a score is calculated that reflects the

statistical significance of the match between the experimental and theoretical spectra.[49,67,75] The "peptide sequence tag" approach extracts a short, unambiguous amino acid sequence from the peak pattern that, when combined with the mass information, is a specific probe to determine the origin of the peptide.[76] These database-searching algorithms can also support posttranslational modifications of specific amino acids. Following completion of the database search by any of the aforementioned algorithms, the identified peptides are compiled into a protein "hit list", which is the output of a typical proteomic experiment.

Top-down data are usually analyzed using the expressed sequence tag (EST) method or the *de novo* sequencing program leading to identification of a source protein.[77] Sequence tag searches are performed using small contiguous strings of identified amino acids (sequence tags) compared against sequences in the database. The *de novo* sequencing represents the direct "reading" of the amino acid sequence from an MS/MS spectrum.

RESEARCH GOALS AND OBJECTIVES

Study of HNE-modification by mass spectrometry

MS/MS with CID-based fragmentation is a widespread method for peptide sequencing and determination of posttranslational modifications. However, the limitation with the CID-based fragmentation technique in characterization of HNE-modification in a peptide is that the cleavage of the labile HNE group is favored over the peptide backbone dissociation. The HNE-modified peptide results in a neutral loss of HNE (156 Da; 78 or 52 Th for doubly or triply charged peptides) from the precursor or product ions upon CID.[78] This phenomenon of neutral loss of modifying group limits further fragmentation of the precursor ion restricting the

generation of fragment ions that would otherwise provide sequence information. Even though neutral loss indicates the presence of modification by its characteristic signature tag, a significant challenge still persists in the determination of site(s) of HNE modification. The difficulty of correctly assigning the site of HNE modification also exists because, unlike other posttranslational modifications such as phosphorylation or glycosylation, a consensus sequence representing the chemical selectivity of HNE modification is lacking.

This dissertation describes the development and application of mass spectrometric-based qualitative methods to unravel HNE modification sites in peptides and proteins.

REFERENCES

1. Navarro, A. (2004) *Mitochondrial enzyme activities as biochemical markers of aging.* Mol. Aspects Med. 25, 37-48

2. Sohal, R. S. (2002) *Role of oxidative stress and protein oxidation in the aging process.* Free Radic. Biol. Med. 33, 37-44

3. Beckman, K. B. and Ames, B. N. (1998) *The free radical theory of aging matures.* Physiol. Rev. 78, 547-581

4. Stadtman, E. R. (2002) *Importance of individuality in oxidative stress and aging.* Free Radic. Biol. Med. 33, 597-604

5. Stadtman, E. R. (1992) *Protein oxidation and aging.* Science 257, 1220-1224

6. Uchida, K. (2003) *4-hydroxy-2-nonenal: A product and mediator of oxidative stress.* Prog. Lipid Res. 42, 318-343

7. Bloomer, R. J. and Goldfarb, A. H. (2004) *Anaerobic exercise and oxidative stress: A review.* Can. J. Appl. Physiol. 29, 245-263

8. van den Bosch, H., Schutgens, R. B., Wanders, R. J., and Tager, J. M. (1992) *Biochemistry of peroxisomes.* Annu. Rev. Biochem. 61, 157-197

9. Finkel, T. and Holbrook, N. J. (2000) *Oxidants, oxidative stress and the biology of ageing.* Nature 408, 239-247

10. McLennan, H. R. and Degli Esposti, M. (2000) *The contribution of mitochondrial respiratory complexes to the production of reactive oxygen species.* J. Bioenerg. Biomembr. 32, 153-162

11. Boveris, A. and Chance, B. (1973) *The mitochondrial generation of hydrogen peroxide. general properties and effect of hyperbaric oxygen.* Biochem. J. 134, 707-716

12. Kohen, R. and Nyska, A. (2002) *Oxidation of biological systems: Oxidative stress phenomena, antioxidants, redox reactions, and methods for their quantification.* Toxicol. Pathol. 30, 620-650

13. Jackson, M. J., Papa, S., Bolanos, J., Bruckdorfer, R., Carlsen, *et al.* (2002) *Antioxidants, reactive oxygen and nitrogen species, gene induction and mitochondrial function.* Mol. Aspects Med. 23, 209-285

14. Requena, J. R., Chao, C. C., Levine, R. L., and Stadtman, E. R. (2001) *Glutamic and aminoadipic semialdehydes are the main carbonyl products of metal-catalyzed oxidation of proteins.* Proc. Natl. Acad. Sci. U. S. A. 98, 69-74

15. Levine, R. L. and Stadtman, E. R. (2001) *Oxidative modification of proteins during aging.* Exp. Gerontol. 36, 1495-1502

16. Stadtman, E. R. and Levine, R. L. (2003) *Free radical-mediated oxidation of free amino acids and amino acid residues in proteins.* Amino Acids 25, 207-218

17. Stadtman, E. R. (2001) *Protein oxidation in aging and age-related diseases.* Ann. N. Y. Acad. Sci. 928, 22-38

18. Dalle-Donne, I., Giustarini, D., Colombo, R., Rossi, R., and Milzani, A. (2003) *Protein carbonylation in human diseases.* Trends Mol. Med. 9, 169-176

19. van der Loo, B., Bachschmid, M., Spitzer, V., Brey, L., Ullrich, V., and Luscher, T. F. (2003) *Decreased plasma and tissue levels of vitamin C in a rat model of aging: Implications for antioxidative defense.* Biochem. Biophys. Res. Commun. 303, 483-487

20. Chen, J. J. and Yu, B. P. (1994) *Alterations in mitochondrial membrane fluidity by lipid peroxidation products.* Free Radic. Biol. Med. 17, 411-418

21. Esterbauer, H., Schaur, R. J., and Zollner, H. (1991) *Chemistry and biochemistry of 4-hydroxynonenal, malonaldehyde and related aldehydes.* Free Radic. Biol. Med. 11, 81-128

22. Ichihashi, K., Osawa, T., Toyokuni, S., and Uchida, K. (2001) *Endogenous formation of protein adducts with carcinogenic aldehydes: Implications for oxidative stress.* J. Biol. Chem. 276, 23903-23913

23. Uchida, K. (2000) *Role of reactive aldehyde in cardiovascular diseases.* Free Radic. Biol. Med. 28, 1685-1696

24. Van Kuijk, F. J., Holte, L. L., and Dratz, E. A. (1990) *4-hydroxyhexenal: A lipid peroxidation product derived from oxidized docosahexaenoic acid.* Biochim. Biophys. Acta 1043, 116-118

25. Uchida, K. and Stadtman, E. R. (1992) *Modification of histidine residues in proteins by reaction with 4-hydroxynonenal.* Proc. Natl. Acad. Sci. U. S. A. 89, 4544-4548

26. Nadkarni, D. V. and Sayre, L. M. (1995) *Structural definition of early lysine and histidine adduction chemistry of 4-hydroxynonenal.* Chem. Res. Toxicol. 8, 284-291

27. Sayre, L. M., Lin, D., Yuan, Q., Zhu, X., and Tang, X. (2006) *Protein adducts generated from products of lipid oxidation: Focus on HNE and one.* Drug Metab. Rev. 38, 651-675

28. Dwivedi, S., Sharma, A., Patrick, B., Sharma, R., and Awasthi, Y. C. (2007) *Role of 4-hydroxynonenal and its metabolites in signaling.* Redox Rep. 12, 4-10

29. Grimsrud, P. A., Xie, H., Griffin, T. J., and Bernlohr, D. A. (2008) *Oxidative stress and covalent modification of protein with bioactive aldehydes.* J. Biol. Chem. 283, 21837-21841

30. Petersen, D. R. and Doorn, J. A. (2004) *Reactions of 4-hydroxynonenal with proteins and cellular targets.* Free Radic. Biol. Med. 37, 937-945

31. Stadtman, E. R. (1990) *Metal ion-catalyzed oxidation of proteins: Biochemical mechanism and biological consequences.* Free Radic. Biol. Med. 9, 315-325

32. Aldini, G., Dalle-Donne, I., Facino, R. M., Milzani, A., and Carini, M. (2007) *Intervention strategies to inhibit protein carbonylation by lipoxidation-derived reactive carbonyls.* Med. Res. Rev. 27, 817-868

33. Okada, K., Wangpoengtrakul, C., Osawa, T., Toyokuni, S., Tanaka, K., and Uchida, K. (1999) *4-hydroxy-2-nonenal-mediated impairment of intracellular proteolysis during oxidative stress. identification of proteasomes as target molecules.* J. Biol. Chem. 274, 23787-23793

34. Davies, K. J. (2001) *Degradation of oxidized proteins by the 20S proteasome.* Biochimie 83, 301-310

35. Friguet, B., Stadtman, E. R., and Szweda, L. I. (1994) *Modification of glucose-6-phosphate dehydrogenase by 4-hydroxy-2-nonenal. formation of cross-linked protein that inhibits the multicatalytic protease.* J. Biol. Chem. 269, 21639-21643

36. Friguet, B. and Szweda, L. I. (1997) *Inhibition of the multicatalytic proteinase (proteasome) by 4-hydroxy-2-nonenal cross-linked protein.* FEBS Lett. 405, 21-25

37. Berlett, B. S. and Stadtman, E. R. (1997) *Protein oxidation in aging, disease, and oxidative stress.* J. Biol. Chem. 272, 20313-20316

38. Robinson, C. E., Keshavarzian, A., Pasco, D. S., Frommel, T. O., Winship, D. H., and Holmes, E. W. (1999) *Determination of protein carbonyl groups by immunoblotting.* Anal. Biochem. 266, 48-57

39. Yoo, B. S. and Regnier, F. E. (2004) *Proteomic analysis of carbonylated proteins in two-dimensional gel electrophoresis using avidin-fluorescein affinity staining.* Electrophoresis 25, 1334-1341

40. Soreghan, B. A., Yang, F., Thomas, S. N., Hsu, J., and Yang, A. J. (2003) *High-throughput proteomic-based identification of oxidatively induced protein carbonylation in mouse brain.* Pharm. Res. 20, 1713-1720

41. Castegna, A., Aksenov, M., Aksenova, M., Thongboonkerd, V., Klein, J. B., Pierce, W. M., Booze, R., Markesbery, W. R., and Butterfield, D. A. (2002) *Proteomic identification of oxidatively modified proteins in Alzheimer's disease brain. part I: Creatine kinase BB, glutamine synthase, and ubiquitin carboxy-terminal hydrolase L-1.* Free Radic. Biol. Med. 33, 562-571

42. Butterfield, D. A. and Castegna, A. (2003) *Proteomic analysis of oxidatively modified proteins in alzheimer's disease brain: Insights into neurodegeneration.* Cell. Mol. Biol. (Noisy-le-grand) 49, 747-751

43. Uchida, K., Szweda, L. I., Chae, H. Z., and Stadtman, E. R. (1993) *Immunochemical detection of 4-hydroxynonenal protein adducts in oxidized hepatocytes.* Proc. Natl. Acad. Sci. U. S. A. 90, 8742-8746

44. Toyokuni, S., Miyake, N., Hiai, H., Hagiwara, M., Kawakishi, S., Osawa, T., and Uchida, K. (1995) *The monoclonal antibody specific for the 4-hydroxy-2-nonenal histidine adduct.* FEBS Lett. 359, 189-191

45. Levine, R. L., Garland, D., Oliver, C. N., Amici, A., Climent, I., Lenz, A. G., Ahn, B. W., Shaltiel, S., and Stadtman, E. R. (1990) *Determination of carbonyl content in oxidatively modified proteins.* Methods Enzymol. 186, 464-478

46. Requena, J. R., Levine, R. L., and Stadtman, E. R. (2003) *Recent advances in the analysis of oxidized proteins.* Amino Acids 25, 221-226

47. Tyers, M. and Mann, M. (2003) *From genomics to proteomics.* Nature 422, 193-197

48. Gygi, S. P., Corthals, G. L., Zhang, Y., Rochon, Y., and Aebersold, R. (2000) *Evaluation of two-dimensional gel electrophoresis-based proteome analysis technology.* Proc. Natl. Acad. Sci. U. S. A. 97, 9390-9395

49. Lane, C. S. (2005) *Mass spectrometry-based proteomics in the life sciences.* Cell Mol. Life Sci. 62, 848-869

50. Peng, J. and Gygi, S. P. (2001) *Proteomics: The move to mixtures.* J. Mass Spectrom. 36, 1083-1091

51. Ahn, N. G., Shabb, J. B., Old, W. M., and Resing, K. A. (2007) *Achieving in-depth proteomics profiling by mass spectrometry.* ACS Chem. Biol. 2, 39-52

52. Mann, M., Hendrickson, R. C., and Pandey, A. (2001) *Analysis of proteins and proteomes by mass spectrometry.* Annu. Rev. Biochem. 70, 437-473

53. Opiteck, G. J. and Jorgenson, J. W. (1997) *Two-dimensional SEC/RPLC coupled to mass spectrometry for the analysis of peptides.* Anal. Chem. 69, 2283-2291

54. Opiteck, G. J., Lewis, K. C., Jorgenson, J. W., and Anderegg, R. J. (1997) *Comprehensive on-line LC/LC/MS of proteins.* Anal. Chem. 69, 1518-1524

55. Hillenkamp, F., Karas, M., Beavis, R. C., and Chait, B. T. (1991) *Matrix-assisted laser desorption/ionization mass spectrometry of biopolymers.* Anal. Chem. 63, 1193A-1203A

56. Fenn, J. B., Mann, M., Meng, C. K., Wong, S. F., and Whitehouse, C. M. (1989) *Electrospray ionization for mass spectrometry of large biomolecules.* Science 246, 64-71

57. Karas, M. and Hillenkamp, F. (1988) *Laser desorption ionization of proteins with molecular masses exceeding 10,000 daltons.* Anal. Chem. 60, 2299-2301

58. Yates, J. R., Ruse, C. I., and Nakorchevsky, A. (2009) *Proteomics by mass spectrometry: Approaches, advances, and applications.* Annu. Rev. Biomed. Eng. 11, 49-79

59. Glish, G. L. and Vachet, R. W. (2003) *The basics of mass spectrometry in the twenty-first century.* Nat. Rev. Drug Discov. 2, 140-150

60. Kebarle, P. and Verkerk, U. H. (2009) *Electrospray: From ions in solution to ions in the gas phase, what we know now.* Mass Spectrom. Rev. 28, 898-917

61. Felitsyn, N., Kitova, E. N., and Klassen, J. S. (2002) *Thermal dissociation of the protein homodimer ecotin in the gas phase.* J. Am. Soc. Mass Spectrom. 13, 1432-1442

62. Whitehouse, C. M., Dreyer, R. N., Yamashita, M., and Fenn, J. B. (1985) *Electrospray interface for liquid chromatographs and mass spectrometers.* Anal. Chem. 57, 675-679

63. Aebersold, R. and Mann, M. (2003) *Mass spectrometry-based proteomics.* Nature 422, 198-207

64. Wysocki, V. H., Resing, K. A., Zhang, Q., and Cheng, G. (2005) *Mass spectrometry of peptides and proteins.* Methods 35, 211-222

65. Ahmed, F. E. (2008) *Utility of mass spectrometry for proteome analysis: Part I. conceptual and experimental approaches.* Expert Rev. Proteomics 5, 841-864

66. Han, X., Aslanian, A., and Yates, J. R., 3rd. (2008) *Mass spectrometry for proteomics.* Curr. Opin. Chem. Biol. 12, 483-490

67. Lu, B., Xu, T., Park, S. K., McClatchy, D. B., Liao, L., and Yates, J. R.,3rd. (2009) *Shotgun protein identification and quantification by mass spectrometry in neuroproteomics.* Methods Mol. Biol. 566, 229-259

68. Aebersold, R. and Goodlett, D. R. (2001) *Mass spectrometry in proteomics.* Chem. Rev. 101, 269-295

69. Wysocki, V. H., Tsaprailis, G., Smith, L. L., and Breci, L. A. (2000) *Mobile and localized protons: A framework for understanding peptide dissociation.* J. Mass Spectrom. 35, 1399-1406

70. Shi, S. D., Hemling, M. E., Carr, S. A., Horn, D. M., Lindh, I., and McLafferty, F. W. (2001) *Phosphopeptide/phosphoprotein mapping by electron capture dissociation mass spectrometry.* Anal. Chem. 73, 19-22

71. Jensen, O. N. (2004) *Modification-specific proteomics: Characterization of post-translational modifications by mass spectrometry.* Curr. Opin. Chem. Biol. 8, 33-41

72. Kjeldsen, F., Haselmann, K. F., Budnik, B. A., Sorensen, E. S., and Zubarev, R. A. (2003) *Complete characterization of posttranslational modification sites in the bovine milk protein PP3 by tandem mass spectrometry with electron capture dissociation as the last stage.* Anal. Chem. 75, 2355-2361

73. Syka, J. E., Coon, J. J., Schroeder, M. J., Shabanowitz, J., and Hunt, D. F. (2004) *Peptide and protein sequence analysis by electron transfer dissociation mass spectrometry.* Proc. Natl. Acad. Sci. U. S. A. 101, 9528-9533

74. Sadygov, R. G., Cociorva, D., and Yates, J. R.,3rd. (2004) *Large-scale database searching using tandem mass spectra: Looking up the answer in the back of the book.* Nat. Methods 1, 195-202

75. Perkins, D. N., Pappin, D. J., Creasy, D. M., and Cottrell, J. S. (1999) *Probability-based protein identification by searching sequence databases using mass spectrometry data.* Electrophoresis 20, 3551-3567

76. Mann, M. and Wilm, M. (1994) *Error-tolerant identification of peptides in sequence databases by peptide sequence tags.* Anal. Chem. 66, 4390-4399

77. Horn, D. M., Zubarev, R. A., and McLafferty, F. W. (2000) *Automated de novo sequencing of proteins by tandem high-resolution mass spectrometry.* Proc. Natl. Acad. Sci. U. S. A. 97, 10313-10317

78. Carbone, D. L., Doorn, J. A., Kiebler, Z., Ickes, B. R., and Petersen, D. R. (2005) *Modification of heat shock protein 90 by 4-hydroxynonenal in a rat model of chronic alcoholic liver disease.* J. Pharmacol. Exp. Ther. 315, 8-15

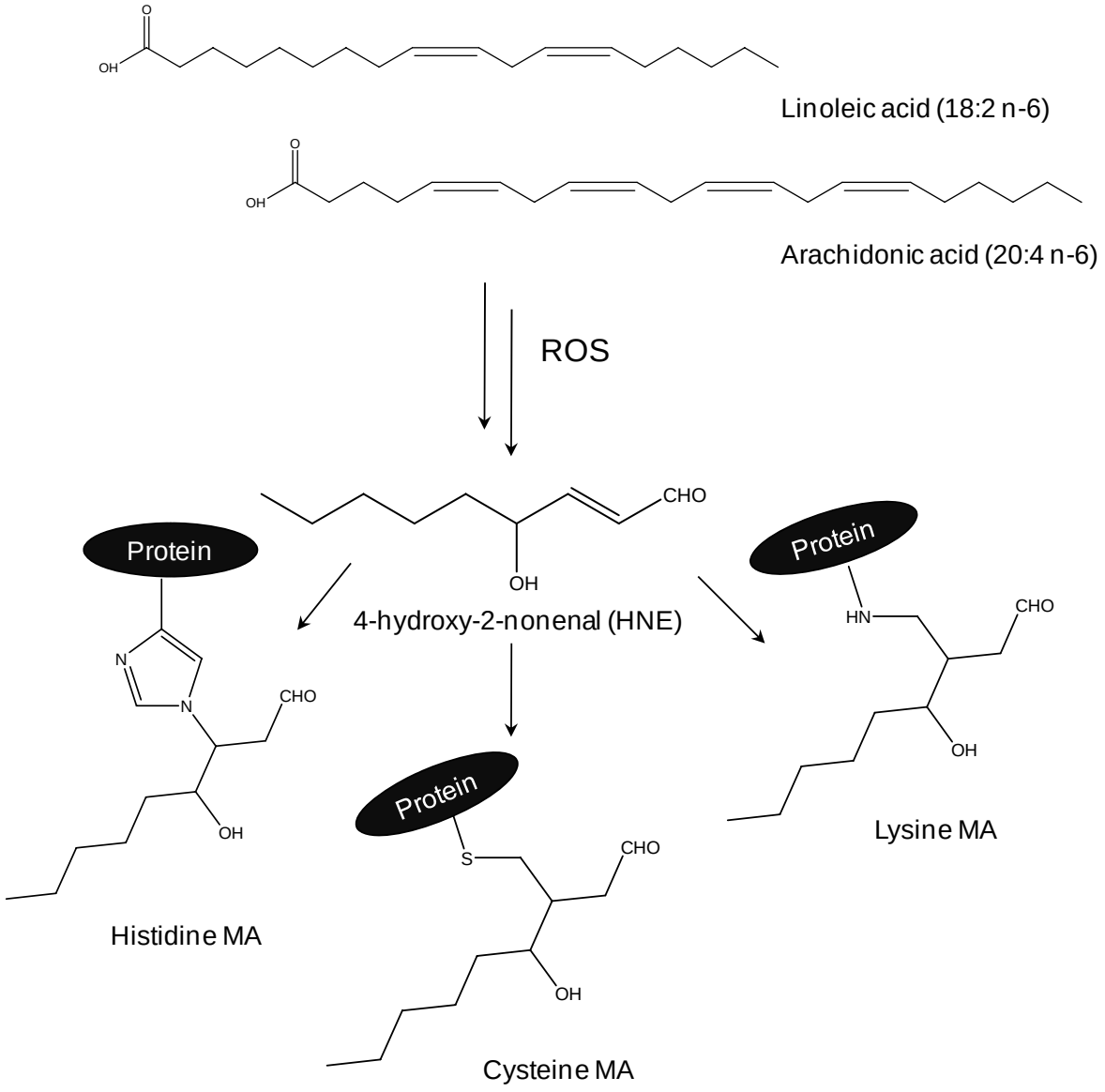

Figure 1. HNE generated by ROS-induced peroxidation of polyunsaturated membrane lipids can covalently modify nucleophilic groups in protein.

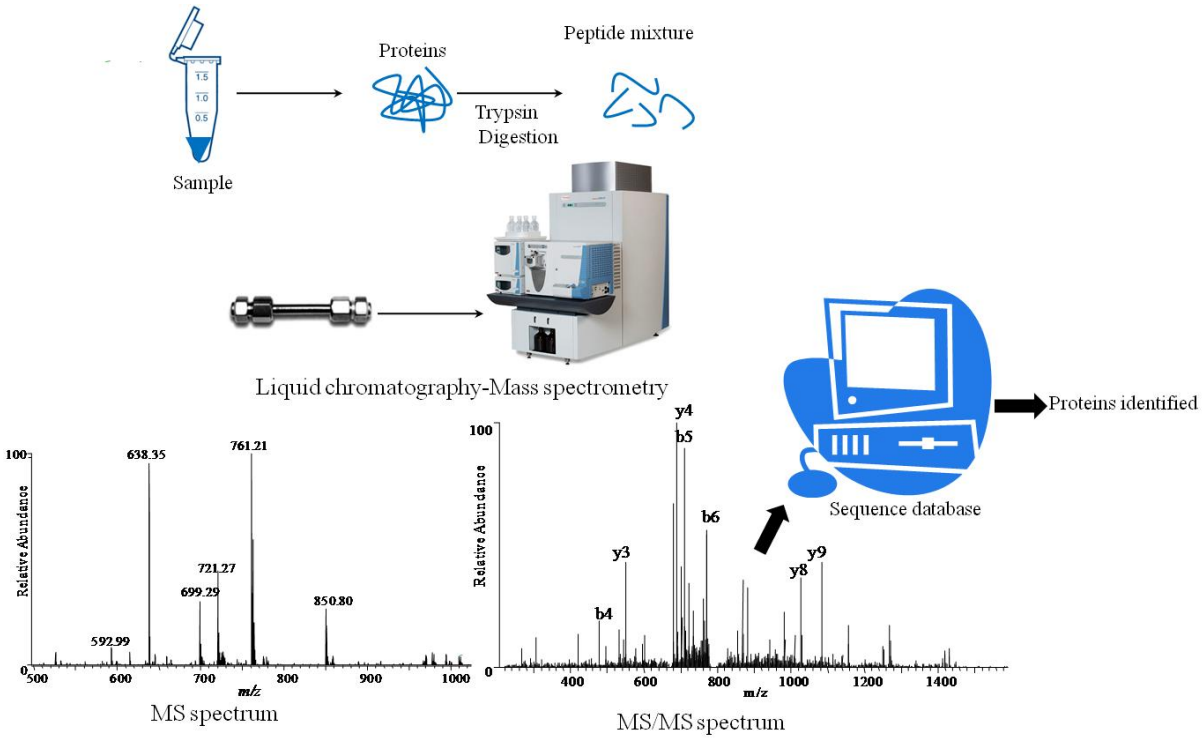

Figure 2. Generic method for bottom-up protein sample analysis by mass spectrometry. The proteins are enzymatically (usually by trypsin) digested to peptides. The resulting peptide mixture are separated by liquid chromatography and eluted into an electrospray ion source where they are neubilized in small, highly charged droplets. The protonated peptide ions enter the mass spectrometer and a mass spectrum of the peptides eluting at this time point is taken (MS or MS1 spectrum). In next stage a peptide ion is selected for fragmentation by energetic collision with gas and the tandem or MS/MS spectrum is recorded. The MS and MS/MS spectra are stored for matching against protein sequence databases. MS spectra reveal the masses of the peptide and MS/MS spectra provide their primary sequence information. The outcome of the experiments is the identity of the peptides and, therefore, the proteins making up the purified protein population.

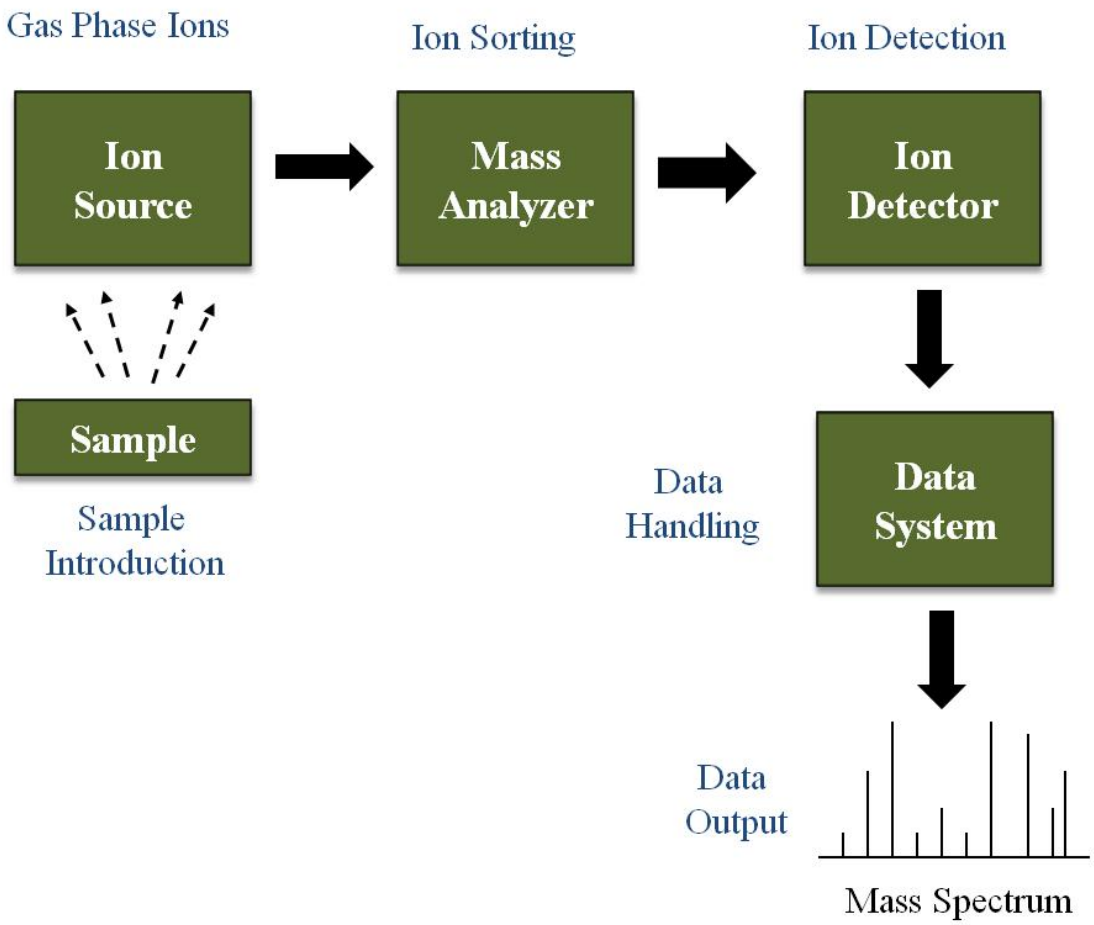

Figure 3. Components of a mass spectrometer.

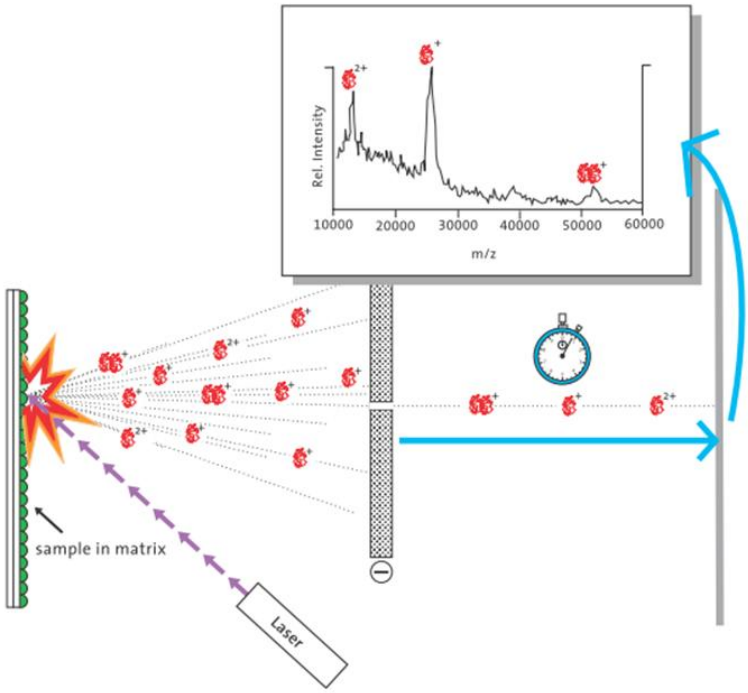

Figure 4. Schematic of the matrix-associated laser desorption ionization (MALDI) method.

(http://nobelprize.org/nobel_prizes/chemistry/laureates/2002/chemadv02.pdf)

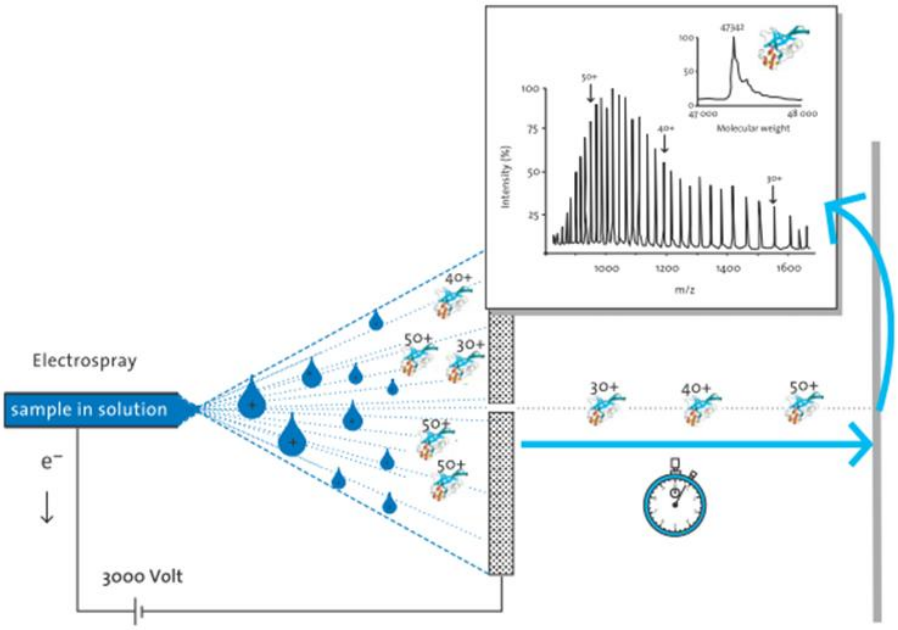

Figure 5. Schematic of the electrospray ionization (ESI) method.

http://nobelprize.org/nobel_prizes/chemistry/laureates/2002/chemadv02.pdf

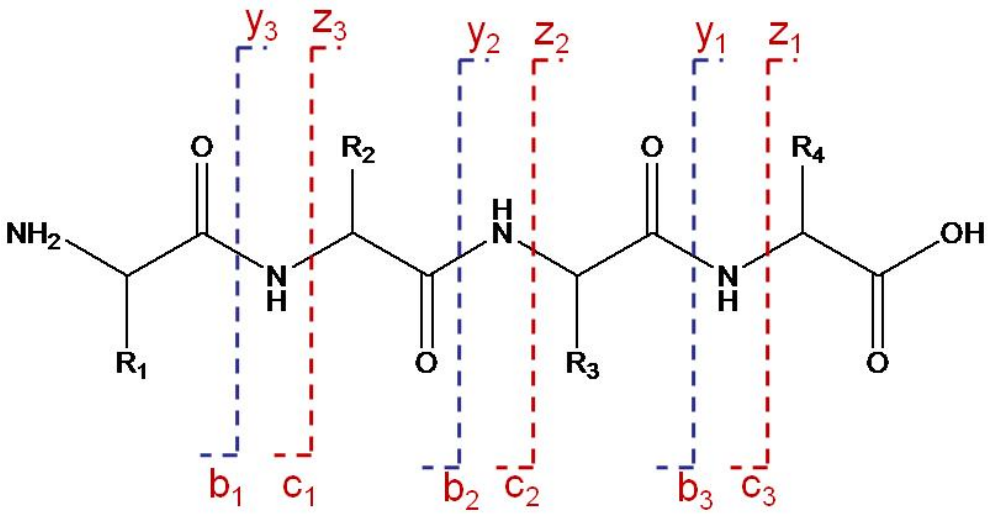

Figure 6. Nomenclature of b- and y-, as well as c- and z-ions generated most commonly upon collision-induced dissociation and electron capture dissociation of peptide ions.

CHAPTER II

FOURIER TRANSFORM ION CYCLOTRON RESONANCE MASS SPECTROMETRY OF COVALENT ADDUCTS OF PROTEINS AND 4-HYDROXY-2-NONENAL, A REACTIVE END-PRODUCT OF LIPID PEROXIDATION

Navin Rauniyar, Stanley M. Stevens Jr, Laszlo Prokai

Department of Molecular Biology & Immunology,

University of North Texas Health Science Center,

Fort Worth, TX 76107-2699, USA

Published in: *Anal. Bioanal. Chem.* 2007, 389, 1421-8

ABSTRACT

Covalent adduction of the model protein apomyoglobin by 4-hydroxy-2-nonenal, a reactive end-product of lipid peroxidation, was characterized by nanoelectrospray ionization Fourier transform ion cyclotron resonance mass spectrometry (FTICR). The high mass resolving power and mass measurement accuracy of the instrument facilitated a detailed compositional analysis of the complex reaction product without the need for deconvolution and transformation to clearly show the pattern of adduction and component molecular weights. Our study has also demonstrated the value of electron capture dissociation over collision-induced dissociation for the tandem mass spectrometric determination of site of modification for the 4-hydroxy-2-nonenal adduct of oxidized insulin B chain as an example.

Keywords

Fourier transform ion cyclotron resonance mass spectrometry • Electrospray ionization • Protein carbonylation • 4-Hydroxy-2-nonenal • Electron capture dissociation

INTRODUCTION

Reactive oxygen species (ROS) such as superoxide anion ($O_2^{\cdot -}$) , hydrogen peroxide (H_2O_2), and the hydroxyl radical ($HO\cdot$) that are produced at higher levels during oxidative stress can induce numerous proteomic changes in vivo.[1] Oxidative damage of proteins can result in several key events that alter cellular activity including changes in protein activity, proteasomal quality control, cellular redox-balance, and interference with the cell cycle.[2] Protein carbonylation in particular is an event caused by direct attack of ROS, metal-catalyzed oxidation, reaction with reducing sugars, and conjugation with highly reactive carbonyl compounds produced as end-products of lipid peroxidation.[1] The last of these processes, an event in which oxidation of polyunsaturated lipids present in biological membranes occurs, forms carbonyl compounds such as the α, β-unsaturated aldehyde 4-hydroxy-2-nonenal (HNE), acrolein, and others.

Aldehydes formed by lipid peroxidation react with nucleophilic groups of proteins and are found to be selective for certain amino acid residues including cysteine (Cys), lysine (Lys), and histidine (His).[3] As shown in Fig. 1, reaction between these aldehydes and amino acids occurs via Michael-type addition or Schiff base (imine) formation.[4,5] In HNE-based Michael-type addition, modification involves addition of the imidazole group of His (H), ε-amino group of Lys (L), or the sulfhydryl (–SH) group of Cys (C) to the α,β-unsaturated bond of HNE.[6] Several reported studies have demonstrated modifications of proteins at various amino acid residues by HNE leading to alteration in their structure and biological activity. For example, cytochrome c oxidase and apolipoprotein B-100 undergo modification exclusively at His by HNE[7,8], whereas epithelial fatty acid-binding protein was modified at Cys.[9] Cathepsin B was

reported to be modified both at Cys and His[10], and glyceraldehyde-3-phosphate dehydrogenase at Cys, His, and Lys residues.[11] Glucose-6- phosphate dehydrogenase undergoes selective modification at Lys by HNE.[12] Chemical modification of proteins by HNE can induce significant changes in their activity and thus knowledge of the exact modification sites provides detailed insight into oxidative stress-mediated cellular dysfunction.[13]

For the identification of post-translational modifications such as carbonylation, Fourier transform ion cyclotron resonance (FTICR) mass spectrometry[14] has unprecedented advantages over other instrumentation including ultra-high resolution, exceptionally high mass accuracy, and unique ion manipulation capabilities such as electron capture dissociation (ECD).[15] Characterization of protein carbonylation using FTICR/MS can be particularly effective, since the increase in molecular weight of intact proteins due to addition of aldehyde moieties such as HNE to Lys, His, or Cys residues is measured with ultra-high accuracy. Tandem mass spectrometry (MS/MS) can also be employed using both top-down (MS/MS of intact proteins typically by ECD) and bottom-up approaches (MS/MS of peptides derived from protease digestion) to provide further information on the exact site of protein modification. Identification of specific targets of covalent adduction of reactive aldehydes such as HNE is important to understand the chemistry behind the modification and subsequent variation in protein activity mediated by the modification.

In CID and IRMPD methods of dissociation, the amide bond of the peptide backbone is cleaved forming primarily b- or y-type fragment ions.[16] During CID-based fragmentation, however, there is a probability of neutral loss of the modifying group, which is dependent on the chemistry of the modification and its residue interaction, rendering it frequently difficult to correctly identify the peptide modification site. In comparison to CID where the

elimination of a labile covalent modification is sometimes favored over peptide backbone fragmentation, ECD provides complementary (N–Cα amine-bond cleavage which results in the formation of c- and z-type fragment ions) and perhaps more valuable sequence information, since unstable modifications are typically retained on the amino acid residue during the fragmentation process.[17]

The purpose of this study was to detect the extent of HNE modification of apomyoglobin by FTICR electrospray ionization mass spectrometry (ESI-MS). Bolgar and Gaskell have reported the formation of three to ten HNE adducts per protein molecule in apomyoglobin with modification occurring only at His residues.[17] Fenaille *et al*. have also reported nine His residues in apomyoglobin modified by HNE, after tryptic digestion and immunoaffinity purification of HNE-labeled peptides.[18] In this study we provide evidence of Schiff base addition of HNE to apomyoglobin in addition to Michael addition using FTICR/MS. We also show the advantages of electron capture dissociation (ECD) for gas-phase peptide fragmentation compared to conventional collision-induced dissociation (CID) using HNE-modified oxidized insulin B chain as a model peptide.

EXPERIMENTAL

Chemicals

Apomyoglobin from horse skeletal muscle and oxidized insulin B chain were purchased from Sigma-Aldrich (St. Louis, MO). 4-Hydroxy-2-nonenal was obtained from Alpha Diagnostic (San Antonio, TX). Water and acetonitrile were of high-performance liquid chromatography grade and purchased from Honeywell Burdick and Jackson (Morristown, NJ). All other chemicals were obtained from Sigma-Aldrich.

Preparation of apomyoglobin-HNE adduct

HNE adducts of apomyoglobin were generated via the method described by Bolgar and Gaskell[17] with slight modification. Apomyoglobin (137 μM) was incubated in an aqueous solution (2 mM) of HNE, buffered with 25 mM ammonium bicarbonate (final volume of 0.5 mL). The temperature was maintained at 37 °C for 2 h. The reaction was then terminated by the addition of 0.25 mL of 1% formic acid. The volume of the reaction mixture was adjusted to 2.5 mL with 25 mM ammonium bicarbonate and subjected to gel filtration by G-25 column (PD-10, GE Healthcare, Piscataway, NJ) in order to remove the unreacted substances. The desalted protein fraction was eluted in 3.5 mL of 0.1% formic acid and dried in a vacufuge concentrator (Eppendorf Scientific, Westbury, NY). The sample was resuspended in 49.5% acetonitrile/49.5% H_2O/1% acetic acid and used directly for nano-electrospray ionization mass spectrometric analysis.

Preparation of insulin-HNE adduct

Oxidized insulin B chain was incubated in an aqueous solution of HNE (2 mM), buffered with 50 mM K_2HPO_4 (pH 7.4). The temperature was maintained at 37 °C for 2 h (final volume 0.5 mL). The resulting modified peptides were desalted by octadecylsilica (C18) ZipTip (Millipore, Billerica, MA) microcolumns. The bound peptides were washed with 0.1% acetic acid and then recovered by elution with 20 μL of 49.5% acetonitrile/49.5% H_2O/1% acetic acid and used directly for nanoelectrospray mass spectrometric analysis.

Mass spectrometry

Electrospray ionization mass spectrometry was performed on a hybrid linear ion trap-7-

Tesla FTICR mass spectrometer (LTQ-FT, Thermo, San Jose, CA) equipped with a nanoelectrospray ionization source and operated with the Xcalibur (version 2.0) data acquisition software. HNE-adducted proteins or peptides were directly infused at 500 nL min^{-1} through a 50-μm-I.D. (pulled to 30-μm I.D.) New Objective (Woburn, MA) PicoTip. ESI spray voltage and capillary temperature were maintained at 2.0 kV and 250 °C, respectively. FTICR full-scan mass spectra were generally acquired at 100,000 nominal mass resolving power (M/ΔM at *m/z* 400 and taking the full width at half maximum intensity, FWHM, as ΔM) from *m/z* 500 to 2,000 using the automatic gain control mode of ion trapping. CID in the linear ion trap was performed using a 3.0-u isolation width and 35% normalized collision energy with helium as the target gas. ECD characterization of HNE-labeled peptides in the FTICR cell was carried out using an electrode current of 1.2 A and an ion irradiation time of 30 ms.

RESULTS AND DISCUSSION

HNE-apomyoglobin adduct characterization

The high mass resolving power provided by FTICR/MS was employed to accurately measure HNE adduct formation on apomyoglobin, since the various protein-derived charge state isotope clusters were easily resolved. To determine the extent of modification, apomyoglobin was resuspended in ESI spray solvent and analyzed by ESI-FTICR/MS as shown in Fig. 2. The charge state distribution of this protein was centered around the $[M+15H]^{15+}$ ion upon ESI. The inset in Fig. 2 (upper panel) shows the isotopic resolution of the +15 charge state of native apomyoglobin obtained at 100,000 nominal mass resolving power. The mass measurement accuracy of the instrument was calculated by comparing the measured isotope mass values of the

+15 charge state of apomyoglobin with the corresponding isotope mass values of the theoretical simulation of the same charge state (bottom panel). The average mass measurement accuracy obtained for the analysis of native apomyoglobin was approximately 1.5 ppm after external calibration of the FTICR instrument (mass measurement accuracies observed for full scan FTICR mass spectra were routinely less than 4 ppm).

Figure 3a represents a full-scan FTICR mass spectrum obtained for HNE-modified apomyoglobin which shows a complex pattern of peaks at each charge state of the modified protein. This complexity is due in part to the varying number and distribution of Schiff base or Michael addition HNE adducts. Figure 3b is an expanded *m/z* range of the +15 charge state of HNE-adducted apomyoglobin. The extent of modification was determined by comparing the experimentally derived peaks with isotopic simulations corresponding to various distributions of Michael-type (+156 Da) and/or Schiff base (+138 Da) adducts. FTICR/MS analysis allowed for the identification of three to nine sites of HNE modification in apomyoglobin. The increase in mass sequentially by 156 corroborates the proposed Michael-type addition mechanism for modification of apomyoglobin by HNE (see Fig. 1). Interestingly, ions corresponding to Schiff base addition of HNE to apomyoglobin could also be detected (Fig. 3c, upper), although the intensity of these ions is low compared to those of the apomyoglobin-HNE Michael-type adducts. Theoretical simulation of each HNE adduct within this particular *m/z* range was performed to support this finding (Fig. 3c, lower panel). Future studies will incorporate a bottom-up approach to characterize Schiff base adducts putatively identified from this analysis.

In this study, we investigated the extent of modification and mechanism by which adduct formation occurred by directly profiling the HNE reaction with apomyoglobin using the high mass resolving power and mass measurement accuracy of FTICR/MS. Extensive modification of

apomyoglobin by HNE has previously been reported to occur[17] where the complexity of the ESI mass spectra obtained required processing and transformation (deconvolution) to clearly show the pattern of adduction and component molecular weights using a triple quadrupole mass analyzer.[17] However, deconvolution techniques may not be ideal when characterizing modifications of intact proteins, since artifact peaks and peak distortions may be introduced into the analysis.[19]

The ESI-FTICR mass spectrum also showed a complex pattern of apomyoglobin-HNE adducts with multiple peaks observed at each charge state; however, evaluation of the pattern of adduction and the determination of component molecular weights were possible without deconvolution and additional data manipulation. We were able to identify the covalent attachment of up to nine HNE molecules to the protein. Most peaks could be assigned to products of Michael-type addition that represented the predominant mechanism of HNE reaction[20] over the competing Schiff base condensation. In horse apomyoglobin, 11 His residues are present and can be assumed to be targets for Michael-type addition, as indicated in previous studies.[17,18] In addition to confirming earlier results by accurate *m/z* measurement at high mass resolving power, we have also detected the possible formation of Schiff base adducts on the protein apomyoglobin.

CID and ECD tandem mass spectrometry of HNE-insulin adducts

In contrast to CID, the ECD technique has encouraging potential for the characterization of protein carbonylation, since labile post-translational modifications such as HNE attachment are retained during MS/MS fragmentation. The CID and ECD product-ion spectra of oxidized insulin B chain modified by one and two HNEs are shown in Figs. 4 and 5, respectively, along

with the corresponding MS/MS spectra of the unmodified peptides. The CID-derived MS/MS spectrum of the singly HNE-modified insulin peptide was complicated by numerous fragments produced due to the overall size of the peptide (>3 kDa) as well as the presence of HNE neutral loss fragment ions (Fig. 4b). From our experience with CID fragmentation of HNE-modified peptides, it is often difficult to assign the exact site(s) of modification. Frequently, no signature mass tag remains in the spectra due to HNE neutral loss from the peptide, which can be easily recognized upon comparing the CID product-ion spectra of the unmodified and modified peptides (Fig. 4a and b). As indicated in Fig. 4b, the predominant peaks observed in the MS/MS spectrum of the singly HNE-modified oxidized insulin B chain correspond to b-type fragment ions with and, mostly, without the HNE moiety (occurrence of neutral loss denoted by asterisk). Nevertheless, the high mass resolving power of the FTICR instrument was particularly effective in distinguishing isobaric fragment ions generated from the front-end linear ion trap. For example, an expanded *m/z* range of the CID product-ion spectrum shows clear separation of the b_{16}^{2+} and y_8 monoisotopic peaks which differ by *m/z* 0.031. A theoretical simulation of these two fragment ions at 20,000 mass resolving power is superimposed on the expanded *m/z* region in Fig. 4c, demonstrating that some ambiguity with fragment ion assignment would exist with conventional high-performance instrumentation such as time-of-flight (TOF) mass spectrometers.

Although the improved mass resolving power and mass measurement accuracy of the FTICR instrument facilitated tandem mass spectrometric characterization of the HNE-modified insulin peptide, the exact HNE modification site was difficult to determine due to limited sequence coverage and neutral loss fragmentation obtained by the CID process. Consequently, ECD was employed as an alternative method for the MS/MS analysis of the HNE-modified

insulin peptide. Figure 5 shows the ECD-derived fragmentation spectra of unmodified (Fig. 5a) and doubly HNE-modified (Fig. 5b) oxidized insulin B chain. Upon comparison of these two spectra, a shift in mass of +156 Da for the c_5 ion with an additional increase of 156 Da for the c_{10} ion was observed. Since ECD preserves the HNE modification during MS/MS fragmentation, the amino acid residue containing the intact modification was identified. Specifically, the mass spectrum in Fig. 5b shows that oxidized insulin B chain is modified by HNE through the formation of Michael-type adducts at His-5 and His-10 (Fig. 6). To our knowledge, this is the first reported example demonstrating the potential of ECD for an improved characterization of a protein- or peptide-HNE adducts. Future work will include the implementation of data-dependent neutral loss-driven MS^3 and ECD-based tandem mass spectrometric methods for the characterization of protein carbonylation sites.

Sequence information obtained from MS/MS spectra using CID and ECD were complementary and hence both can be beneficial for the identification of PTMs. For example, the neutral loss of HNE observed in CID fragmentation spectra could serve as a signature tag for the presence of that group in the peptide. ECD can then be utilized to provide enhanced information regarding peptide sequence and site(s) of modification. The use of ECD for tandem mass spectrometric analysis is not, however, widely implemented for this purpose, since only FTICR mass spectrometers would allow for the reliable and efficient application of this technique to induce dissociation of protonated peptides and proteins.

CONCLUSION

The reported study has demonstrated the value of FTICR instrumentation in addressing

the chemical aspects of the impact of oxidative stress on proteins. Oxidative stress has been implicated in aging and in almost every major chronic disease.[21] Oxidative stress-associated damage to proteins can significantly affect their activity, localization, turnover, and interaction with other molecules. Protein inactivation by formation of covalent adducts with HNE has been particularly well documented.[10-13] All ROS examined thus far, including reactive nitrogen species, also give rise to protein carbonyls which, therefore, have been regarded as broad biomarkers of oxidative stress.[22] Understanding the mechanisms and selectivity of protein carbonylation should provide new diagnostic biomarkers for oxidative damage, and yield basic information to aid the development of an efficacious antioxidant therapy.

ACKNOWLEDGMENT

This research has been supported by the grant AG025384 from the National Institutes of Health. Laszlo Prokai is the Robert A. Welch Professor at the University of North Texas Health Science Center.

REFERENCES

1. Shacter, E. (2000) *Quantification and significance of protein oxidation in biological samples.* Drug Metab. Rev. 32, 307-326

2. Castegna, A., Aksenov, M., Thongboonkerd, V., Klein, J. B., Pierce, W. M., Booze, R., Markesbery, W. R., and Butterfield, D. A. (2002) *Proteomic identification of oxidatively modified proteins in alzheimer's disease brain. part II: Dihydropyrimidinase-related protein 2, alpha-enolase and heat shock cognate 71.* J. Neurochem. 82, 1524-1532

3. Fenaille, F., Guy, P. A., and Tabet, J. C. (2003) *Study of protein modification by 4-hydroxy-2-nonenal and other short chain aldehydes analyzed by electrospray ionization tandem mass spectrometry.* J. Am. Soc. Mass Spectrom. 14, 215-226

4. Esterbauer, H., Zollner, H. (1989) *Methods for determination of aldehydic lipid peroxidation products*. Free Radic Biol Med 7, 197-203

5. Poli, G. and Schaur, R. J. (2000) *4-hydroxynonenal in the pathomechanisms of oxidative stress.* IUBMB Life 50, 315-321

6. Uchida, K. and Stadtman, E. R. (1992) *Modification of histidine residues in proteins by reaction with 4-hydroxynonenal.* Proc. Natl. Acad. Sci. U. S. A. 89, 4544-4548

7. Musatov, A., Carroll, C. A., Liu, Y. C., Henderson, G. I., Weintraub, S. T., and Robinson, N. C. (2002) *Identification of bovine heart cytochrome c oxidase subunits modified by the lipid peroxidation product 4-hydroxy-2-nonenal.* Biochemistry 41, 8212-8220

8. Bolgar, M. S., Yang, C. Y., and Gaskell, S. J. (1996) *First direct evidence for lipid/protein conjugation in oxidized human low density lipoprotein.* J. Biol. Chem. 271, 27999-28001

9. Bennaars-Eiden, A., Higgins, L., Hertzel, A. V., Kapphahn, R. J., Ferrington, D. A., and Bernlohr, D. A. (2002) *Covalent modification of epithelial fatty acid-binding protein by 4-hydroxynonenal in vitro and in vivo. evidence for a role in antioxidant biology.* J. Biol. Chem. 277, 50693-50702

10. Crabb, J. W., O'Neil, J., Miyagi, M., West, K., and Hoff, H. F. (2002) *Hydroxynonenal inactivates cathepsin B by forming michael adducts with active site residues.* Protein Sci. 11, 831-840

11. Ishii, T., Tatsuda, E., Kumazawa, S., Nakayama, T., and Uchida, K. (2003) *Molecular basis of enzyme inactivation by an endogenous electrophile 4-hydroxy-2-nonenal: Identification of modification sites in glyceraldehyde-3-phosphate dehydrogenase.* Biochemistry 42, 3474-3480

12. Szweda, L. I., Uchida, K., Tsai, L., and Stadtman, E. R. (1993) *Inactivation of glucose-6-phosphate dehydrogenase by 4-hydroxy-2-nonenal. selective modification of an active-site lysine.* J. Biol. Chem. 268, 3342-3347

13. Doorn, J. A., Hurley, T. D., and Petersen, D. R. (2006) *Inhibition of human mitochondrial aldehyde dehydrogenase by 4-hydroxynon-2-enal and 4-oxonon-2-enal.* Chem. Res. Toxicol. 19, 102-110

14. Marshall, A. G., Hendrickson, C. L., and Jackson, G. S. (1998) *Fourier transform ion cyclotron resonance mass spectrometry: A primer.* Mass Spectrom. Rev. 17, 1-35

15. Meng, F., Forbes, A. J., Miller, L. M., and Kelleher, N. L. (2005) *Detection and localization of protein modifications by high resolution tandem mass spectrometry.* Mass Spectrom. Rev. 24, 126-134

16. Wells, J. M. and McLuckey, S. A. (2005) *Collision-induced dissociation (CID) of peptides and proteins.* Methods Enzymol. 402, 148-185

17. Bolgar, M. S. and Gaskell, S. J. (1996) *Determination of the sites of 4-hydroxy-2-nonenal adduction to protein by electrospray tandem mass spectrometry*. Anal. Chem. 68, 2325-2330

18. Fenaille, F., Tabet, J. C., and Guy, P. A. (2002) *Immunoaffinity purification and characterization of 4-hydroxy-2-nonenal- and malondialdehyde-modified peptides by electrospray ionization tandem mass spectrometry.* Anal. Chem. 74, 6298-6304

19. Hagen, J. J., Monnig, C. A. (1994) Method for estimating molecular mass from electrospray spectra. Anal. Chem. 66, 1877-1883

20. Bakhtiar, R. and Guan, Z. (2006) *Electron capture dissociation mass spectrometry in characterization of peptides and proteins.* Biotechnol. Lett. 28, 1047-1059

21. Berlett, B. S. and Stadtman, E. R. (1997) *Protein oxidation in aging, disease, and oxidative stress.* J. Biol. Chem. 272, 20313-20316

22. Dalle-Donne, I., Giustarini, D., Colombo, R., Rossi, R., and Milzani, A. (2003) *Protein carbonylation in human diseases.* Trends Mol. Med. 9, 169-176

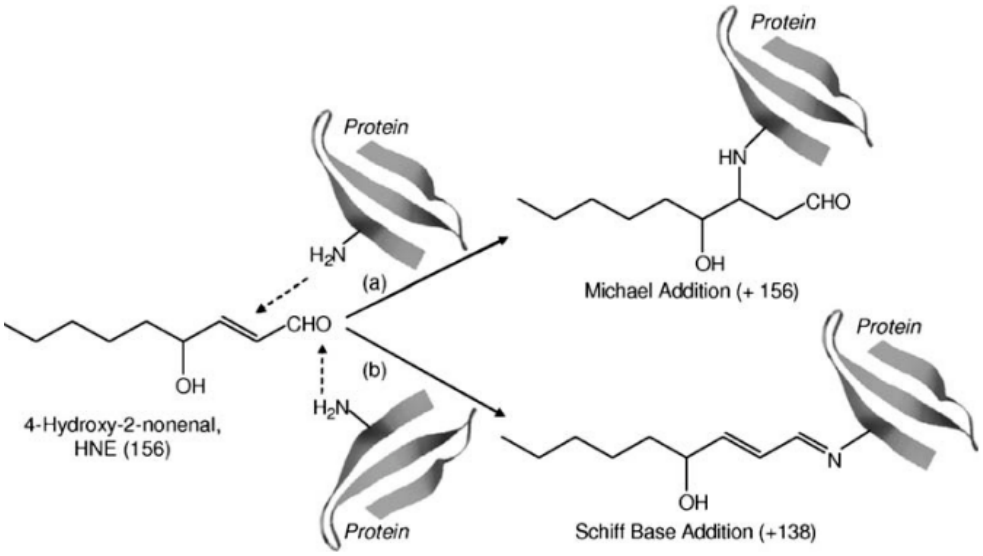

Figure 1. Primary mechanisms observed for the reaction of amine groups of proteins and peptides with 4-hydroxy-2-nonenal (HNE) are Michael-type addition (a) and formation of Schiff base adducts (b). HNE can also form Michael-type adducts (+156) with the imidazole =NH group of histidine (His) and sulfhydryl (–SH) groups of Cys side-chains (products not shown)

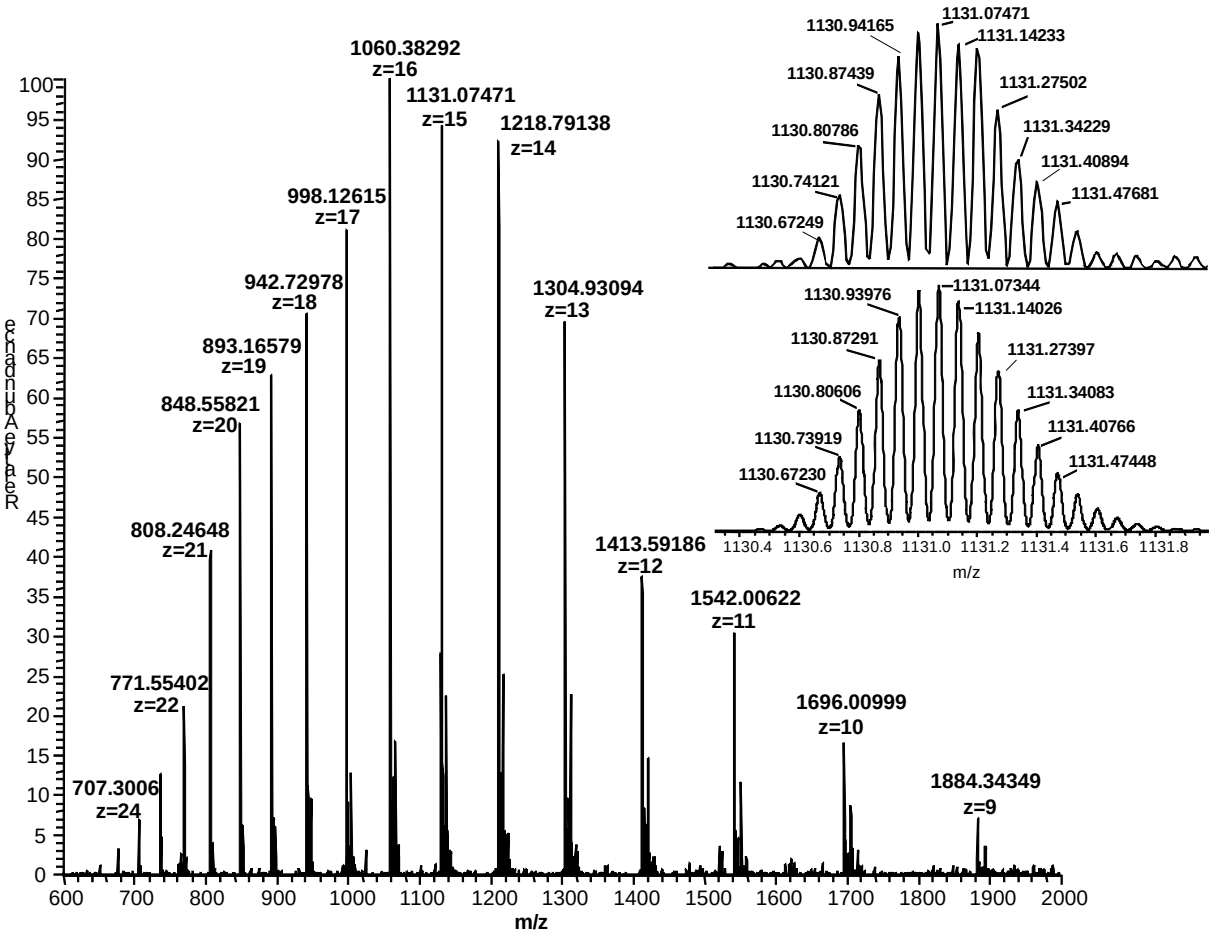

Figure 2. High resolution mass spectrum of unmodified apomyoglobin obtained by nanoESI hybrid linear ion trap-FTICR/MS (LTQ-FT, ThermoFisher). The top panel in the *inset* is an expanded *m/z* region showing isotopic resolution of the +15 charge state of unmodified apomyogobin. The mass accuracy and intensity distribution of this isotope envelope are in good agreement with a theoretical simulation (*bottom panel*)

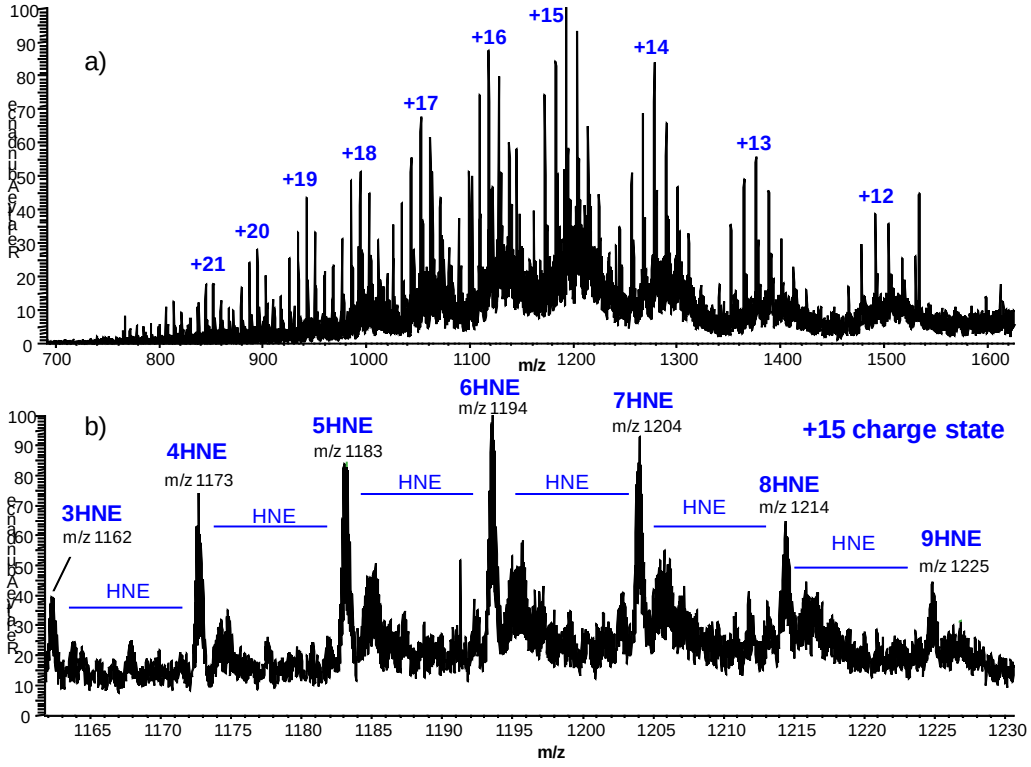
a)
+21
+20
+19
+18
+17
+16
+15
+14
+13
+12
Abundance
m/z
b)
3HNE
m/z 1162
4HNE
m/z 1173
5HNE
m/z 1183
6HNE
m/z 1194
7HNE
m/z 1204
8HNE
m/z 1214
9HNE
m/z 1225
HNE
+15 charge state

c)

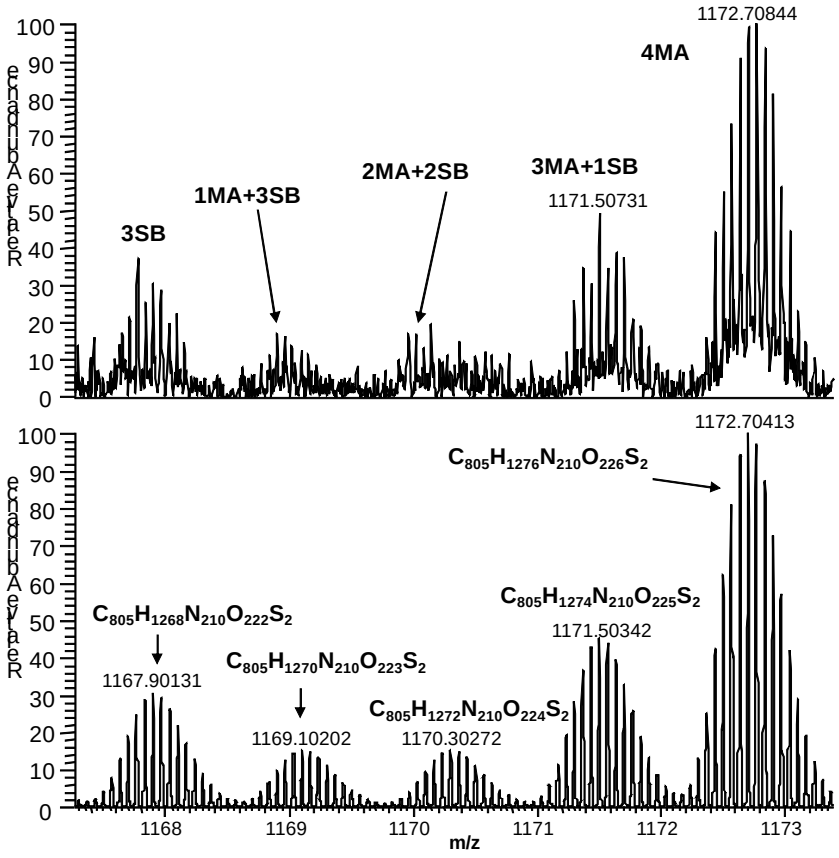

Figure 3. (a) FTICR mass spectrum of HNE-modified apomyoglobin. The charge state distribution ranged from $[M+12H]^{11+}$ to $[M+21H]^{21+}$. **(b)** Expanded m/z range of the +15 charge state of HNE-adducted apomyoglobin. Three to nine HNE adducts on apomyoglobin were observed. **(c)** Expanded *m/z* range of the +15 charge state of HNE- adducted apomyoglobin that contains between three to four Michael-type adducts (*MA*) of HNE. In addition to Michael-type addition of HNE to apomyoglobin, the formation of Schiff base adducts are also indicated (*SB*) in the *upper panel*. Theoretical isotopic simulation attests the presence of these adducts (*bottom*)

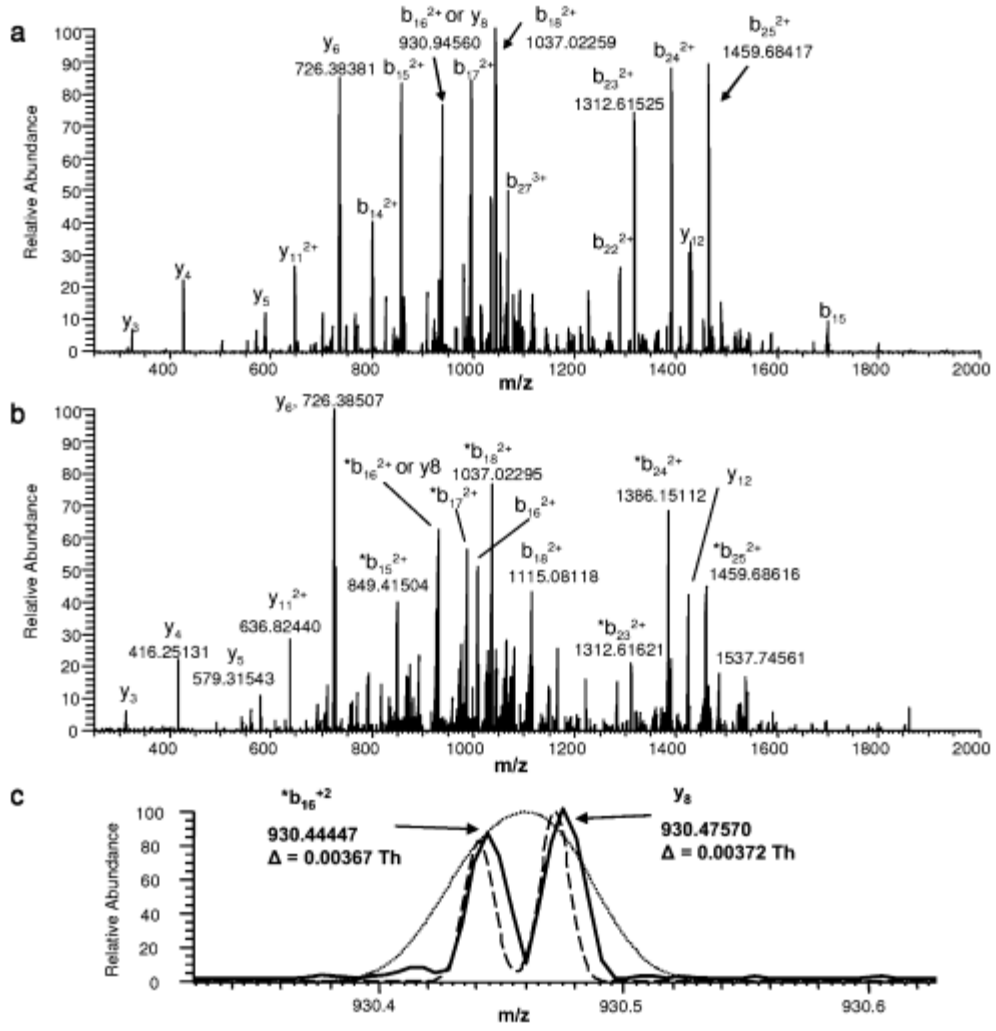

Figure 4. Collision-induced dissociation (CID) mass spectrum of oxidized insulin B chain un-modified **(a)** and modified with one HNE molecule. **(b)** Fragment ions representing neutral loss of the HNE modification were apparent (indicated by asterisks). An expanded *m/z* range of the CID product-ion spectrum **(c)** shows clear separation of the b_{16}^{2+} and y_8 monoisotopic peaks ($\Delta_{measured}$=0.03123 Th, $\Delta_{theoretical}$=0.03109 Th) by FTICR (*solid line*). Theoretical simulations of these two fragment ions are shown at mass resolving powers of 75,000 (*dashed line*) and 20,000 (*dotted line*), respectively

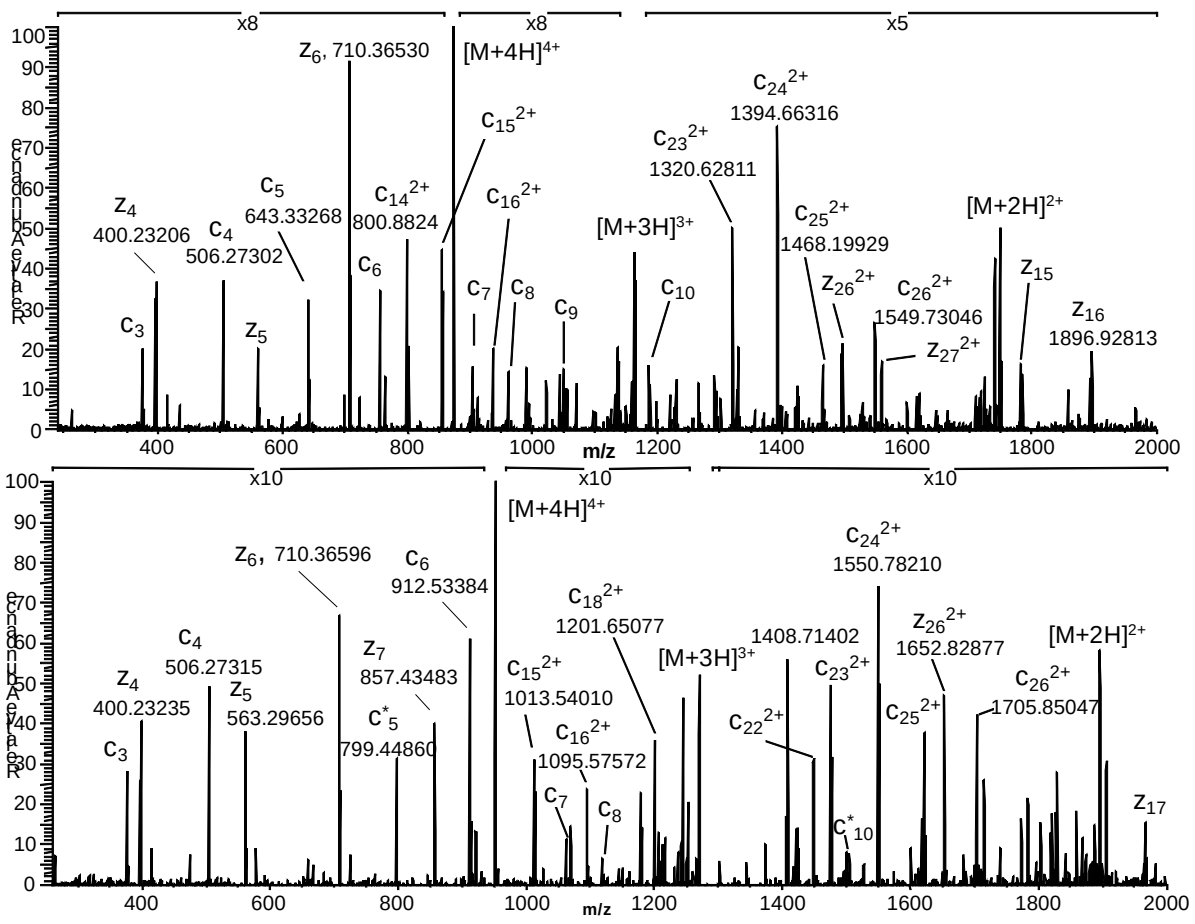

Figure 5. Electron capture dissociation (ECD) mass spectrum of oxidized insulin B chain, $[M+4H]^{4+}$ precursor ions, unmodified **(a)** and modified with two HNE molecules. **(b)** Retention of the HNE modification on the fragment ions allowed for definitive sequence and modification assignment as demonstrated by the increase in mass of 156 Da on the c_5 and c_{10} ions (indicated by $^{\#}$)

FVNQH$^{\#}$$_{(HNE)}LC_{SO3H}$GS H$^{\#}$$_{(HNE)}$LVEALYLVC$_{SO3H}$GERGFFYTPKA

Figure 6. Amino acid sequence of the oxidized insulin B chain with potential HNE-modification sites by Michael-type addition indicated by the *number sign* (#). (SO_3H denotes Cys oxidation)

CHAPTER III

IDENTIFICATION OF CARBONYLATION SITES IN APOMYOGLOBIN AFTER EXPOSURE TO 4-HYDROXY-2-NONENAL BY SOLID-PHASE ENRICHMENT AND LIQUID CHROMATOGRAPHY–ELECTROSPRAY IONIZATION TANDEM MASS SPECTROMETRY

Navin Rauniyar[¶], Katalin Prokai-Tatrai[¶§], and Laszlo Prokai[¶]

[¶]Department of Molecular Biology & Immunology and

[§]Department of Pharmacology & Neuroscience,

University of North Texas Health Science Center,

Fort Worth, Texas 76107

Published in: *J Mass Spectrom*. 2010, 45, 398-410

ABSTRACT

Identification of protein carbonylation because of covalent attachment of a lipid peroxidation end-product was performed by combining proteolytic digestion followed by solid-phase hydrazide enrichment and liquid chromatography (LC)–electrospray ionization (ESI) tandem mass spectrometry (MS/MS) using both collision-induced dissociation (CID) and electron capture dissociation (ECD). To evaluate this approach, we selected apomyoglobin and 4-hydroxy-2-nonenal (4-HNE) as a model protein and a representative end-product of lipid peroxidation, respectively. Although the characteristic elimination of 4-HNE (156 Da) in CID was found to serve as a signature tag for the modified peptides, generation of nearly complete fragment ion series because of efficient peptide backbone cleavage (in most cases over 75%) and the capability to retain the labile 4-HNE moiety of the tryptic peptides significantly aided the elucidation of primary structural information and assignment of exact carbonylation sites in the protein, when ECD was employed. We have concluded that solid-phase enrichment with both CID- and ECD-MS/MS are advantageous during an in-depth interrogation and unequivocal localization of 4-HNE-induced carbonylation of apomyoglobin that occurs via Michael addition to its histidine residues.

Keywords

4-Hydroxy-2-nonenal • Protein carbonylation • LC–MS/MS • Collision-induced dissociation • Electron capture dissociation • Solid-phase hydrazide chemistry

INTRODUCTION

4-Hydroxy-2-nonenal (4-HNE), an α,β-unsaturated hydroxyalkenal, is generated through the oxidation-induced β-cleavage of hydroperoxides derived from polyunsaturated fatty acids in response to oxidative stress and aging.[1,2] 4-HNE-related modifications to proteins have been implicated in the onset and/or progression of various neurodegenerative diseases because of the formation of covalent protein-4-HNE adducts that cause irreversible inactivation or degradation of cellular protein functions.[3–7] 4-HNE-induced modifications to proteins or peptides occur mainly on nucleophilic residues preferentially via Michael addition, in particular on the imidazole moiety of histidines (His, H), the sulfhydryl group of cysteines (Cys, C) and the ε-amino group of lysines (Lys, K), as shown in Fig. 1.[2,8,9]

Protein carbonyls can serve as useful biomarkers of degenerative diseases associated with oxidative stress, emphasizing the importance of identifying proteins (or, rather, peptide motifs) susceptible to attack by carbonyl modification. In addition, localization of carbonylation sites in proteins is fundamental to understand the mechanisms of 4-HNE-induced cytotoxicity at the molecular level. This information would allow us to recognize reactive centers in proteins, and relate protein structure to its function (e.g., loss of enzyme activity upon 4-HNE treatment), ultimately guiding drug design and discovery.[7] The determination of 4-HNE modification sites, in general, is far from trivial because no consensus sequence for the chemical selectivity of 4-HNE modification has been found. The initial challenge is to detect substoichiometric levels of 4-HNE-modified peptides amidst high background of non-modified peptides. A front-end enrichment of 4-HNE-modified peptides prior to mass spectrometric analysis usually mitigates the obstacles related to undersampling during data-dependent liquid chromatography–

electrospray ionization tandem mass spectrometry (LC–ESI-MS/MS) of complex mixtures because of broad dynamic range of concentrations and wide range of ESI efficiencies of peptides in complex proteolytic digests.[10] Various enrichment techniques for the selective isolation of carbonylated proteins and peptides have been developed.[11–16]

Another difficulty has been the localization of the sites of 4-HNE modifications by MS/MS. Collision-induced dissociation (CID) employed most commonly in the current practice of MS/MS is prone to yield predominant fragment ions corresponding to the neutral loss of 4-HNE in modified peptides, which may preclude identification of the primary sequence from the spectra.[17] A neutral loss-driven MS^3 method (MS/MS/MS), in which MS^3 is triggered upon encountering neutral loss corresponding to 4-HNE during MS/MS, has proved to be an efficient approach to circumvent this problem.[16,17] However, ambiguity of correct assignment of the 4-HNE modification site does remain even with this technique, when more than one candidate amino acid residue is present, because MS^3 is triggered on the neutral loss ion from the MS/MS spectrum. These caveats highlight the importance of developing methods that allow for not only the detection of 4-HNE-modified peptides, but also pinpoint the exact site(s) of the 4-HNE-modification(s).

Electron capture dissociation (ECD) is an alternative method of peptide-ion activation and fragmentation usually implemented on Fourier-transform (FT) ion cyclotron resonance (ICR) instruments.[18] During ECD fragmentation, multiply charged precursor ions are irradiated with low-energy electrons (<0.2 eV).[19] The capture of a thermal electron by a multiply protonated peptide/protein cation induces its backbone fragmentation at N–Cα bonds to produce c- and z-type fragment ions.[20] This method of peptide fragmentation offers several advantages over CID-based tandem mass spectrometric approaches. Among others, ECD lacks preference

for cleavage at any particular site(s) and this non-selectivity affords extensive sequence coverage assisting, thereby, the elucidation of the primary sequence. Consequently, the technique has been widely used for the characterization of various posttranslational modifications in peptides and proteins.[19–22] ECD occurs in the ICR cell and the *m*/*z* values of the resulting fragment ions are measured with high mass accuracy; therefore, the chances of false identifications are also minimized. Hence, ECD provides high confidence in structure assignment and permits the exact localization of amino acid modifications that are labile under CID conditions.[23] The implementation of electron-injection systems based on indirectly heated dispenser cathodes that provide higher electron fluxes, wider electron beams and better control of the electron energy[24] has decreased the electron irradiation time needed for ECD to the millisecond range. This improvement has enabled online LC–ECD-MS/MS for the characterization of proteins in complex biological matrices.[23–27]

In our study, we first demonstrated the impact of enriching carbonylated tryptic peptides for data-dependent LC–ESI-MS/MS to detect substoichiometric quantities of such modified peptides using apomyoglobin as a model protein. We then expanded our scope to examine the advantages of using both CID and ECD as complementary methods of ion dissociation, which was expected to enable an in-depth interrogation of 4-HNE-induced carbonylation in this protein.

EXPERIMENTAL

Materials

Apomyoglobin from equine skeletal muscle was purchased from Sigma-Aldrich (St Louis, MO, USA). 4-HNE was obtained from Cayman Chemical (Ann Arbor, MI, USA). Water,

acetonitrile and methanol were of high-performance liquid chromatography (HPLC) grade and purchased from Honeywell Burdick and Jackson (Morristown, NJ, USA). Trypsin and the endoproteinase Glu-C were obtained from Promega (Madison, WI, USA) and Roche Applied Science (Indianapolis, IN, USA), respectively. All other chemicals were obtained from Sigma-Aldrich.

Preparation of apomyoglobin-4-HNE adduct

Apomyoglobin (1 mg/ml) was incubated with 2 mM 4-HNE in phosphate buffer (50 mM, pH 7.4) at 37 °C for 2 h. Then, the protein was precipitated by adding 4 volumes of ice-cold acetone and keeping the mixture at −20 °C for 2h. The sample was centrifuged at 13 000 rpm for 10 min at 4 °C. The protein pellet was resuspended in 50 mM ammonium bicarbonate and subjected to proteolytic digestion at 37 °C for 18 h by adding 8 μg of trypsin or endoproteinase Glu-C (V8 Protease), respectively. Following digestion, proteolytic activity was terminated by acidifying the reaction mixture with acetic acid to pH <3.0.

Solid-phase hydrazide (SPH) enrichment of 4-HNE-modified peptides

For capturing the peptide carbonyls from the proteolytic digest of the 4-HNE-modified apomyoglobin, 5 μl of the digest was added into 100 μl of reaction buffer containing 0.2% (v/v) acetic acid, 10% (v/v) acetonitrile in 89.8% (v/v) water, (pH 3.6). Then, 6 mg of hydrazide on glass beads[16] were added and the resulting mixture was rotated end-over-end overnight at room temperature. After centrifugation to settle the beads, the supernatant was collected and saved for LC–ESI-MS/MS analysis. The beads were washed subsequently four times with reaction buffer followed by 1 M NaCl, distilled water, 80:20 (v/v) acetonitrile: water, and a second round of

distilled water (400 µl each) to remove the unmodified tryptic peptides. Then, the peptide carbonyls (captured as hydrazones) were released from the beads in their original forms (Fig. 2) with 200 µl of formic acid (10%, v/v) at 60 °C for 30 min. This step was repeated one more time and the solutions containing the peptide carbonyls were combined and lyophilized. The residue was reconstituted in 20 µl of loading solvent containing 0.1% (v/v) acetic acid and 5% (v/v) acetonitrile in 94.9% (v/v) water. Five microliter aliquots were used for LC–ESI-MS/MS analyses.

LC–ESI-MS/MS with CID or ECD

LC–ESI-MS/MS was performed on a hybrid linear ion trap-FTICR (7-Tesla) mass spectrometer (LTQ-FT, Thermo Finnigan, San Jose, CA, USA) equipped with a nano-electrospray ionization source and operated with the Xcalibur (version 2.2) and Tune Plus (version 2.2) data acquisition software. Online HPLC was performed with an Eksigent (Dublin, CA, USA) nano-LC-2D system using a 15 cm × 75 µm i.d. PepMap C18 column (LC Packings, Sunnyvale, CA, USA) as the analytical column. Mobile phases consisted of solvent A [0.1% (v/v) acetic acid and 99.9% (v/v) water] and solvent B [0.1% (v/v) acetic acid and 99.9% (v/v) acetonitrile]. Five microliter of the 4-HNE-modified apomyoglobin tryptic peptides were automatically loaded onto the IntegraFrit™ sample trap (2.5 cm × 75 µm i.d.) (New Objective, Woburn, MA, USA), for sample concentration and desalting, at a flow rate of 1.5 µl/min in a loading solvent of 0.1% (v/v) acetic acid and 5% (v/v) acetonitrile in 94.9% (v/v) water. Separations were performed using the following gradient program: (1) 5 min in 95.2% solvent A for equilibration; (2) linear gradient to 40% solvent B over 90 min and holding at 40% solvent B for isocratic elution for 5 min; (3) increasing in 5 min to 90% solvent B and maintaining for 5

min; and finally (4) 95.2% solvent A in the next 20 min. The flow rate through the column was 250 nl/min. Peptides eluted through a Picotip emitter (internal diameter 10±1 μm; New Objective) were directly supplied into the nano-electrospray source of the mass spectrometer.

For LC–CID-MS/MS, the data-dependent mode of acquisition was utilized in which an accurate *m*/*z* survey scan was performed in the FT-ICR cell followed by parallel MS/MS linear ion trap analysis of the top five most intense precursor ions. FT-ICR full-scan mass spectra were acquired at 100 000 mass resolving power (*m*/*z* 400) from *m*/*z* 350 to 1500 using the automatic gain control mode of ion trapping. CID was performed in the linear ion trap using a 3.0-Th isolation width and 35% normalized collision energy with helium as the collision gas. The precursor ion that had been selected for CID was dynamically excluded from further MS/MS analysis for 60 s.

For data-dependent LC–ECD-MS/MS, FT-ICR parameters were adapted from Cooper *et al*.[27,28] with certain modifications. Briefly, the instrument alternated between a full FT-MS survey scan (*m*/*z* 350–1500) and three subsequent ECD-MS/MS scans of the three most abundant precursor ions, in which isolation of the precursor ions by use of the linear ion trap was followed by ECD in the ICR cell. Survey scans were acquired in the ICR cell with a resolution of 50 000 at *m*/*z* 400. At a resolution setting of 50 000, the scan speed was about 2 scans/s. ECD spectra were collected with a resolution of 25 000 (at *m*/*z* 400). For ECD, the precursor ions were isolated in the linear ion trap with an isolation width of 4.0-Th and transferred to the ICR cell. Electrons were produced by an indirectly heated (with current typically around 1.1 A) barium–tungsten cylindrical dispenser cathode, and ions trapped in the ICR cell were irradiated for 120 ms at −5 V cathode potential. A minimum signal to noise (S/N) ratio of 500 was required before precursor ions were subjected to ECD. Singly charged ions and those with unassigned charge

states were disregarded. The precursor ion that has been selected for ECD fragmentation was dynamically excluded from further MS/MS analysis for 180 s.

The MS-Product module of ProteinProspector (http://prospector.ucsf.edu) was used to calculate the *m*/*z* values from the predicted tryptic peptides of apomyoglobin where His residues were replaced with 4-HNE-His Michael adducts (M + 156). The predicted *m*/*z* values were then compared with those measured for the precursor ions during full FT-ICR MS scan. Also, *m*/*z* of b- and y-type ions obtained during CID-MS/MS and *m*/*z* of c- and z-type fragment ions obtained during ECD-MS/MS of peptides were compared to the fragment ion masses generated by MS-Product. All mass spectra were manually searched for the presence of b- and y-, or c- and z-type product ions, respectively.

RESULTS AND DISCUSSIONS

SPH enrichment of apomyoglobin tryptic peptides carbonylated by 4-HNE

The ionization efficiency of posttranslationally modified peptides by ESI and matrix-assisted laser desorption/ionization (MALDI) is generally less than those of the regular, native peptides in a complex mixture.[29] For this reason, from the tryptic digest of 4-HNE-exposed apomyoglobin, peptides carbonyls were separated from the native tryptic peptides by solid-phase hydrazide (SPH) strategy and subsequently analyzed by nano-electrospray LC–CIDMS/MS and LC–ECD-MS/MS. The employed SPH reagent[16] captures only 4-HNE-carbonylated peptides (i.e., Michael adducts) by immobilizing them to the glass beads as hydrazones. Interfering unmodified peptides can, therefore, be removed. Then, the captured peptides can be released from the solid support by acid-catalyzed hydrolysis to the corresponding peptide carbonyls for

subsequent LC–ESI-MS/MS analyses, as shown in Fig. 2. The base-peak chromatogram and averaged full-scan mass spectrum of crude tryptic digest of apomyoglobin after its reaction with 4-HNE (i.e., carbonylated and unmodified tryptic peptides without employing SPH enrichment) acquired in the 30–100 min retention time range during LC–ESI-MS analysis is shown in Fig. 3 (symbols representing apomyoglobin tryptic peptides are given in Table S1 of the Supporting Information online). The mass spectrum shows ions mostly corresponding to unmodified peptides and only a few 4-HNE-modified tryptic peptides ($T_3^{\#}$, $T_{13}^{\#\#}$ and $T_{17}^{\#}$, where # indicates modification by the lipid peroxidation product by Michael addition, and multiple # signs denote multiple 4-HNE modifications within the given tryptic peptide). However, drastically different results were obtained after enrichment via SPH chemistry. As shown in Fig. 4, acid-catalyzed hydrolysis of the captured hydrazones ('eluate' fraction) and subsequent LC–ESI-MS analysis afforded detection of 4-HNEcarbonylated tryptic peptides that were not revealed by analysis without SPH enrichment. A complete list of unmodified and 4-HNE carbonylated apomyoglobin tryptic peptides observed without and with using SPH enrichment can be found in Table S2 of the Supporting Information online.

Except the unmodified peptide YLEFISDAIIHVLHSK (T_{16}, 103–118) present as a minor component and detected at *m*/*z* 472.01 and 629.01 as its triply and doubly charged precursor ions, no other unmodified peptides were seen in the eluate fraction. In addition, the supernatant fraction from the beads contained only the unmodified tryptic peptides (data not shown). Therefore, this strategy allowed for an efficient and selective enrichment of 4-HNEcarbonylated peptides, overcoming the issue with suppression of their ionization by native peptides. Also, the use of SPH strategy to enrich carbonylated species prior to mass spectrometric analysis is advantageous, when compared to direct immunoaffinity approaches. While the SPH method has

the potential to enrich carbonylated peptides modified by a wide array of lipid peroxidation end-products such as malondialdehyde, acrolein, 4-hydroxy-2-hexenal, etc., an immunoaffinity approach requires separate antibodies against each kind of carbonyl adducts. Derivatization of peptide carbonyls with, for example, 2,4-dinitrophenylhydrazine (DNPH) and, then, performing immunoaffinity-based enrichment with immobilized anti-dinitrophenyl antibodies may preclude the need for separate antibodies.[12] However, the derivatives form at low yields[12] and, in addition, they tend to lose the DNPH-tags with each processing step because of their instability according to our experience.

Localization of sites of 4-HNE carbonylation in apomyoglobin

In the hybrid instrument we employed for our study (LTQ-FT), CID-MS/MS was performed exclusively in the linear ion trap (LTQ), because measuring product-ion spectra by FT-ICR was not practical to perform data-dependent acquisition during online LC separation. Product-ion spectra of 4-HNE-modified peptides varied considerably upon using this method of ion dissociation, as exemplified in Fig. 5. For certain peptides, CID revealed extensive fragmentation of the peptide backbone that enabled localization of the site of 4-HNE modification in the peptide (Fig. 5(a)). However, fragmentation of several carbonylated apomyoglobin tryptic peptides resulted in the gas phase elimination of 4-HNE, and this neutral loss was often far more significant than the dissociation of the peptide backbone (Fig. 5(b)). In these cases, MS/MS spectra displayed strong ion signals because of the ejection of 4-HNE from the precursor ions and few or no sequence-specific fragment ions. Thus, we experienced difficulties in finding fragment ions informative of primary sequence and, hence, the direct deduction of sequence information and profiling of site(s) of modification were not possible. On

the other hand, CID-MS/MS of certain 4-HNE-modified peptides (Fig. 5(c)) provided some degree of information on their amino acid sequence and site of 4-HNE modification despite an apparently strong neutral loss of the covalently attached lipid peroxidation end-product. As examples selected for display in Fig. 5, 4-HNE-carbonylated apomyoglobin tryptic peptides that represented the three types of typical CID-MS/MS spectra were: (a) $H^{\#}$PGDFGADAQGAMTK, (b) LFTGH$^{\#}$PETLEK, and, (c) GH$^{\#}$HEAELKPLAQSH$^{\#}$ATK.

Figure 5(a) shows the CID-MS/MS spectrum and resulting fragmentation summary of the doubly charged 4-HNE-carbonylated peptide $T_{17}^{\#}$ ($H^{\#}$PGDFGADAQGAMTK, fragment 119–133, where $H^{\#}$ indicates 4-HNE Michael adduct on the His residue) at *m*/*z* 829.89. CID resulted in fragmentation of 10 of the 14 amide bonds in the peptide generating 71% peptide sequence coverage (Table 1). The spectrum displayed singly charged b and y fragment ions as well as some b-H_2O ions. The observed 4-HNE modified histidine immonium ion[30] at *m*/*z* 266, together with the 4-HNE neutral loss peak at *m/z* 751.8 (loss of 78 *m*/*z* from $[M+2H]^{2+}$ ion) serve as a diagnostic for the presence of $H^{\#}$ in the peptide. Also, the occurrence of the b_2 ion at *m/z* 391.2, and other b- and y-type ions retaining the 4-HNE group confirm Michael addition of 4-HNE to the N-terminal His of the tryptic peptide $T_{17}^{\#}$, corresponding to His-119 in apomyoglobin.

The CID fragmentation of doubly charged 4-HNE-modified peptide, LFTGH$^{\#}$PETLEK ($T_3^{\#}$, 32–42) at *m*/*z* 714.39 (Fig. 5(b)) produced a prominent signal of 4-HNE neutral loss at *m*/*z* 636.3 in the MS/MS spectrum. No appreciable backbone fragmentation is observed in the CID spectrum, which prevented the direct localization of 4-HNE adduct in the peptide. Nevertheless, His-36 may be regarded as the possible target amino acid of 4-HNE Michael addition because the peptide harbors no other candidate nucleophiles except His-36 and Lys-42. The observed

cleavage by trypsin at Lys-42 during digestion, however, precludes Lys-42 as the site of modification, because 4-HNE-modified lysine in a protein is refractory to proteolysis.

The CID-MS/MS spectrum of the triply protonated and bis-carbonylated apomyoglobin tryptic peptide $T_{13}^{\#\#}$, *m*/*z* 722.73, is shown in Fig. 5(c). The formation of this peptide is because of a blockade of efficient tryptic cleavage due to the presence of proline (Pro, P) after Lys-87.[31] Consequently, the corresponding tryptic peptide contains this mid-chain Lys in addition to the C-terminal Lys (Lys-96). The spectrum displayed 4-HNE neutral loss precursor ion peak and few b- and y-type fragment ion peaks, as well as neutral loss of 4-HNE from some of the y-ion species. The detection of b_2 ion at *m*/*z* 351.2 and y_9 ion at *m*/*z* 1108.6 indicates that the site of 4-HNE modifications could be at His-81 and His-93; however, the spectrum lacks sufficient number of fragment ions (by manifesting fragmentation efficiency of only about 25%) to corroborate these assignments unambiguously. A list of 4-HNE modification sites and fragmentation efficiencies of carbonylated apomyoglobin tryptic peptides revealed by the CID method are summarized in Table 1. The LC–CID-MS/MS method identified 11 tryptic peptides exhibiting Michael adducts of 4-HNE-induced covalent modification of apomyoglobin. For most peptides, a distinct fragmentation pathway with the neutral loss of 156 Da from the precursor and/or product ions was seen in CID of 4-HNE-containing peptides.

Upon CID-induced fragmentation of 4-HNE-modified peptides, the loss of 156 Da often confirms the presence of a covalent adduct with this lipid peroxidation product.[16,17] CID, however, may produce incomplete cleavage of the peptide backbone; thus, it frequently poses difficulty to derive information on the primary structure of a peptide,[32] and the location of 4-HNE can be assigned only if there is a single possible modification site. In addition, CID

cleavage of peptide bond is influenced by the flanking amino acid residues that cumulatively determine the intensities observed in product-ion spectra.[33] Therefore, the high sequence coverage and ability to retain posttranslational modifications upon ECD were utilized to unambiguously localize 4-HNE-induced carbonylation.

By employing data-dependent LC–ECD-MS/MS combined with SPH enrichment, several 4-HNE-modified tryptic peptides were successfully identified. Because neighboring amino acids have little influence on backbone cleavage upon ECD except at the N-terminal proline (Pro, P),[34] extensive sets of sequence ions were generally observed because of the cleavage of the N–Cα bonds of the peptide backbone. Triply charged precursor ions were chosen, which afforded improved sequence coverage compared to doubly charged ions upon performing ECD.[28,35] In general, fragmentation efficiency in ECD improves with increasing charge state.[36,37]

The ECD-MS/MS of representative 4-HNE-modified tryptic peptides of apomyoglobin (identical to those for which CIDMS/MS spectra were displayed in Fig. 5(a–c)) are shown in Figs 6–8. Figure 6 illustrates the ECD-MS/MS spectrum and resulting fragmentation summary for the triply charged ion H$^{\#}$PGDFGADAQGAMTK ($T_{17}^{\#}$, 119–133) at m/z 553.60. The ECD fragmentation resulted in the cleavage of 11 out of 14 (11 out of 13, when adjusted for Pro) N–Cα bonds in the peptide, all of which were contiguous and provided 85% peptide sequence coverage (Table 1). The predominant fragment ions resulting from single backbone cleavages are c (c_2–c_{12}) and z (z_3–z_7, z_9) ion series. This is a reliable sequence tag and the product ions afforded the localization of the site of 4-HNE addition to His-119 of apomyoglobin. Information supplied by ECD-MS/MS for H$^{\#}$PGDFGADAQGAMTK (Fig. 6) served as complementary and additional to that of CID-MS/MS (Fig. 5(a)), because the latter also permitted the unequivocal localization of the modification site.

The ECD-MS/MS spectrum obtained from the triply protonated, 4-HNE-modified parent ion LFTGH$^{\#}$PETLEK ($T_3^{\#}$, 32–42) at *m*/*z* 470.60 is shown in Fig. 7. In contrast to cleavage of 2 out of 10 peptide (CO–NH) bonds giving fragmentation efficiency of 20% during LC–CID-MS/MS, 8 out of 10 (8 out of 9, when adjusted for Pro^{34})N–Cα bonds were cleaved during ECD; thus, fragmentation efficiency of 90% was obtained (c_2, c_4, c_6–c_{10} and z_1–z_3, z_5, z_7, z_9 and z_{10}). Because the fragmentation did not involve the loss of 4-HNE, a direct assignment of 4-HNE modification site to His-36 was possible from the collected ECD-MS/MS spectrum (Fig. 7). This site of protein carbonylation was, on the other hand, not revealed by the CID-MS/MS spectrum (Fig. 5(b)).

By using the CID method of peptide fragmentation, neutral loss of 4-HNE from precursor and/or product ions and the lack of sufficient product ions can cause ambiguity in the assignment of 4-HNE modification sites, especially when analyzing multiple carbonylated peptides. The greater peptide coverage and retention of posttranslational modifications on backbone fragments have been valuable features of ECD, when more than one putative modification sites exist.[21] The ECD-MS/MS spectrum of triply protonated and bis-carbonylated precursor peptide $T_{13}^{\#\#}$ (fragment 80–96) at *m*/*z* 722.73 is shown in Fig. 8. The extensive and complementary series of N-terminal and C-terminal peptide fragment ions generated upon ECD-based fragmentation enabled nearly complete sequencing of this 4-HNE-modified peptide. The shift in 156 Da following c_2 (*m*/*z* 368.23) and z_4 (*m*/*z* 596.35), and 312 Da following c_{14}^{2+} (*m*/*z* 933.51) and z_{16}^{2+} (*m*/*z* 1048.58) confirmed the presence of 4-HNE at His-81 and His-93, respectively. In the same MS/MS spectrum, c_3^* (*m*/*z* 661.40) product ion corresponded to the modification of His-81 and His-82 with 4-HNE, indicating the presence of the isomeric coeluting peptide GH$^{\#}$H$^{\#}$EAELKPLAQSHATK because of Michael addition of the lipid peroxidation end-product

at His-81 and His-82 in apomyoglobin. Moreover, a z_{15}^{2+} fragment ion at *m*/*z* 979.04 pointed to another coeluting isomer GHH$^{\#}$EAELKPLAQSH$^{\#}$ATK modified at His-82 and His-93. Ultimately, based on the fragment ions observed in Fig. 8, formation of three different combinations of carbonylation at two His residues (His-81 and His-93; His-81 and His-82; and His-82 and His-93) in the modified apomyoglobin tryptic peptide $T_{13}^{\#\#}$ could be assigned. However, when the intensities of the fragment ions in the ESI-MS/MS spectrum were compared, His-81 and His-93 appeared to be the preferred sites of carbonylation. The CID fragmentation of the same species showed 25% peptide coverage with 4 out of 16 peptide bonds cleaved (Table 1) and, also, the CID-MS/MS spectrum (Fig. 5(c)) was unable to reveal the presence of the other two bis-modified isomers (a peptide showing carbonylation of His-81 and His-82, as well as another one with attachment of 4-HNE to His-82 and His-93 of the protein). This finding has underscored the importance of ECD analysis for the detailed interrogation of the site of 4-HNE modifications in a peptide. Altogether, the ECD-based approach was able to resolve even a heterogeneous MS/MS spectrum by providing identification of fragment ions from isomeric peptides with the same primary sequence but different localizations of 4-HNE attachment.

ECD-MS/MS spectra of additional 4-HNE-modified tryptic peptides are shown in Figs S1–S3 in the Supporting Information online. ECD of the $[M+3H]^{3+}$ ion of VEADIAGH$^{\#}$GQEVLIR ($T_2^{\#}$, 17–31; Fig. S1) at *m*/*z* 588.32 resulted in the cleavage of 13 of the 14 backbone N–Cα bonds in the peptide providing almost complete (93%, Table 1) peptide sequence coverage (c_4, c_5, c_7–c_{14} and z_1 through z_{13}). The complete retention of the 4-HNE moiety on all product ions containing the modified His residue was observed and all fragment ions that contain His residue exhibited a +156 Da mass shift relative to the native peptide. The fragment ions c_8 (*m*/*z* 966.52) and z_8 (*m*/*z* 1091.62) confirmed the Michael addition of 4-HNE to

His in VEADIAGH$^{\#}$GQEVLIR (corresponding to His-24 in the protein). The ECD-induced dissociation of a triply protonated, mono-4-HNE modified tryptic peptide H$^{\#}$GTVVLTALGGILK ($T_{10}^{\#}$, 64–77; Fig. S2) resulted in the cleavage of 11 out of 13 N–Cα bonds. This fragmentation efficiency of 85% with plentitude of c- and z-type product ions and, because the series of c ions all had masses 156 Da higher than those of the native peptide, the localization of 4-HNE residue at His-64 could be done unequivocally. We note, however, that the CID-MS/MS spectrum of the same species (data not shown) revealed 12 of 13 peptide bonds cleaved, leading to 92% peptide coverage.

The ECD-MS/MS spectrum of 4-HNE-modified peptides at *m*/*z* 555.02, a triply charged $[M+3H]^{3+}$ arising from the missed cleavage at Lys either at N- or C-terminus of $T_{10}^{\#}$ is shown in Fig. S3 in the Supporting Information online. The resulting tryptic peptides H$^{\#}$GTVVLTALGGILKK (T_9 –$T_{10}^{\#}$, 64–78) and KH$^{\#}$GTVVLTALGGILK (T_{10} –$T_{11}^{\#}$, 63–77) were coeluting isomers; thus, they were trapped together in the ICR cell for ECD. Hence, the spectrum was complicated by product ions obtained from dissociation of both peptides. None of the 4-HNE-containing product ions was accompanied by the loss of 4-HNE (−156 Da). The product ions, c_2 at *m*/*z* 368.23 from H$^{\#}$GTVVLTALGGILKK and c_3^* at *m*/*z* 496.32 from KH$^{\#}$GTVVLTALGGILK, featured 4-HNE modification at His-64.

His-97 was also confirmed as another site of 4-HNE attachment, because H$^{\#}$KIPIK (T_{14}–$T_{15}^{\#}$, 97–102) could be identified by CID-MS/MS of its $[M+2H]^{2+}$ ion. However, the ECD of this carbonylated tryptic peptide did not yield good-quality MS/MS spectra (data not shown). ECD has been shown to require at least triply charged precursor ions (z = 3) to generate adequate sequence coverage for, e.g., phosphorylated peptides.[28] Hence, we also performed Glu-C digestion of 4-HNE-modified apomyoglobin to obtain longer proteolytic fragments within which

we could interrogate carbonylation in the region covered by the T_{14}–T_{15} (97–102) tryptic peptide of the protein. The obtained Glu-C peptide fragment [LKPLAQSHATKHKIPIKYLE]$^{\#}$ (86–105) contained several basic amino acid residues and was large enough to afford precursor ions with z ≥ 3 to yield good-quality ECD-MS/MS spectra (Fig. S4 in the Supporting Information online). The spectrum and resulting fragmentation summary for the $[M+4H]^{4+}$ (z= 4) precursor ion of this mono-carbonylated peptide ion arising from Glu-C cleavage indicated the presence of two isomeric peptides with 4-HNE modification at His-93 or His-97. Therefore, these carbonylated species apparently coeluted during LC-MS/MS analysis resulting in the generation of product ions from both isomeric peptides in the ECD-MS/MS spectrum. Nevertheless, the use of Glu-C afforded the identification of sites of 4-HNE modification to His-93 and His-97 by LC–ECD-MS/MS. The corresponding CID-MS/MS spectrum, on the other hand, lacked fragment ions discerning the mono-carbonylated isomers of 4-HNE-modified LKPLAQSHATKHKIPIKYLE (data not shown).

The data-dependent acquisition did not supply ECD-MS/MS spectra for mono- or bis-carbonylated isomers of YLEFISDAIIHVLHSK during the online chromatographic separation. This could be because, even though the ECD method of peptide fragmentation had an advantage of providing high peptide sequence coverage and unambiguous localization of modifications, the longer analysis time associated with ECD compared to CID typically resulted in the selection of fewer peptides to fragment in a data-dependent LC–MS/MS analysis.[38] In particular, multiply charged peptides of lower intensity would escape selection for ECD with this mode of data acquisition.[38]

Table 1 summarizes ECD *versus* CID fragmentation efficiencies of 4-HNE-carbonylated apomyoglobin tryptic peptides we identified. With data-dependent LC–ECD-MS/MS, we

identified eight tryptic peptides carrying 4-HNE Michael adducts. ECD cleaved more bonds in respective peptides than CID; nevertheless, data-dependent LC–CID-MS/MS was able to detect peptides that were missed by data-dependent LC–ECD-MS/MS. On the other hand, ECD-MS/MS spectra readily allowed identification of fragment ions that are distinct in each peptide and, hence, facilitated identification of peptide sequences and sites of 4-HNE modifications as well. Also, ECD readily identified two mono-, three bis- and a tris-carbonylated isomers of the tryptic peptide GHHEAELKPLAQSHATK and two mono-carbonylated isomers of the Glu-C peptide LKPLAQSHATKHKIPIKYLE of apomyoglobin. Some of these isomers (Table 1) were not apparent upon employing CID either because of poor fragmentation and, hence, lack of fragment ions discerning the isomers, or because of the tendency to lose 4-HNE group from the fragment ions. In addition, ECD is usually available on FT-ICR instruments; thus, the higher measured mass accuracy and resolution obtained through such mass spectrometers provide specificity that greatly facilitates correct identification of the peptide sequence[39–41] and precise annotation of modifications.[42] In our study, mass measurement accuracy was <10 ppm.

We identified several His modifications in apomyoglobin. His residues in proteins have been reported to be major targets for 4-HNE carbonylation via formation of Michael adducts on the imidazole ring of His.[8,30] It has been established that >99% of 4-HNE-related protein modification occurs via Michael addition.[43] By using SPH-based enrichment combined with data-dependent LC–MS/MS of proteolytic digests, we found that apomyoglobin treated with 4-HNE resulted in the carbonylation by Michael addition to His-24, His-36, His-64, His-81, His-82, His-93, His-97, His-113, His-116 and His-119, representing 10 out of the 11 His residues in the protein. Table 1 summarizes the 4-HNE-modified apomyoglobin tryptic peptides identified by CID-MS/MS and ECD-MS/MS in our study. Our work described here demonstrated the value

of combined CID- and ECD-based MS/MS approaches to study posttranslation modification of protein by lipid peroxidation end-product such as 4-HNE. While CID may have the tendency to eject 4-HNE from the modified peptides often with predominance that prevents adequate breakdown of the peptide backbone to permit sequence identification, the accompanying neutral loss (M-156) provides valuable information regarding the occurrence of this modification. On the other hand, ECD-MS/MS of the 4-HNE-modified peptides gives conclusive data concerning Michael addition of the lipid peroxidation end-product to specific amino acids, because this labile side-chain modification remains intact during the fragmentation process.

We did not observe 4-HNE Michael adducts of Lys, in addition to the predominant His modifications identified, in apomyoglobin that has no Cys residue (another target for 4-HNE modification[6]) in its sequence. This might have been because of the instability of Michael adducts on the Lys residues.[9] In addition, SPH enrichment is amenable for isolating only carbonyl modifications by Michael addition type; hence, dehydrated Michael adducts of His[44] or Schiff-bases cannot be enriched using this method. On the other hand, a method that enables the detection of Schiff-base adducts of 4-HNE to peptides by higher-order MS/MS has been reported recently.[45]

Even though the advantage of ECD in providing rich series of N-terminal c ions and C-terminal z ions generating extensive sequence coverage and the ability to retain modifying groups in the fragment ions is appreciable, ECD efficiency (the sum of the total product ion abundances divided by the precursor ion abundance obtained) is usually ≤30%.[46] Therefore, ECD and CID are complementary methods and the implementation of both will definitely furnish a wealth of information that neither one can provide alone.[47,48] Several beneficial features of CID and ECD make these methods of ion dissociation unique in their own way.[48] More

recently, electron transfer dissociation (ETD) has been developed to induce fragmentation of the peptide backbone along pathways that are analogous to those observed in ECD. In ETD, a combination of gas-phase ion/ion chemistry and MS/MS is employed in which singly charged radical anions transfer an electron to multiply protonated peptides.[49,50] Like with ECD, successful applications of ETD have been demonstrated in analysis of posttranslational modifications.[51] Therefore, our observations regarding ECD-induced fragmentation of 4-HNEmodified peptides are likely to be valid to ETD as well.

CONCLUSION

Our study has demonstrated the advantage of enrichment before LC–MS/MS analysis to detect 4-HNE-induced carbonylation of proteins by the 'bottom-up' approach. In addition, we have shown the benefits of complementary methods of ion dissociation to determine the chemical nature and sites of protein modification by this highly reactive end-product of lipid peroxidation. While the characteristic loss of 4-HNE (156 Da) upon CID was found to serve as a signature tag for the presence of 4-HNE in peptides, a preferred ejection of the neutral species often precluded the formation of sequence ions permitting the localization of the modification site(s). The application of ECD enabled, on the other hand, the unambiguous localization of 4-HNE additions to His residues of the model protein apomyoglobin. ECD fragment ion spectra were also simpler to interpret than MS/MS spectra obtained by CID, because of the presence of extensive singly charged fragment ion series and the absence of neutral loss products. In addition to using the conventional CID, our results have also shown the advantage of incorporating ECD

into data-dependent LC–MS/MS strategies to facilitate an in-depth interrogation of 4-HNE-induced protein carbonylation.

Future work aims at the implementation of the described approach for characterization of 4-HNE and other carbonyl modifications in proteins extracted from various complex matrices such as cells and tissues, which may lead to the identification of new biomarkers of oxidative stress. Since limits of detection are of paramount importance, this endeavor should preferably include prior enrichment of modified peptides, such as the SPH chemistry we employed, to reduce sample complexity, compensate for the low stoichiometric ratios of 4-HNE-modified peptides to unmodified peptides after proteolytic digestion, and/or to minimize ion suppression during LC–ESI-MS analysis.

ACKNOWLEDGEMENTS

We thank Dr Stanley M. Stevens, Jr., for the expert assistance in ECD and helpful discussions. This research has been supported by the grant AG025384 from the National Institutes of Health and a joint intramural grant from the UNT and UNTHSC. Laszlo Prokai is the Robert A. Welch Professor at the University of North Texas Health Science Center (endowment BK-0031).

REFERENCES

1. Esterbauer, H., Schaur, R. J., and Zollner, H. (1991) *Chemistry and biochemistry of 4-hydroxynonenal, malonaldehyde and related aldehydes.* Free Radic. Biol. Med. 11, 81-128

2. Uchida, K. (2003) 4-*Hydroxy-2-nonenal: a product and mediator of oxidative stress.* Prog. Lipid Res. 42, 318-343

3. Zarkovic, K. (2003) *4-Hydroxynonenal and neurodegenerative diseases*. Mol. Aspects Med. 24, 293-303.

4. Lopachin, R. M., Gavin, T., and Barber, D. S. (2008) *Type-2 alkenes mediate synaptotoxicity in neurodegenerative diseases.* Neurotoxicology 29, 871-882

5. Negre-Salvayre, A., Coatrieux, C., Ingueneau, C., and Salvayre, R. (2008) *Advanced lipid peroxidation end products in oxidative damage to proteins. potential role in diseases and therapeutic prospects for the inhibitors.* Br. J. Pharmacol. 153, 6-20

6. Carini, M., Aldini, G., and Facino, R. M. (2004) *Mass spectrometry for detection of 4-hydroxy-trans-2-nonenal (HNE) adducts with peptides and proteins.* Mass Spectrom. Rev. 23, 281-305

7. Aldini, G., Dalle-Donne, I., Facino, R. M., Milzani, A., and Carini, M. (2007) *Intervention strategies to inhibit protein carbonylation by lipoxidation-derived reactive carbonyls.* Med. Res. Rev. 27, 817-868

8. Uchida, K. and Stadtman, E. R. (1992) *Modification of histidine residues in proteins by reaction with 4-hydroxynonenal.* Proc. Natl. Acad. Sci. U. S. A. 89, 4544-4548

9. Nadkarni, D. V. and Sayre, L. M. (1995) *Structural definition of early lysine and histidine adduction chemistry of 4-hydroxynonenal.* Chem. Res. Toxicol. 8, 284-291

10. Garza, S. and Moini, M. (2006) *Analysis of complex protein mixtures with improved sequence coverage using (CE-MS/MS)^n*. Anal. Chem. *78*, 7309-7316

11. Carbone, D. L., Doorn, J. A., Kiebler, Z., Ickes, B. R., and Petersen, D. R. (2005) *Modification of heat shock protein 90 by 4-hydroxynonenal in a rat model of chronic alcoholic liver disease.* J. Pharmacol. Exp. Ther. 315, 8-15

12. Fenaille, F., Tabet, J. C., and Guy, P. A. (2002) *Immunoaffinity purification and characterization of 4-hydroxy-2-nonenal- and malondialdehyde-modified peptides by electrospray ionization tandem mass spectrometry.* Anal. Chem. 74, 6298-6304

13. Mirzaei, H. and Regnier, F. (2005) *Affinity chromatographic selection of carbonylated proteins followed by identification of oxidation sites using tandem mass spectrometry.* Anal. Chem. 77, 2386-2392

14. Mirzaei, H. and Regnier, F. (2006) *Enrichment of carbonylated peptides using girard P reagent and strong cation exchange chromatography.* Anal. Chem. 78, 770-778

15. Chavez, J., Wu, J., Han, B., Chung, W. G., and Maier, C. S. (2006) *New role for an old probe: Affinity labeling of oxylipid protein conjugates by N'-aminooxymethylcarbonylhydrazino d-biotin.* Anal. Chem. 78, 6847-6854

16. Roe, M. R., Xie, H., Bandhakavi, S., and Griffin, T. J. (2007) *Proteomic mapping of 4-hydroxynonenal protein modification sites by solid-phase hydrazide chemistry and mass spectrometry.* Anal. Chem. 79, 3747-3756

17. Stevens, S. M.,Jr, Rauniyar, N., and Prokai, L. (2007) *Rapid characterization of covalent modifications to rat brain mitochondrial proteins after ex vivo exposure to 4-hydroxy-2-nonenal by liquid chromatography-tandem mass spectrometry using data-dependent and neutral loss-driven MS(3) acquisition.* J. Mass Spectrom. 42, 1599-1605

18. Zubarev, R. A., Kelleher, N. L., and McLafferty, F. W. (1998) *Electron capture dissociation of multiply charged protein cations. A nonergodic process*. J. A. Chem. Soc. 120, 3265-3266

19. Cooper, H. J., Hakansson, K., and Marshall, A. G. (2005) *The role of electron capture dissociation in biomolecular analysis.* Mass Spectrom. Rev. 24, 201-222

20. Zubarev, R. A. (2004) *Electron-capture dissociation tandem mass spectrometry.* Curr. Opin. Biotechnol. 15, 12-16

21. Bakhtiar, R. and Guan, Z. (2006) *Electron capture dissociation mass spectrometry in characterization of peptides and proteins.* Biotechnol. Lett. 28, 1047-1059

22. Rauniyar, N., Stevens, S. M. Jr., and Prokai, L. (2007) *Fourier transform ion cyclotron resonance mass spectrometry of covalent adducts of proteins and 4-hydroxy-2-nonenal, a reactive end-product of lipid peroxidation*. Anal. Bioanal. Chem. 389, 1421-1428

23. Tsybin, Y. O., Ramstrom, M., Witt, M., Baykut, G., and Hakansson, P. (2004) *Peptide and protein characterization by high-rate electron capture dissociation fourier transform ion cyclotron resonance mass spectrometry.* J. Mass Spectrom. 39, 719-729

24. Ramstrom, M., Hagman, C., Tsybin, Y. O., Markides, K. E., Hakansson, P., Salehi, A., Lundquist, I., Hakanson, R., and Bergquist, J. (2003) *A novel mass spectrometric approach to the analysis of hormonal peptides in extracts of mouse pancreatic islets.* Eur. J. Biochem. 270, 3146-3152

25. Palmblad, M., Tsybin, Y. O., Ramstrom, M., Bergquist, J., and Hakansson, P. (2002) *Liquid chromatography and electron-capture dissociation in fourier transform ion cyclotron resonance mass spectrometry.* Rapid Commun. Mass Spectrom. 16, 988-992

26. Davidson, W. and Frego, L. (2002) *Micro-high-performance liquid chromatography/Fourier transform mass spectrometry with electron-capture dissociation for the analysis of protein enzymatic digests.* Rapid Commun. Mass Spectrom. 16, 993-998

27. Cooper, H. J., Akbarzadeh, S., Heath, J. K., and Zeller, M. (2005) *Data-dependent electron capture dissociation FT-ICR mass spectrometry for proteomic analyses.* J. Proteome Res. 4, 1538-1544

28. Creese, A. J. and Cooper, H. J. (2008) *The effect of phosphorylation on the electron capture dissociation of peptide ions.* J. Am. Soc. Mass Spectrom. 19, 1263-1274

29. Stensballe, A., Jensen, O. N., Olsen, J. V., Haselmann, K. F., and Zubarev, R. A. (2000) *Electron capture dissociation of singly and multiply phosphorylated peptides.* Rapid Commun. Mass Spectrom. 14, 1793-1800

30. Bolgar, M. S. and Gaskell, S. J. (1996) *Determination of the sites of 4-hydroxy-2-nonenal adduction to protein by electrospray tandem mass spectrometry*. Anal. Chem. 68, 2325-2330

31. Barret, A. J., Rawlings, N. D., and Woessner, J. F. (2004) *Trypsin*. Handbook of Proteolytic Enzymes. Elsevier Academic Press: San Diego, CA , p. 1483.

32. Savitski, M. M., Nielsen, M. L., Kjeldsen, F., and Zubarev, R. A. (2005) *Proteomics-grade de novo sequencing approach.* J. Proteome Res. 4, 2348-2354

33. Tabb, D. L., Friedman, D. B., and Ham, A. J. (2006) *Verification of automated peptide identifications from proteomic tandem mass spectra.* Nat. Protoc. 1, 2213-2222

34. Cooper HJ, Hudgins RR, Hakansson K, Marshall AG. Secondary fragmentation of linear peptides in electron capture dissociation. *International Journal of Mass Spectrometry* **2003**, *228*, 723-728

35. Rauniyar, N., Stevens, S. M., Prokai-Tatrai, K., and Prokai, L. (2009) *Characterization of 4-hydroxy-2-nonenal-modified peptides by liquid chromatography-tandem mass spectrometry using data-dependent acquisition: Neutral loss-driven MS3 versus neutral loss-driven electron capture dissociation.* Anal. Chem. 81, 782-789

36. Zubarev, R. A., Horn, D. M., Fridriksson, E. K., Kelleher, N. L., Kruger, N. A., Lewis, M. A., Carpenter, B. K., and McLafferty, F. W. (2000) *Electron capture dissociation for structural characterization of multiply charged protein cations.* Anal. Chem. 72, 563-573

37. Iavarone, A. T., Paech, K., and Williams, E. R. (2004) *Effects of charge state and cationizing agent on the electron capture dissociation of a peptide.* Anal. Chem. 76, 2231-2238

38. Creese, A. J. and Cooper, H. J. (2007) *Liquid chromatography electron capture dissociation tandem mass spectrometry (LC-ECD-MS/MS) versus liquid chromatography collision-induced dissociation tandem mass spectrometry (LC-CID-MS/MS) for the identification of proteins.* J. Am. Soc. Mass Spectrom. 18, 891-897

39. Zubarev, R. A., Hakansson, P., and Sundqvist, B. (1996) *Accuracy requirements for peptide characterization by monoisotopic molecular mass measurements.* Anal. Chem. *68*, 4060-4063

40. Wu, S., Kaiser, N. K., Meng, D., Anderson, G. A., Zhang, K., and Bruce, J. E. (2005) *Increased protein identification capabilities through novel tandem MS calibration strategies.* J. Proteome Res. 4, 1434-1441

41. Scherl, A., Shaffer, S. A., Taylor, G. K., Hernandez, P., Appel, R. D., Binz, P. A., and Goodlett, D. R. (2008) *On the benefits of acquiring peptide fragment ions at high measured mass accuracy.* J. Am. Soc. Mass Spectrom. 19, 891-901

42. Wisniewski, J. R., Zougman, A., Kruger, S., and Mann, M. (2007) *Mass spectrometric mapping of linker histone H1 variants reveals multiple acetylations, methylations, and*

phosphorylation as well as differences between cell culture and tissue. Mol. Cell. Proteomics 6, 72-87

43. Bruenner, B. A., Jones, A. D., and German, J. B. (1995) *Direct characterization of protein adducts of the lipid peroxidation product 4-hydroxy-2-nonenal using electrospray mass spectrometry.* Chem. Res. Toxicol. 8, 552-559

44. Liu, Z., Minkler, P. E., and Sayre, L. M. (2003) *Mass spectroscopic characterization of protein modification by 4-hydroxy-2-(E)-nonenal and 4-oxo-2-(E)-nonenal.* Chem. Res. Toxicol. 16, 901-911

45. Rauniyar, N. and Prokai, L. (2009) *Detection and identification of 4-hydroxy-2-nonenal Schiffbase adducts along with products of Michael addition using data-dependent neutral loss-driven MS3 acquisition: method evaluation through an in vitro study on cytochrome c oxidase modifications.* Proteomics *9*, 5188-5193

46. Gorshkov, M. V., Masselon, C. D., Nikolaev, E. N., Udseth, H. R., Pasa-Tolic, L., and Smith, R. D. (2004) *Considerations for electron capture dissociation efficiency in FTICR mass spectrometry.* Int. J. of Mass Spectrom. 234, 131-136

47. Nielsen, M. L., Savitski, M. M., and Zubarev, R. A. (2005) *Improving protein identification using complementary fragmentation techniques in fourier transform mass spectrometry.* Mol. Cell. Proteomics 4, 835-845

48. Zubarev, R. A., Zubarev, A. R., and Savitski, M. M. (2008) *Electron Capture/Transfer versus collisionally Activated/Induced dissociations: Solo or duet?* J. Am. Soc. Mass Spectrom. 19, 753-761

49. Syka, J. E., Coon, J. J., Schroeder, M. J., Shabanowitz, J., and Hunt, D. F. (2004) *Peptide and protein sequence analysis by electron transfer dissociation mass spectrometry.* Proc. Natl. Acad. Sci. USA 101, 9528-9533

50. Han, H., Xia, Y., Yang, M., and McLuckey, S. A. (2008) *Rapidly alternating transmission mode electron-transfer dissociation and collisional activation for the characterization of polypeptide ions*. Anal. Chem. 80*,* 3492-3497

51. Wiesner, J., Premsler, T., and Sickmann, A. (2008) *Application of electron transfer dissociation (ETD) for the analysis of posttranslational modifications*. Proteomics 8*,* 4466-4483

Table 1. Identification of 4-HNE-modification site(s) by ECD and CID after SPH enrichment and LC–ESI-MS/MS.

Tryptic peptide	Positions	Peptide sequence[a]	ECD			CID		
			Charge state	Sequence tags (N–C_α bonds cleaved)[b]	Sequence %	Charge state	Sequence tags (peptide bonds cleaved)[b]	Sequence %
T_2	17-31	VEADIAGH$^{\#}$GQEVLIR	3	13/14	93	2	8/14	57
T_3	32-42	LFTGH$^{\#}$PETLEK	3	8/9[d]	89	2	2/10	20
T_{10}	64-77	H$^{\#}$GTVVLTALGGILK	3	11/13	85	2	12/13	92
T_9-T_{10}	63-77	KH$^{\#}$GTVVLTALGGILK	3	9/14	64	2	6/14	43
T_{10}-T_{11}	64-78	H$^{\#}$GTVVLTALGGILKK	3	14/14	100	2	11/14	79
T_9-T_{11}	63-78	KH$^{\#}$GTVVLTALGGILKK	4	15/15	100	3	9/15	60
T_{13}	80-96	GH$^{\#}$H$^{\#}$EAELKPLAQSH$^{\#}$ATK	4	12/15[d]	80	3	4/16	25
T_{13}	80-96	GH$^{\#}$HEAELKPLAQSH$^{\#}$ATK	3	15/15[d]	100	3	4/16	25
T_{13}	80-96	GH$^{\#}$H$^{\#}$EAELKPLAQSHATK	3	12/15[d]	80	-	N.A.	-
T_{13}	80-96	GHH$^{\#}$EAELKPLAQSH$^{\#}$ATK	3	15/15[d]	100	-	N.A.	-
T_{13}	80-96	GH$^{\#}$HEAELKPLAQSHATK	3	12/15[d]	80	3	8/16	50

T_{13}	80-96	GHHEAELKPLAQSH$^{\#}$ATK	3	14/15[d]	93	3	6/16	38
T_{12}-T_{11}	79-96	KGH$^{\#}$HEAELKPLAQSH$^{\#}$ATK	-	N.A.	-	3	3/17	18
T_{14}-T_{15}	97-102	H$^{\#}$KIPIK	-	N.A.	-	2	5/5	100
T_{16}	103-118	YLEFISDAIIH$^{\#}$VLH$^{\#}$SK	-	N.A.	-	3	4/15	27
T_{16}	103-118	[YLEFISDAIIHVLHSK]$^{\#}$[c]	-	N.A.	-	3	6/15	40
T_{17}	119-133	H$^{\#}$PGDFGADAQGAMTK	3	11/13[d]	85	2	10/14	71
G_{11}[e]	86-105	LKPLAQSH$^{\#}$ATKHKIPIKYLE	4	13/17[d]	76	3	5/19	26
		LKPLAQSHATKH$^{\#}$KIPIKYLE	4	13/17[d]	76	-	N.A.	-

[a] H$^{\#}$ denotes Michael adduct of 4-HNE to histidine (His).

[b] Number of N–C_α (ECD) or peptide (CO–NH, CID) bonds cleaved relative to the total number of N-Cα (ECD) or peptide bonds (CID) present in the peptide.

[c] The fragment ions distinguishing the 4-HNE localization site (His-113 or His-116) was not observed.

[d] The cleavage of N–C_α of proline (Pro, P) does not give ECD fragment ion (not counted).

[e] Glu-C peptide fragment of apomyoglobin.

N.A.: CID/ECD spectrum was not acquired.

Table S1. Apomyoglobin[a] tryptic fragments

Peptide sequence	Symbol	Position
GLSDGEWQQVLNVWGK	T_1	1-16
VEADIAGHGQEVLIR	T_2	17-31
LFTGHPETLEK	T_3	32-42
FDK	T_4	43-45
FK	T_5	46-47
HLK	T_6	48-50
TEAEMK	T_7	51-56
ASEDLK	T_8	57-62
K	T_9	63
HGTVVLTALGGILK	T_{10}	64-77
K	T_{11}	78
K	T_{12}	79
GHHEAELKPLAQSHATK	T_{13}	80-96
HK	T_{14}	97-98
IPIK	T_{15}	99-102
YLEFISDAIIHVLHSK	T_{16}	103-118
HPGDFGADAQGAMTK	T_{17}	119-133
ALELFR	T_{18}	134-139
NDIAAK	T_{19}	140-145
YK	T_{20}	146-147
ELGFQG	T_{21}	148-153

[a]Amino acid sequence of equine skeletal muscle apomyoglobin:

GLSDGEWQQV[10] LNVWGKVEAD[20] IAGHGQEVLI[30] RLFTGHPETL[40] EKFDKFKHLK[50] TEAEMKASED[60] LKKHGTVVLT[70] ALGGILKKKG[80] HHEAELKPLA[90] QSHATKHKIP[100] IKYLEFISDA[110] IIHVLHSKHP[120] GDFGADAQGA[130] MTKALELFRN[140] DIAAKYKELG[150] FQG[153]

Table S2. Summary of 4-HNE-modified apomyoglobin tryptic peptides observed before and after solid-phase hydrazide (SPH) enrichment

Tryptic fragment (one letter code)	Positions	Peptide Sequence	Number of 4-HNE adducts
Before enrichment			
T_1	1-16	GLSDGEWQQVLNVWGK	0
T_2	17-31	VEADIAGHGQEVLIR	0
T_3	32-42	LFTGHPETLEK	0
T_3-T_4	32-45	LFTGHPETLEKFDK	0
T_3-T_5	32-47	LFTGHPETLEKFDKFK	0
T_9-T_{10}	63-77	KHGTVVLTALGGILK	0
T_{10}	64-77	HGTVVLTALGGILK	0
T_9-T_{11}	63-78	KHGTVVLTALGGILKK	0
T_{10}-T_{11}	64-78	HGTVVLTALGGILKK	0
T_{10}-T_{12}	64-79	HGTVVLTALGGILKKK	0
T_{16}	103-118	YLEFISDAIIHVLHSK	0
T_{17}	119-133	HPGDFGADAQGAMTK	0
		HPGDFGADAQGAM$^{@}$TK	0
T_{18}	134-139	ALELFR	0
T_{20}-T_{21}	146-153	YKELGFQG	0
T_3	32-42	LFTGHPETLEK	1
T_{13}	80-96	GHHEAELKPLAQSHATK	2
T_{17}	119-133	HPGDFGADAQGAMTK	1
After enrichment			
T_2	17-31	VEADIAGHGQEVLIR	1
T_3	32-42	LFTGHPETLEK	1
T_{10}	64-77	HGTVVLTALGGILK	1
T_9-T_{10}	63-77	KHGTVVLTALGGILK	1
T_{10}-T_{11}	64-78	HGTVVLTALGGILKK	1
T_9-T_{11}	63-78	KHGTVVLTALGGILKK	1
T_{10}-T_{12}	64-79	HGTVVLTALGGILKKK	1
T_{13}	80-96	GHHEAELKPLAQSHATK	1,2,3
T_{12}-T_{13}	79-96	KGHHEAELKPLAQSHATK	2
T_{14}-T_{15}	97-102	HKIPIK	1
T_{16}	103-118	YLEFISDAIIHVLHSK	0,1,2
T_{17}	119-133	HPGDFGADAQGAMTK	1

$^{@}$ = Oxidized methionine residue

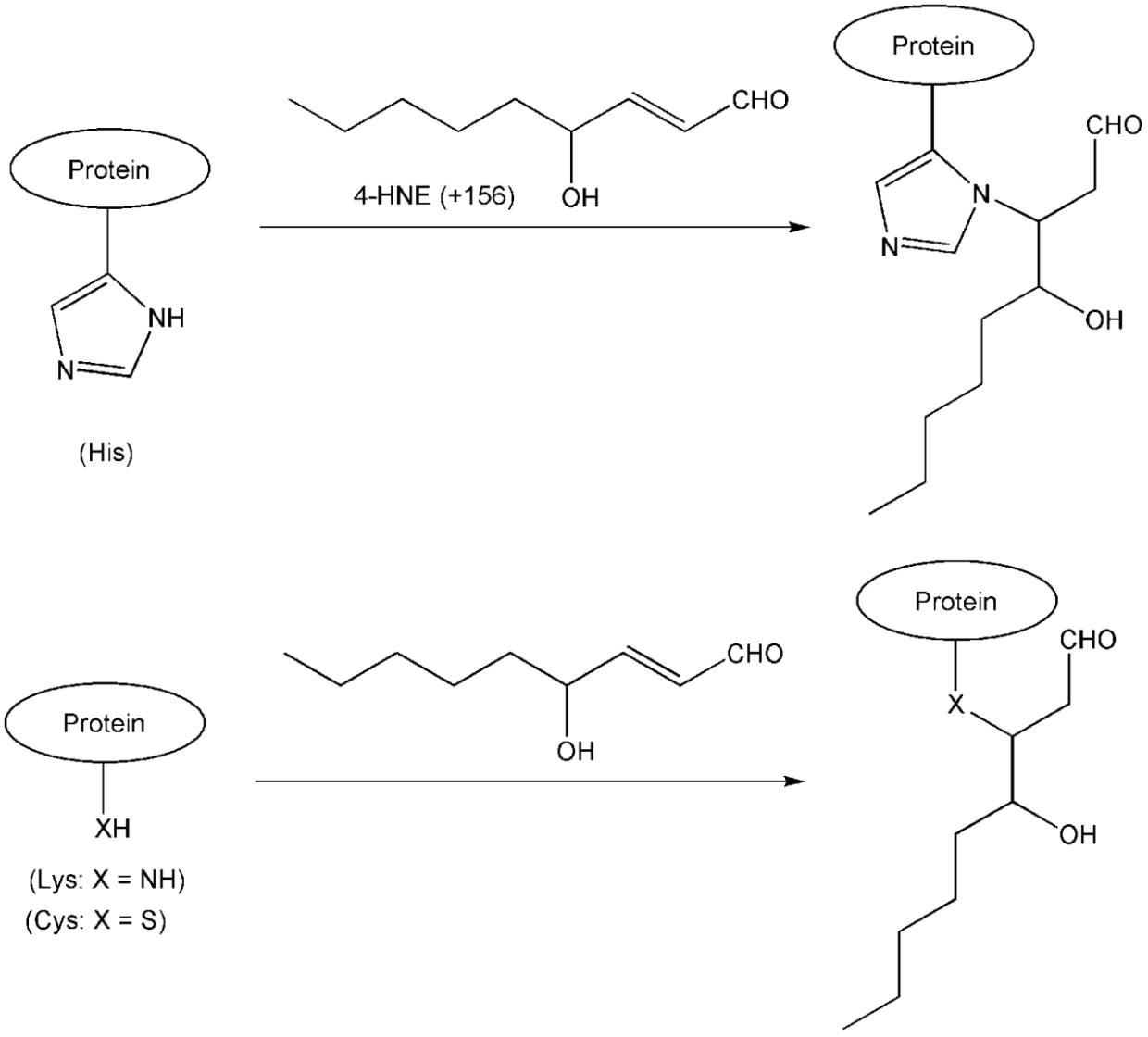

Figure 1. Primary reaction chemistry observed for 4-hydroxy-2-nonenal (4-HNE) modification of proteins. The α,β-unsaturated aldehyde is susceptible to Michael addition by a variety of nucleophiles including the histidine (His) imidazole group, lysine (Lys) ε-amino group, or thiol group of cysteine (Cys).

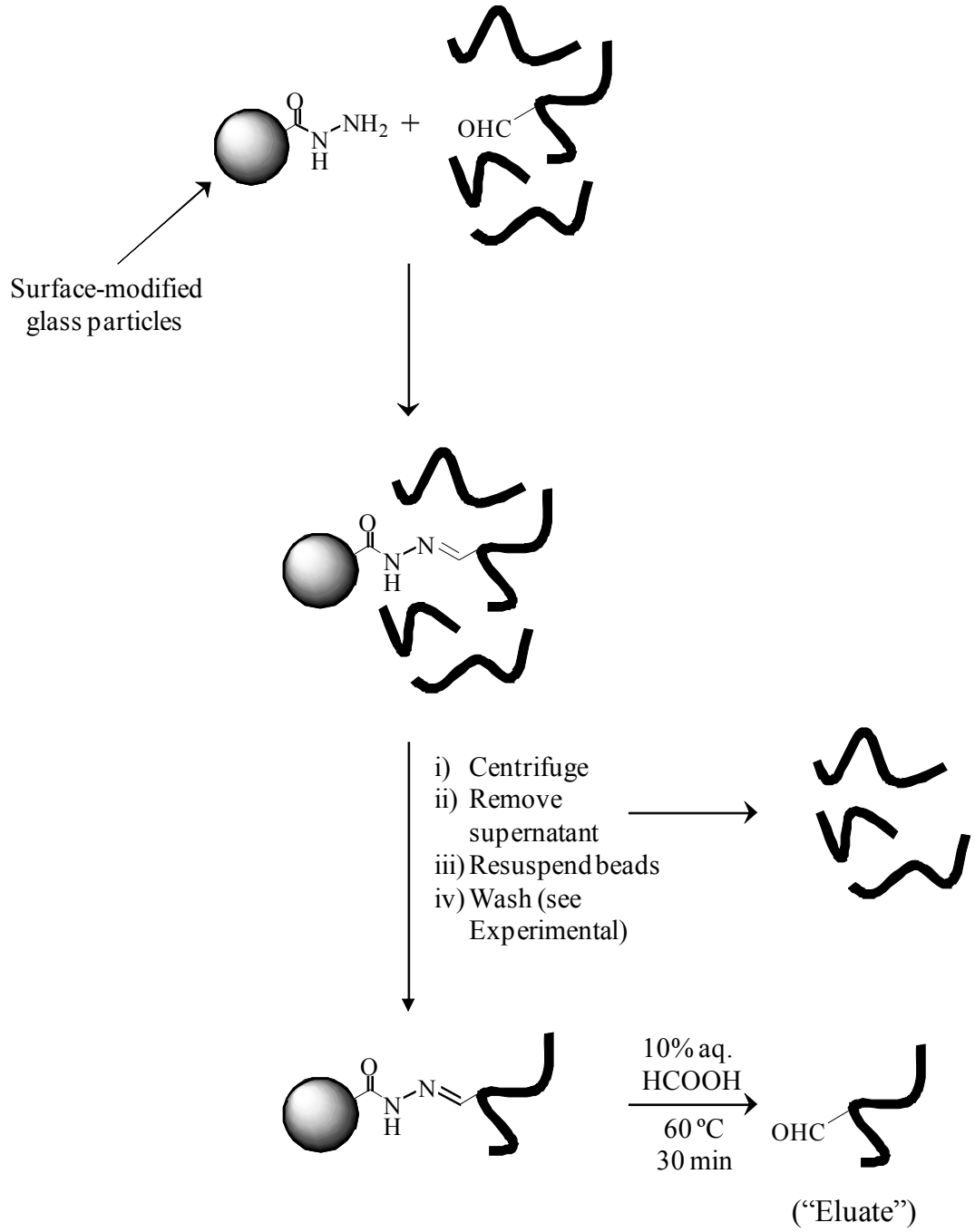

Figure 2. Schematic illustration of the procedure used for solid-phase hydrazide (SPH) enrichment of 4-HNE-carbonylated tryptic peptides of apomyoglobin.

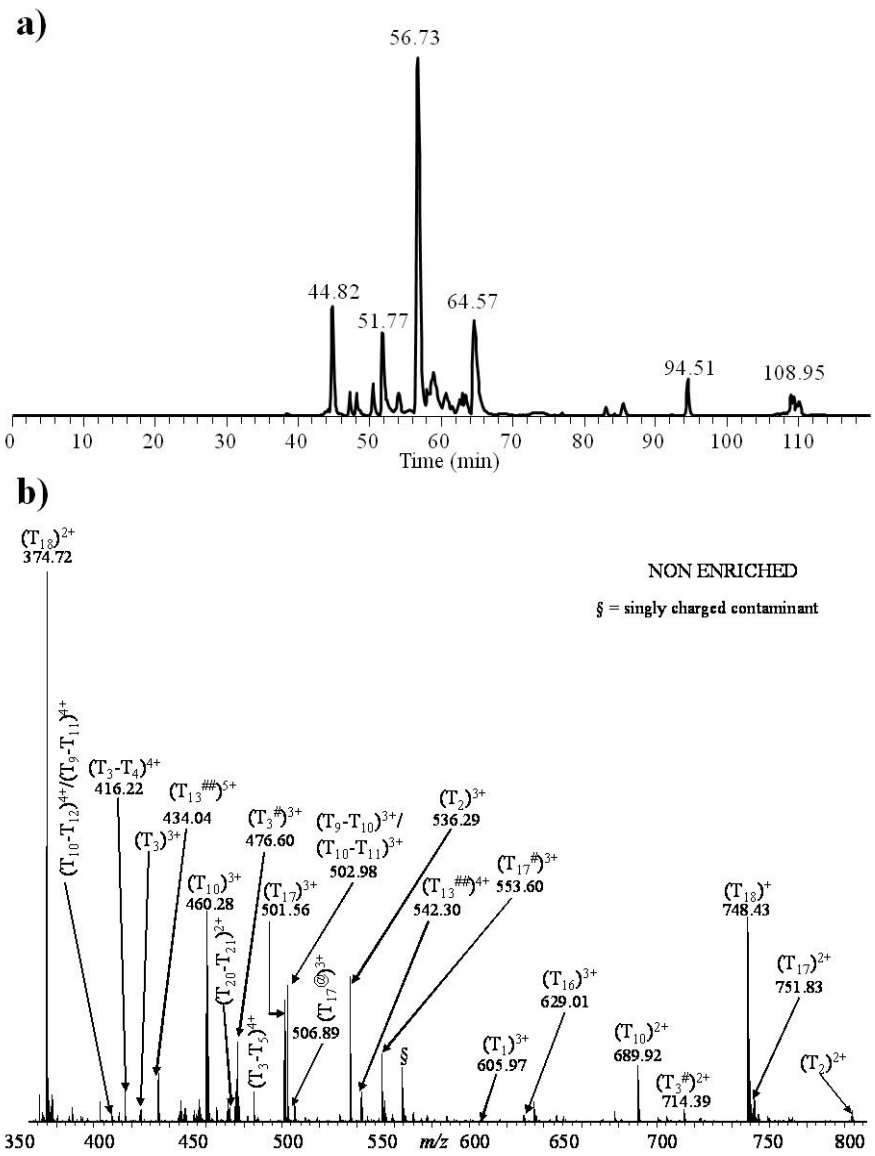

Figure 3. LC–ESI-MS analysis of tryptic digest of apomyoglobin from the crude reaction product with 4-HNE (i.e., unmodified and carbonylated tryptic peptides without prior enrichment of modified peptides: **a)** Base-peak chromatogram and **b)** averaged full-scan mass spectrum from acquisitions in the 30-100 min retention time window. The symbols T_1–T_{21} represent apomyoglobin tryptic peptides (refer to Table S1 in the Supporting Information). The number signs (#) indicate 4-HNE moieties attached to the respective tryptic peptide, multiple signs denote multiple modifications.

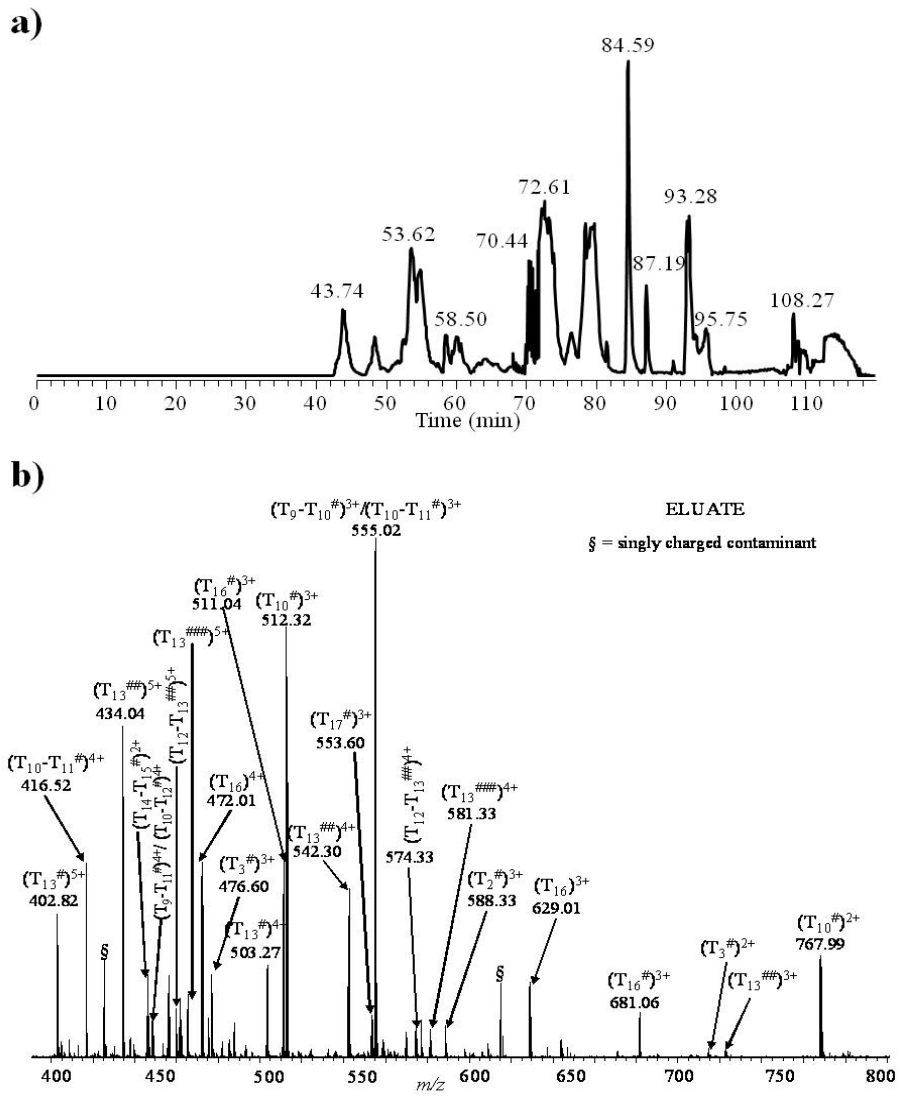

Figure 4. LC–ESI-MS analysis of tryptic digest of 4-HNE modified apomyoglobin after SPH enrichment (see Fig. 2): **a)** Base-peak chromatogram and **b)** averaged full-scan mass spectrum of the "eluate" fraction from acquisitions in the 30-100 min retention time window. The symbols T_1–T_{21} represent apomyoglobin tryptic peptides (refer to Table S1 in the Supporting Information). The number signs (#) indicate 4-HNE moieties attached to the respective tryptic peptide, multiple signs denote multiple modifications within the corresponding sequence.

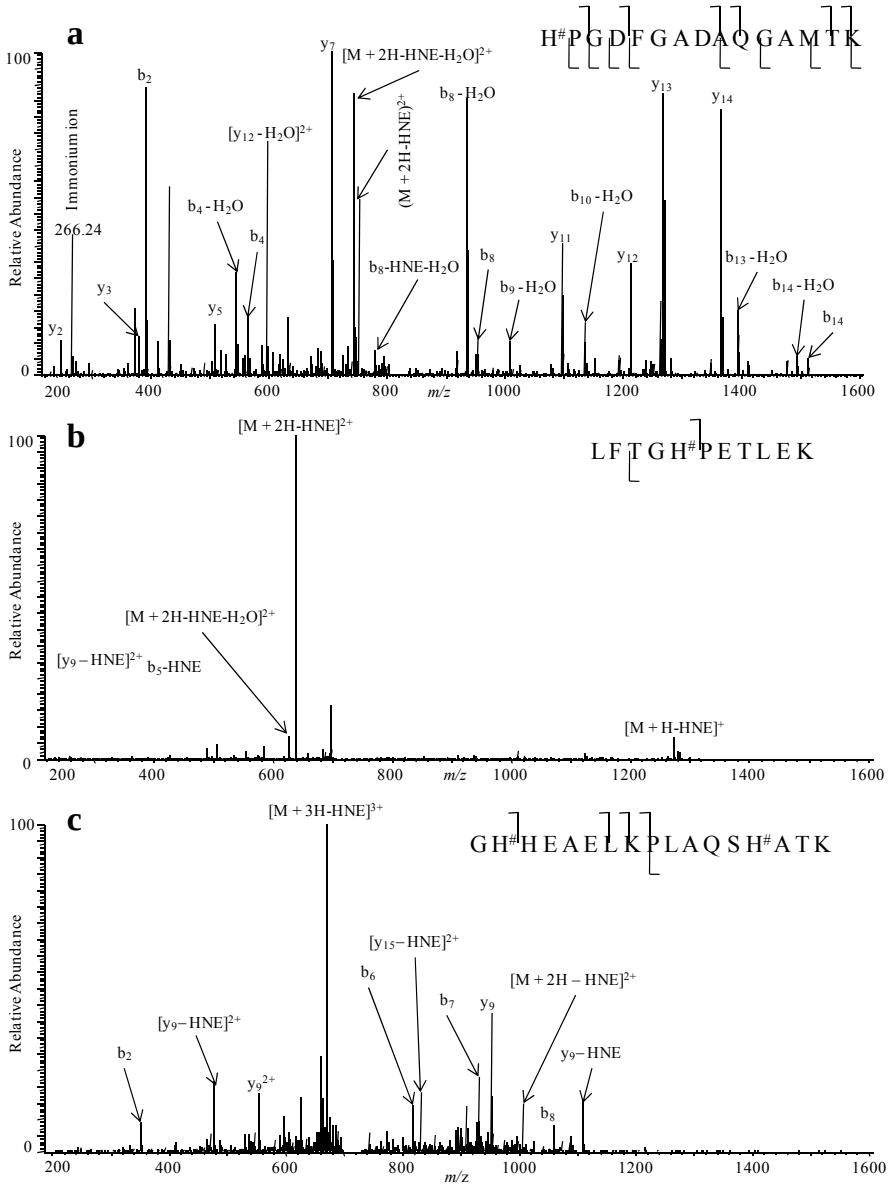

Figure 5. 4-HNE carbonylated apomyoglobin tryptic peptides representing the three types of fragmentation patterns upon CID: **(a)** CID-MS/MS spectrum of the doubly-charged 4-HNE-carbonylated precursor ion, H#PGDFGADAQGAMTK ($T^{17\#}$, 119-133) at *m/z* 829.89, **(b)** CID MS/MS spectrum of the doubly-charged 4-HNE-carbonylated precursor ion, LFTGH#PETLEK ($T_3^{\#}$, 32-42) at *m/z* 714.39, and, **(c)** CID-MS/MS spectrum of the triply-charged and bis-carbonylated precursor ion, [GHHEAELKPLAQSHATK]## ($T_{13}^{\#\#}$, 80-96) at *m/z* 722.73. Observed fragmentations are indicated on the amino acid sequence (inset). Histidines (H) marked with the number signs (#) denote side-chain 4-HNE modification.

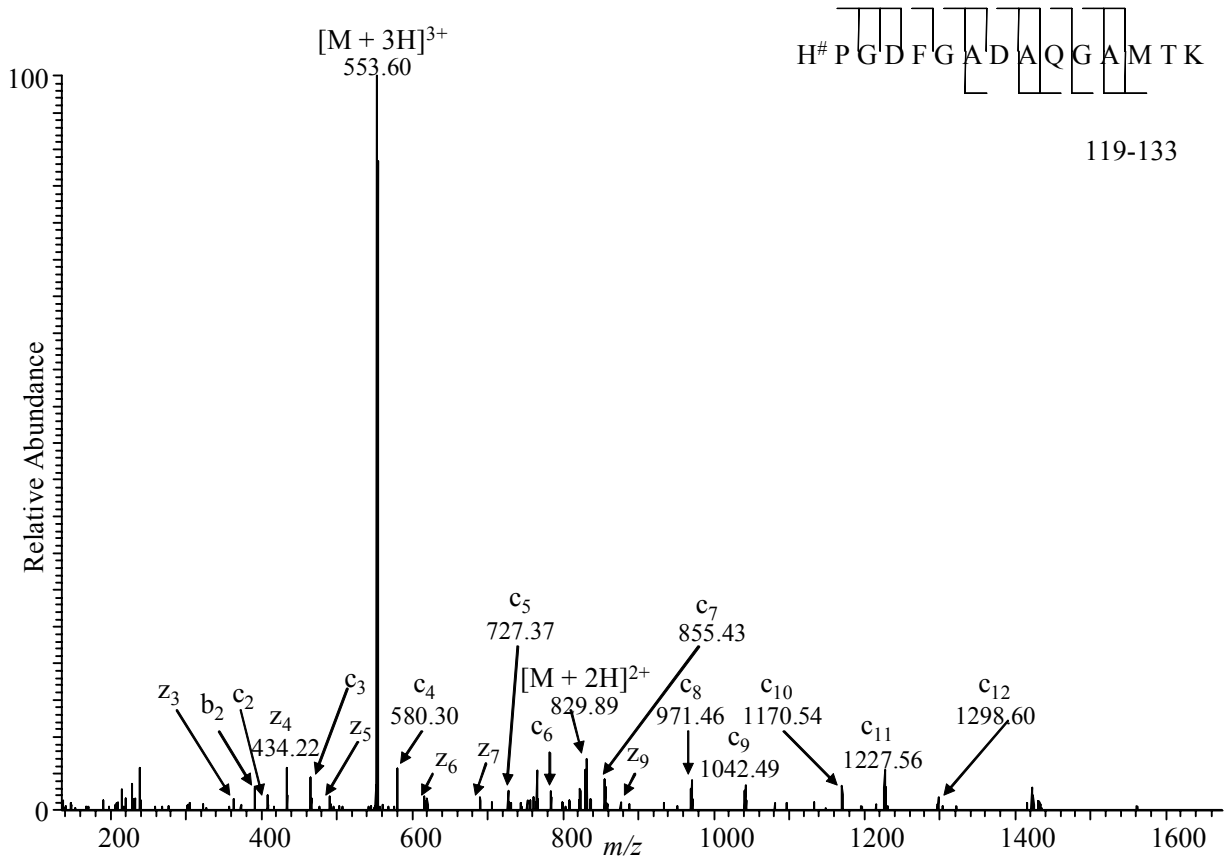

Figure 6. ECD-MS/MS spectrum of the $[M+3H]^{3+}$ 4-HNE-modified tryptic peptide ion, HPGDFGADAQGAMTK ($T_{17}^{\#}$, 119-133), at *m/z* 553.60. The fragmentation of the peptide backbone is indicated (inset). Histidines (H) marked with the number signs (#) denote side-chain 4-HNE modification.

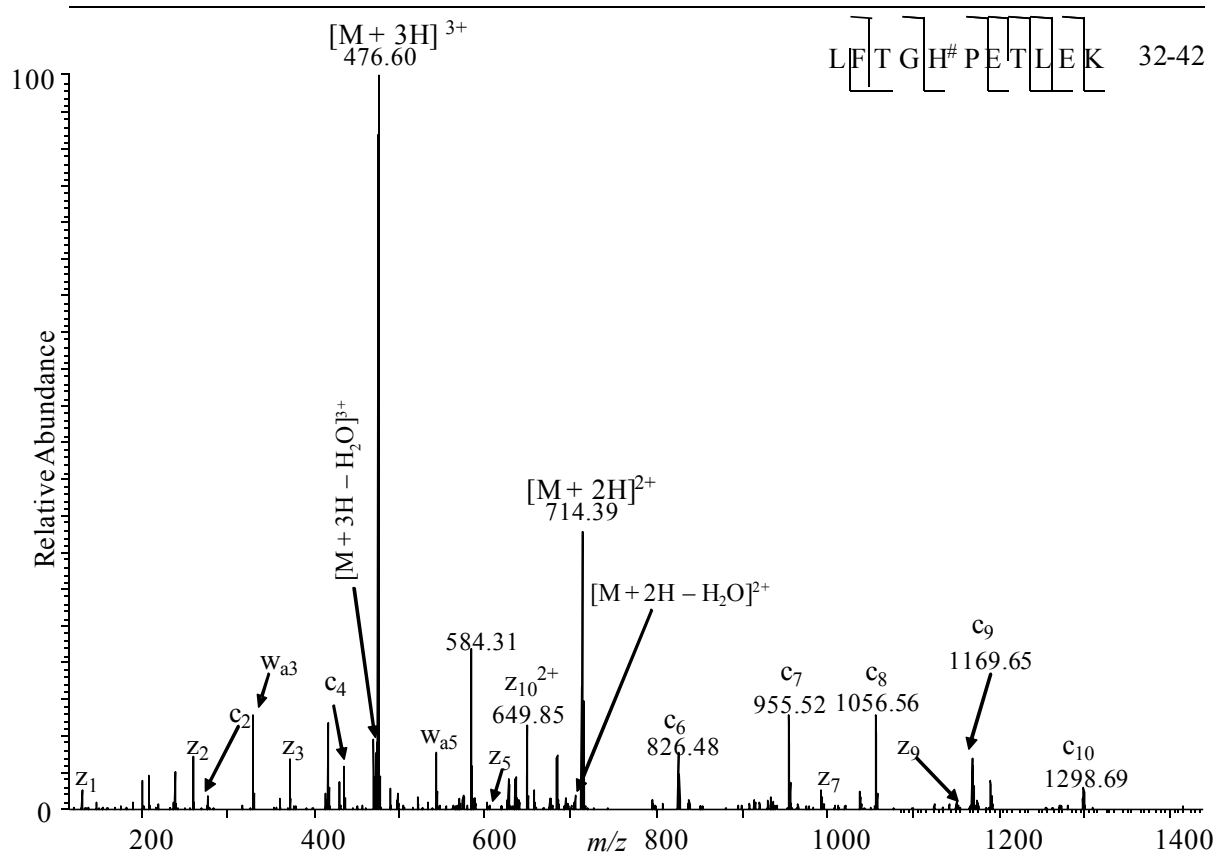

Figure 7. ECD-MS/MS spectrum of the $[M+3H]^{3+}$ 4-HNE-carbonylated peptide ion, LFTGH$^{\#}$PETLEK ($T_3^{\#}$, 32-42), at *m/z* 476.60. The fragmentation of the peptide backbone is indicated (inset). Histidines (H) marked with the number signs (#) denote side-chain 4-HNE modification.

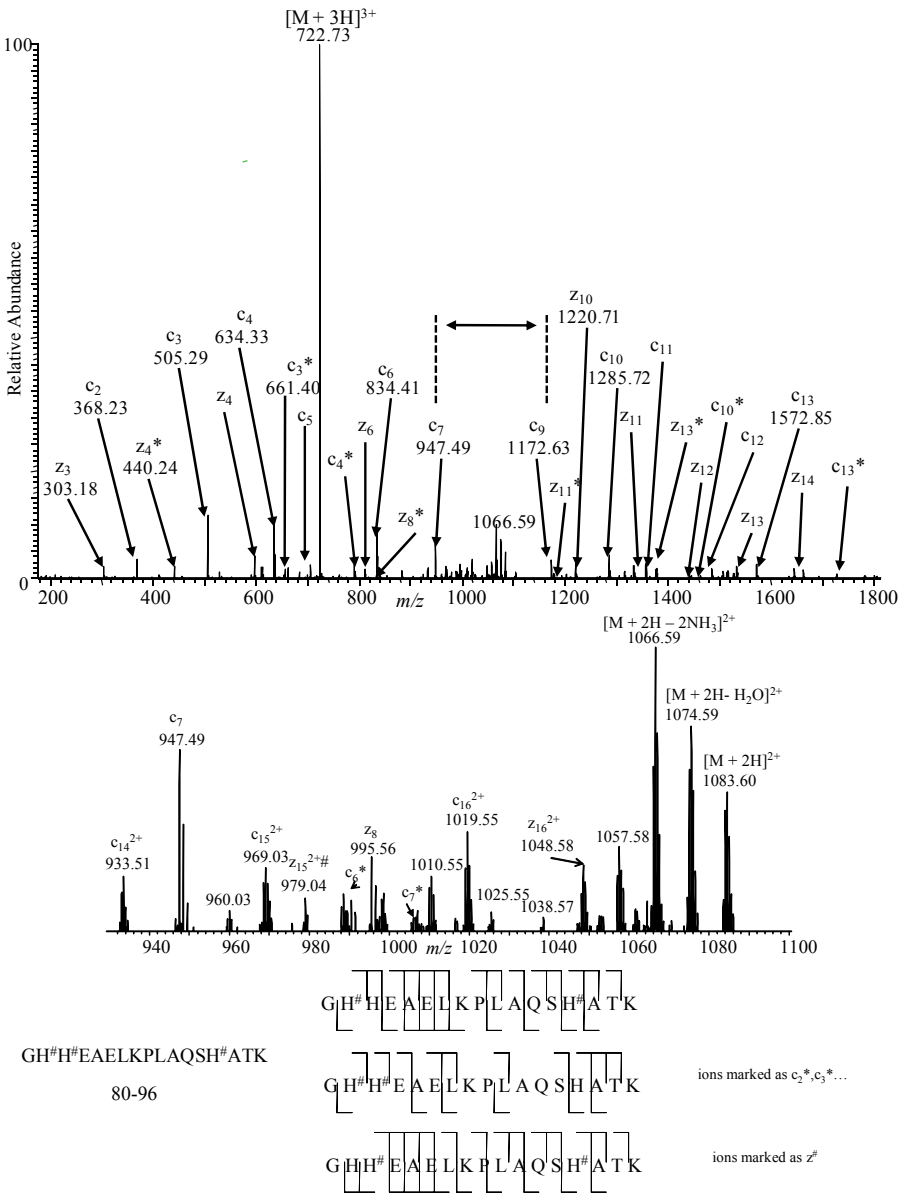

Figure 8. ECD-MS/MS spectrum of the triply-charged, bis-carbonylated tryptic peptide [GHHEAELKPLAQSHATK]$^{\#\#}$ ($T_{13}^{\#\#}$, 80-96), *m/z* 722.73. Inset shows the *m/z* 930-1100 range magnified. The mass spectrum consists of fragment ions generated from 4-HNE adduct to His-81 & 93 (not marked), His-81 &-82 (ions marked with *) and His-82 & 93 (ion marked with #) in apomyoglobin. The fragmentation summary of the peptide backbone is indicated. Histidines (H) marked with the number signs (#) denote side-chain 4-HNE modification.

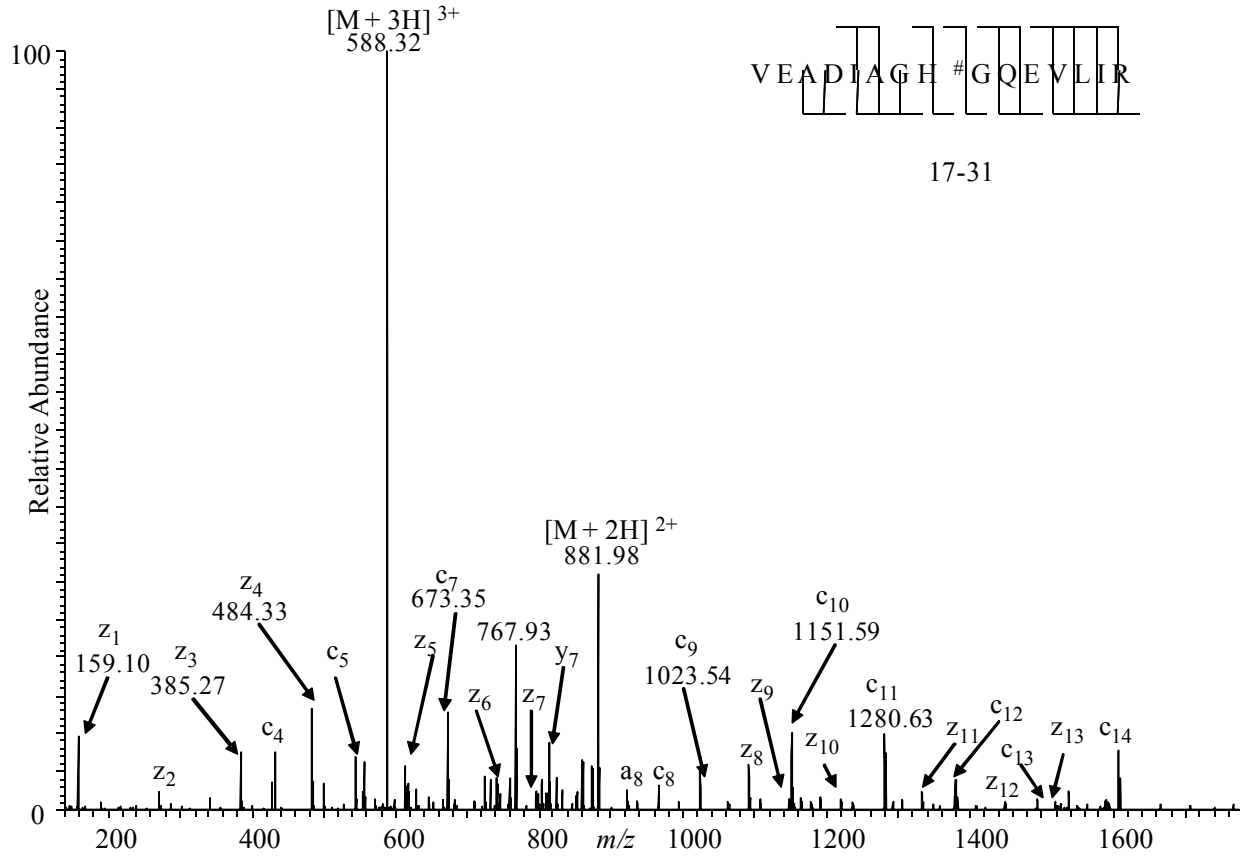

Figure S1. ECD-MS/MS spectrum of the triply-charged 4-HNE-carbonylated peptide ion, VEADIAGH$^{\#}$GQEVLIR ($T_2^{\#}$, 17-31), at *m/z* 588.32. Fragmentation behavior is indicated for the amino acid sequence (inset). Histidine (H) marked with a # sign denotes 4-HNE modification.

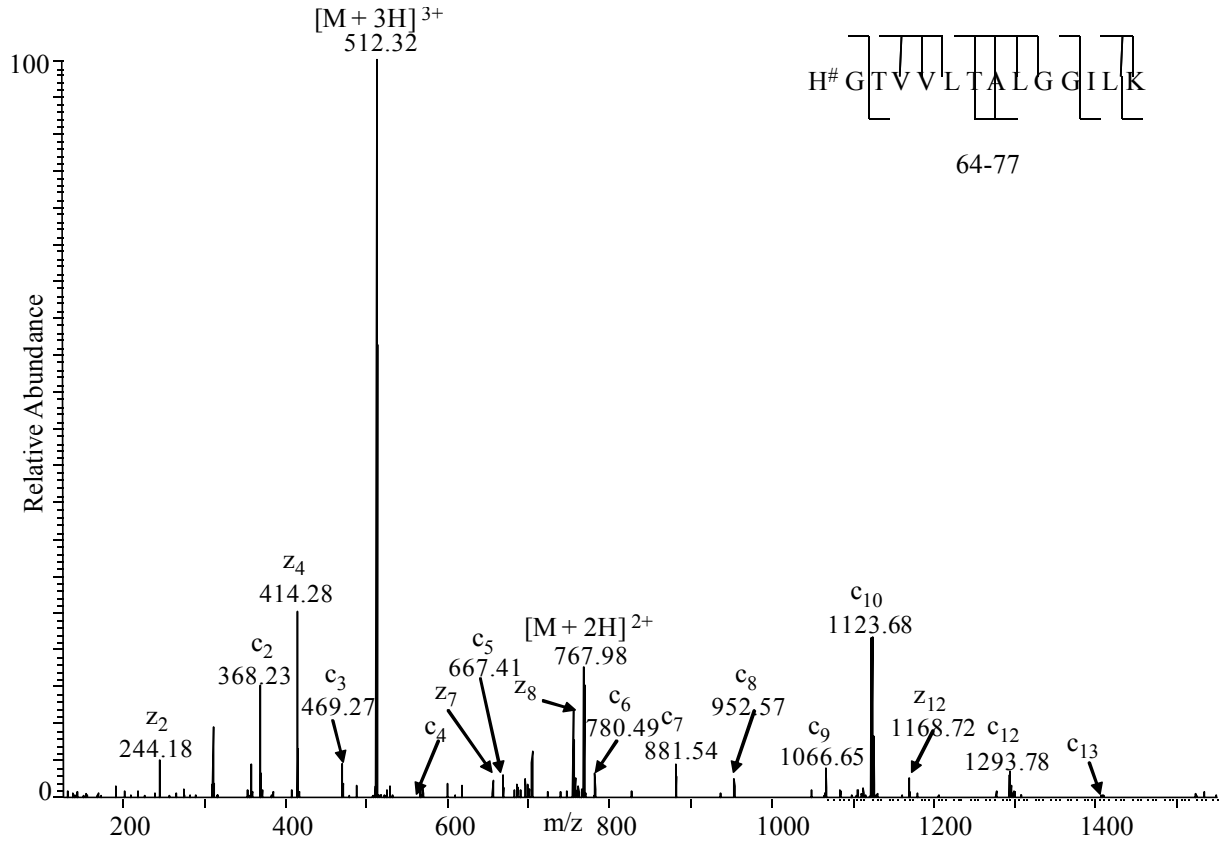

Figure S2. ECD-MS/MS spectrum of the $[M+3H]^{3+}$ 4-HNE-carbonylated peptide ion, $H^{\#}GTVVLTALGGILK$ ($T_{10}{}^{\#}$, 64-77), at *m/z* 512.32. The fragmentation of the peptide backbone is indicated (inset). Histidine (H) marked with a # sign denotes modification with 4-HNE.

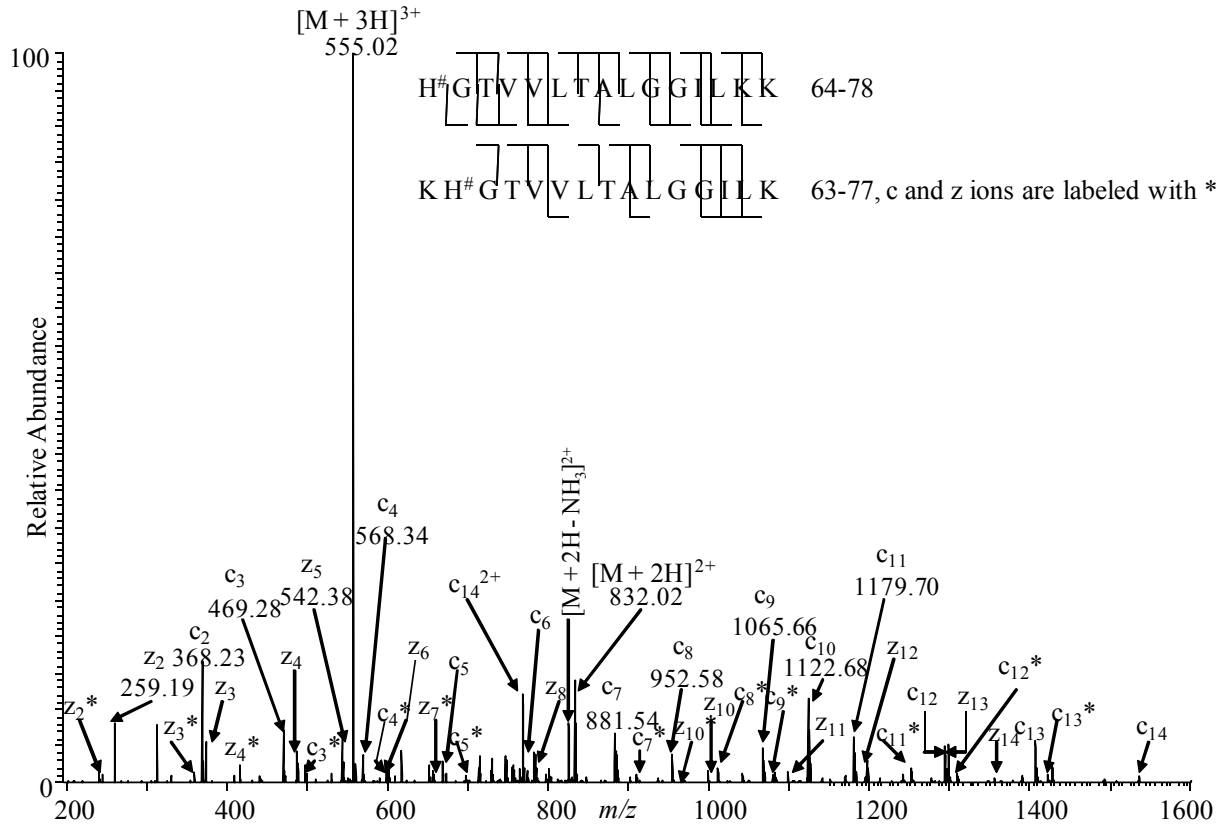

Figure S3. ECD-MS/MS spectrum of the coeluting triply-charged 4-HNE-carbonylated peptides ions, H#GTVVLTALGGILKK (T_{10}-T_{11}#, 64-78) and KH#GTVVLTALGGILK (T_9-T_{10}#, 63-77), at *m/z* 555.02. Unmarked product ions and product ions marked with asterisk (*) represents the ions obtained from cleavage of the triply-charged precursor ions of H#GTVVLTALGGILKK and KH#GTVVLTALGGILK, respectively. The fragmentation of the peptide backbone is indicated (inset). Histidine (H) marked with a # sign denotes modification with 4-HNE.

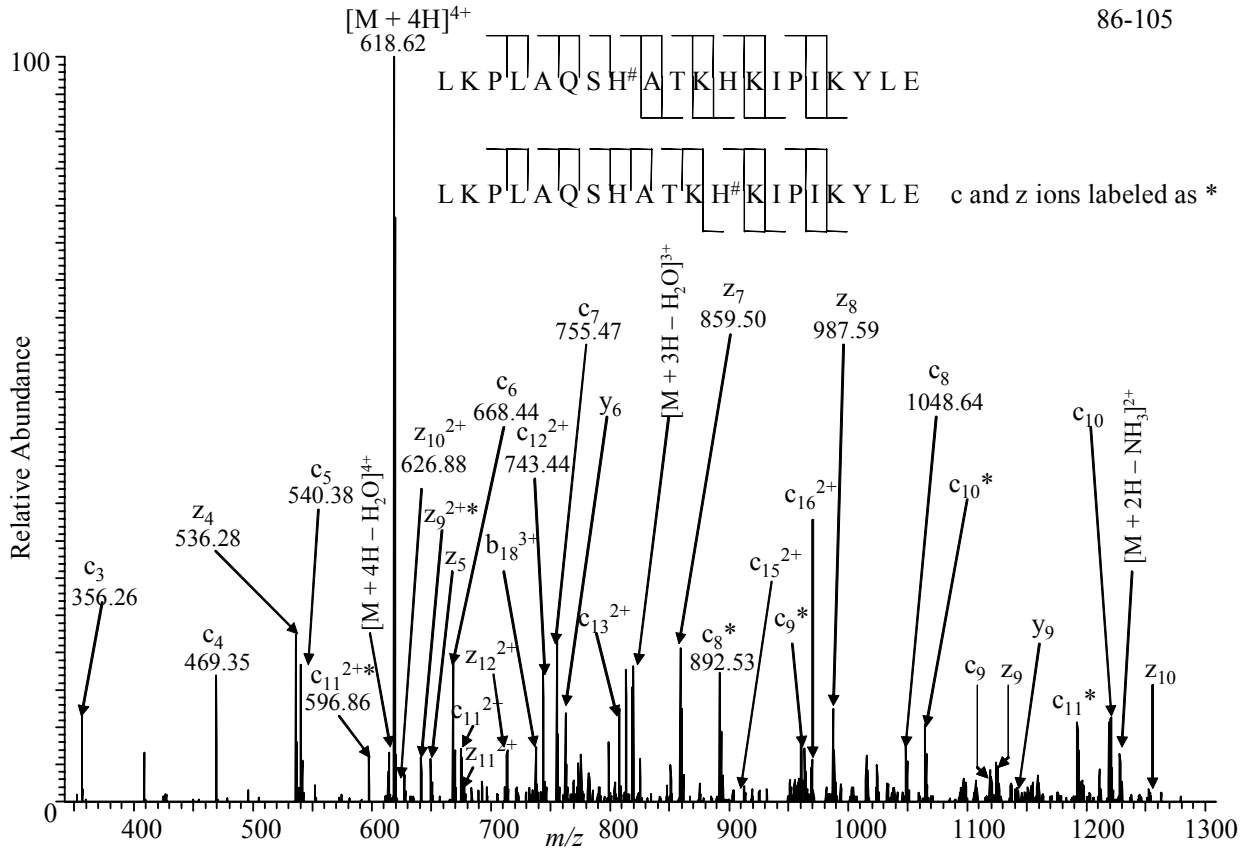

Figure S4. ECD-MS/MS spectrum of quadruply-charged (*m/z* 618.62) parent ions of isomeric 4-HNE-carbonylated peptides [LKPLAQSHATKHKIPIKYLE]# (86-105) obtained by Glu-C digestion of the 4-HNE-adducted apomyoglobin and after SPH enrichment. Fragment ions obtained from ECD of the peptide with 4-HNE adduct to His-93 are displayed without asterisks. Fragment ions of the isobaric coeluting peptide with 4-HNE adduct to His-97 are labeled with an asterisk. The fragmentation of the peptide backbone is indicated (inset). Histidine (H) marked with a # sign denotes modification with 4-HNE.

CHAPTER IV

CHARACTERIZATION OF 4-HYDROXY-2-NONENAL-MODIFIED PEPTIDES BY LIQUID CHROMATOGRAPHY-TANDEM MASS SPECTROMETRY USING DATA-DEPENDENT ACQUISITION: NEUTRAL LOSS-DRIVEN MS^3 VERSUS NEUTRAL LOSS-DRIVEN ELECTRON CAPTURE DISSOCIATION

Navin Rauniyar[¶], Stanley M. Stevens[¶], Jr., Katalin Prokai-Tatrai[§], and Laszlo Prokai[¶]

[¶]Department of Molecular Biology & Immunology and

[§]Department of Pharmacology & Neuroscience,

University of North Texas Health Science Center,

Fort Worth, Texas 76107

Published in: *Anal. Chem.* 2009, 81, 782-789

ABSTRACT

Reactive oxygen species generated during oxidative stress can lead to unfavorable cellular consequences, predominantly due to formation of 4-hydroxy-2-nonenal (HNE) during lipid peroxidation. Data-dependent and neutral loss (NL)-driven MS^3 acquisition have been reported for the identification of HNE adducts by mass spectrometry-based proteomics. However, the limitation associated with this method is the ambiguity in correct assignment of the HNE modification site when more than one candidate site is present as MS^3 is triggered on the neutral loss ion. We introduce NL-triggered electron capture dissociation tandem mass spectrometry (NL-ECD-MS/MS) for the characterization of HNE-modification sites in peptides. With this method performed using a hybrid linear ion trap-Fourier transform ion cyclotron resonance (FTICR) mass spectrometer, ECD in the FTICR unit of the instrument is initiated on precursor ions of peptides showing the neutral loss of 156 Da corresponding to an HNE molecule in the prescan acquired via collision-induced dissociation tandem mass spectrometry in the linear ion trap. In addition to manifold advantages associated with the ECD method of backbone fragmentation, including extensive sequence fragments, ECD tends to retain the HNE group during MS/MS of the precursor ion, facilitating the correct localization of the modification site. The results also suggest that predisposition of a peptide molecular ion to lose HNE during collision-induced dissociation-based fragmentation is independent of its charge state (2+ or 3+). In addition, we have demonstrated that coupling of solid-phase enrichment of HNE-modified peptides facilitates the detection of this posttranslational modification by NL-driven strategies for low-abundance proteins that are susceptible to substoichiometric carbonylation during oxidative stress.

INTRODUCTION

Oxidative stress typically results in peroxidation of polyunsaturated fatty acids present in lipids of the cell membrane bilayer, and as a consequence, various reactive aldehydes are generated. 4-Hydroxy-2-nonenal (HNE) is a highly reactive α,β-unsaturated electrophilic aldehyde that has been shown to form Michael adducts with cysteine (Cys, C), histidine (His, H), and lysine (Lys, K) residues[1] and has been reported to inactivate several enzymes.[2] HNE-protein Michael adducts are one of the most useful biomarkers for the occurrence and extent of oxidative stress.[3] HNE also forms a Schiff base with the ε-NH_2 group of Lys.[4] Identification of the sites of amino acid modification by this reactive end product of lipid peroxidation will help in the understanding of its impact on protein function and activity and, also, its effect on downstream targets or other interacting proteins.

Mass spectrometry-based approaches to characterize posttranslational HNE modification to proteins and peptides are promising because the peptide sequence and, hence, the protein identity and the position of HNE can be directly determined through tandem mass spectrometry (MS/MS). Collision-induced dissociation (CID) is the most widely used peptide fragmentation technique implemented in MS/MS. However, HNE-containing peptides may result in a neutral loss of HNE (156 Da; 78 or 52 Da for doubly or triply charged peptides) from the precursor or product ions upon CID.[5] A neutral loss-driven MS^3 (NL-MS^3) method for the characterization of HNE modified peptides has been reported recently.[6,7] In this strategy, the neutral loss of HNE observed upon MS/MS of HNE-modified peptides triggers MS^3 analysis of the neutral-loss product ion to reveal the sequence of the peptide. However, MS^3 of the neutral loss ion provides no diagnostic mass tag that would allow for unambiguous HNE modification site identification, if

more than one possible amino acid residue that could potentially react with HNE is present. Though neutral loss indicates the presence of modification by its characteristic signature tag, a significant challenge still persists in the determination of site(s) of HNE modification or of other posttranslational modifications (PTMs), such as phosphorylation, sulfation, glycosylation, and oxidation.[8] Because cleavage of the labile PTMs is favored over peptide backbone dissociation, neutral loss limits further fragmentation that would provide sequence information and, thus, may not afford identification of the modified peptide. Moreover, the difficulty of correctly assigning the site of HNE modification is amplified when more than one possible candidate site is present within the peptide, because the consensus sequence representing the chemical selectivity of HNE modification is lacking. A potential solution to these problems affecting the MS/MS characterization of HNE-modified peptides is to stabilize Michael adducts with sodium borohydride reduction, which prevents the neutral loss upon CID.[9] However, this chemical and very attractive enrichment strategy applicable only to conversion precludes the use of a subsequent carbonylated peptides.[7] Electron capture dissociation (ECD) is an alternative fragmentation technique and is usually implemented with FTICR mass analyzers.[10] The partial neutralization of multiply charged peptides following capture of low-energy electrons results in interresidue backbone cleavage.[11] The typical fragmentation pathway of a peptide backbone in ECD consists of cleavage of the amine linkage (N-Cα) rather than at the amide bond characteristic to CID. ECD cleavage results in production of c- and z-type, as opposed to that of b- and y-type, fragment ions typically observed in CID.[12] More recently, electron transfer dissociation (ETD) has been developed to induce fragmentation of the peptide backbone along pathways that are analogous to those observed in ECD. In ETD, a combination of gas-phase ion/ion chemistry and MS/MS is employed in which singly charged radical anions transfer an

electron to multiply protonated peptides.[13,14] The peptide bond dissociations upon ECD are "ergodic" in nature, in which internal energy gained upon electron capture is randomized before dissociation.[15-17] Nevertheless, this method of peptide fragmentation offers several advantages over CID. ECD allows labile PTMs (such as HNE) to remain attached during backbone fragmentation facilitating characterization of posttranslational modification, in contrast to CID, in which the labile modification group may be expelled first.[18,19] Hence, ECD permits the determination of the exact location of labile modifications with amino acid resolution.[12] Mechanisms and fundamental features as well as benefits of ECD have been reviewed in detail.[20] Several studies have demonstrated the efficiency of ECD in characterizing different types of posttranslational modifications, such as phosphorylation,[21,22] acylation,[23] glycosylation,[24] sulfation,[25] and other types of modifications in peptides and proteins. We also have shown previously the potential of ECD in retaining and identifying HNE modification sites in the oxidized insulin B chain.[19] The use of online separation of peptides prior to MS has been well-known to decrease the complexity of spectra, reduce ion suppression in the spray, and result in a preconcentration of the analytes.[26] Implementation of electron-injection systems based on indirectly heated dispenser cathodes that provide higher electron fluxes, wider electron beams, and better control of the electron energy[12] has decreased electron irradiation time to the millisecond range to afford ECD, which has enabled coupling of the technique with online liquid chromatography/FTICR-MS and made high-throughput data-dependent LC-ECD-MS/MS possible for characterization of proteins or analysis of peptides in tissue extracts.[12,26-29] For the analysis of phosphopeptides, Sweet *et al.* have reported a novel method that exploits the neutral loss feature of CID and performs ECD on the precursor ion exhibiting a neutral loss of 98 Da (corresponding to H_3PO_4).[30] This method, termed neutral loss-triggered ECD (NL-ECD-

MS/MS), was applied for the identification of phosphorylation sites in α- and β-casein. Although CID provided, along with the sequence of nonphosphorylated peptides, information on the occurrence of the 98-Da neutral loss from the precursor, ECD was initiated to correctly determine the number and sites of phosphorylation in singly or multiply phosphorylated peptides.

To characterize HNE modifications, a NL-ECD-MS/MS approach would also be beneficial, since ECD will be triggered only on precursor ions that show a HNE loss of 78 or 52 Th in the CID spectra, depending on the charge state of the peptide (2+ or 3+), thereby reducing the duty cycle associated with full data-dependent ECD analysis. To our knowledge, the applicability of NL-ECD-MS/MS for the characterization of HNE-modified peptides has not been reported previously. The current work evaluates, in comparison with the CID-based NL-MS^3 technique,[6] the performance of NL-ECD-MS/MS to characterize HNE modification.

EXPERIMENTAL SECTION

Materials

Human angiotensin (AGT) I peptide (DRVYIHPFHL) and AGT II octapeptide (DRVYIHPF) were purchased from Anaspec (San Jose, CA). Peptides LVLEVAQHLGESTVR and IVYGHLDDPANQEIER (which correspond to tryptic peptides of ATP synthase subunit beta and aconitate hydratase, respectively, found to be targets for HNE modification[6]) were custom synthesized by Peptide 2.0, Inc. (Chantilly, VA) and used without further purification. 4-Hydroxy-2-nonenal was obtained from Cayman Chemical (Ann Arbor, MI).

4-Hydroxy-2-nonenal modification of peptides

HNE adducts of peptides (1 mg/mL) were prepared by reaction with 2mM HNE in 0.1 M phosphate buffer, pH 7.4, at 37 °C for 2 h. Excess HNE was removed by extracting the solution three times with ethyl acetate. The resultant aqueous (stock) solutions of HNE-modified peptides were used without further purification in the experiments detailed below.

Solid-phase enrichment

To obtain a complex tissue sample, 100 mg of mouse brain was incubated in 500 µL of urea (8 M) for 30 min. The supernatant was aliquoted and reduced with 5 mM DTT at 65 °C for 30 min, followed by alkylation with 20 mM iodoacetamide at room temperature in the dark for 30 min. The sample was diluted 4-fold with 50 mM ammonium bicarbonate and subsequently digested with trypsin (substrate/enzyme ratio of 100/1, wt/wt) at 37 °C for 18 h. One hundred microliters of the brain protein digest was acidified with acetic acid to pH 3.6 and mixed with 120 µL of reaction buffer (0.2% acetic acid, 10% acetonitrile, pH 3.6) spiked with approximately 66, 88, and 20 pmol of HNE-modified DRVYIHPF, LVLEVAQHLGESTVR, and IVYGHLDDPANQEIER from their respective stock solutions. Five microliters of this mixture was used directly for LC-MS analysis to evaluate the mixture before enrichment.

For enrichment of HNE-modified peptides from the mouse brain tryptic digest, 4.2 mg of solid-phase hydrazide (SPH) reagent prepared as described by Roe *et al*.[7] was added, and the resulting mixture was rotated end-over-end overnight at room temperature. The SPH reagent was then pelleted, and the supernatant was removed. The pellet was washed, and the hydrazide-bound peptides were released by incubation with 200 µL of 10% formic acid for 30 min at 60 °C. This step was repeated once, and the solutions containing the released peptides were combined. The

eluate containing the HNE-modified standard peptides was dried in an Eppendorf (Westbury, NY) Vacufuge concentrator and resuspended with 20 μL of 0.1% acetic acid. A 5 μL aliquot of the resuspended solution was used for LC-MS analysis by NL-ECD-MS/MS and NL-MS^3.

ESI mass spectrometry

For analysis without LC separation, the modified peptides were first desalted on an octadecylsilica (C18) solid phase (Ziptip pipet tips, Millipore, Billerica, MA). The bound peptides were washed with 0.1% acetic acid and then recovered by elution with water/methanol/acetic acid (49.5:49.5:1, v/v) and were electrosprayed directly through a PicoTip (New Objective, Inc., Woburn MA) emitters.

LC-NL-MS^3 and LC-NL-ECD-MS/MS

Neutral loss-driven MS^3 and neutral loss-driven ECD tandem mass spectrometry were performed on a hybrid linear ion trap-FTICR (7-T) mass spectrometer (LTQ-FT, Thermo Finnigan, San Jose, CA) equipped with an electrospray ionization source and operated with the Xcalibur (version 2.2) data acquisition software. Online high performance liquid chromatography was performed with an Eksigent nano-LC-2D system using a 15 cm × 75 μm PepMap C18 column (LC Packings) as the analytical column. Mobile phases consisted of solvents A (0.1% acetic acid and 99.9% water (v/v)) and B (0.1% acetic acid and 99.9% acetonitrile (v/v)). Five microliters of the HNE-modified peptide AGT-I and -II or a peptide mixture of the HNE-modified LVLEVAQHLGESTVR and IVYGHLDDPANQEIER were automatically loaded onto the column and equilibrated for 5 min in 5% solvent B, followed by a 90-min gradient to 40% solvent B at a constant flow rate of 250 nL/min. Analysis was performed using NL-initiated MS^3 and NL-initiated ECD data-dependent acquisition mode.

NL-MS^3-driven data-dependent acquisition was performed as described previously.[6] If a neutral loss of 78 or 52 Th (from a doubly or triply charged HNE-modified peptide) is observed, the neutral loss fragment ion is then selected and subjected to another CID fragmentation (i.e., MS^3) in the NL-MS^3 method. Briefly, first an accurate *m/z* survey scan was performed in the FTICR cell, followed by parallel MS/MS linear ion trap analysis of the top five most intense precursor ions selected from interim survey spectra (resolving power of <12 500 at *m/z* 400) obtained by fast Fourier transformation (FFT) about 0.15 s after starting the acquisition of the transients from the receiver plates of the FTICR unit. FTICR full-scan mass spectra were acquired at 100 000 mass resolving power (at *m/z* 400) from *m/z* 350 to 1500 using the automatic gain control mode of ion trapping (500 000 target ion count). Collision-induced dissociation in the linear ion trap was performed using a 3.0 Th isolation width and 35% normalized collision energy with helium as the target gas. Isolation and subsequent CID fragmentation of ions exhibiting a 78 or 52 Th difference (representing neutral loss of HNE from 2+ or 3+ precursor ions, respectively) from the precursor ion was triggered if the neutral loss fragment ions passed specified selection criteria (they were among the three most intense ions in the MS/MS spectra).

The reported NL-ECD-MS/MS approach for characterization of HNE modification in peptides was adapted from the method of mapping phosphorylation sites in tryptic peptides of β-casein and α-casein.[30] In the NL-ECD-MS/MS method, the LTQ-FT performed a full mass scan (*m/z* 200-2000) during the first scan event, followed by CID fragmentation of the most abundant peptides eluted at a particular chromatographic time point from the nano-LC column. Ultimately, if a neutral loss of 78 or 52 Th from a doubly or triply charged precursor ion was observed in the CID mass spectrum, then ECD fragmentation was initiated on the same precursor ion, as opposed to selection of the neutral loss peak in NL-MS^3. Xcalibur 2.2 was used for data

acquisition. For NL-ECD-MS/MS, FTICR acquisition parameters were adapted from Sweet *et al*.[30] with slight modification. Briefly, full-scan mass spectra were acquired in the ICR cell with a resolving power of 50 000 at m/z 400. Precursor ions (selected from interim survey spectra obtained at a resolving power of <12 500 at *m/z* 400) were isolated with an isolation width of 4 Th and subjected to CID in the linear ion trap with helium as the target gas. The dissociation of the precursor ion was induced using an activation time of 30 ms and at a normalized collision energy of 35%. ECD of the precursor ion was triggered if a neutral loss of 156 Da (loss of 78 or 52 Th from 2+ or 3+ charged peptide) was observed from one of the three most abundant fragment ions in the previous MS/MS scan. For ECD, the precursor ions were isolated in the linear ion trap with an isolation width of 4 Th and transferred to the ICR cell. Ions were irradiated for 120 ms at 5 eV during ECD. The precursor ion that has been selected for ECD fragmentation is dynamically excluded from further MS/MS analysis for 180 s. The methods were evaluated using HNE-modified synthetic peptides.

RESULTS AND DISCUSSION

CID- and ECD-based fragmentation of HNE-modified peptides

Scheme 1 shows the steps incorporated in the NL-MS^3 and NL-ECD-MS/MS experiments. Figure 1a displays the CID MS/MS spectrum of $[M + 2H]^{2+}$ of the HNE-modified AGT I peptide DRVYIHPFHL, obtained through ESI-MS without LC separation. This peptide has two potential HNE modification sites, His-6 and His-9, to form Michael adducts. The characteristic neutral loss peak observed at *m/z* 648.75 corresponds to the loss of HNE (156 Da) from the doubly charged precursor ion *m/z* 726.91. Also observed are the product ions b_9 (*m/z*

583.17, 2+), y_2 (*m/z* 269.08), and y_4 (*m/z* 513.17) that are accompanied by the loss of HNE. The product ions b_8 (*m/z* 1028.25) and b_9 (*m/z* 661.25, 2+) show the presence of HNE at His-9, and the overall peptide fragmentation efficiency was 56%. MS^3 of the neutral loss ion *m/z* 648.75 was performed manually in the linear ion trap (LTQ) that produced the fragment ions (Figure 1b) necessary to identify the peptide sequence. Since a neutral loss of HNE was observed during CID analysis of the modified AGT I peptide, this peptide was used to evaluate the performance of NL-ECD-MS/MS for the analysis of HNE modification. In the NL-ECD-MS/MS method, the observed neutral loss of 78 Th from the precursor ion *m/z* 726.9012 (m/z_{calc} 726.9035; 3.2 ppm error in mass accuracy) during the CID-MS/MS scan triggered ECD of the same precursor ion in the subsequent MS/MS scan (Figure1c). In this ECD spectrum, the backbone fragmentation resulted in eight out of the total eight interresidue bonds (the cleavage of the N-terminal side of proline is not considered due to its resistance to ECD because of the cyclic structure of this residue) being cleaved, and HNE was retained on the peptide, as shown by the ECD product ions c_8 (*m/z* 1045.5538) and c_9 (*m/z* 1338.7269). This result led to the unequivocal mapping of the HNE modification site to His-9 in the AGT-I peptide. A loss of HNE moiety from the charge-reduced precursor ion was observed; however, it did not interfere with the correct identification of the site of modification. Generally, the backbone fragments of ECD tend to retain posttranslational modifications, such as phosphorylation,[21,22] acylation,[23] glycosylation,[24] and sulfation.[25] Additionally, there are no fragment ions consistent with the modification of His-6. These results corroborate the fact that neutral loss of HNE (*m/z* 78 for the doubly charged peptide) in CID-based fragmentation serves as a signature tag that shows the presence of HNE-modified peptides in complex mixtures. The extensive backbone fragmentation by ECD, while retaining the labile HNE group, allows for direct localization of the HNE-modified residues. In

addition to c and z product ions, the losses of 28, 45, and 62 Da from charge-reduced precursor ions are also observed in the ECD spectrum.[31]

NL-MS^3 and NL-ECD-MS/MS-based analyses were further employed to HNE-modified LVLEVAQHLGESTVR and IVYGHLDDPANQEIER, which correspond to tryptic peptides of ATP synthase subunit beta and aconitate hydratase, respectively. We have previously shown that His in these tryptic fragments of the proteins are susceptible to *ex vivo* HNE modification (Michael adducts) in the rat brain mitochondria.[6] The peptide mixture was separated online by nanoHPLC and analyzed by NL-MS^3 and NL-ECD-MS/MS as described in the Experimental Section. Parts a and b of Figure 2 are MS/MS and MS/MS/MS spectra of the HNE-modified peptide LVLEVAQHLGESTVR obtained from NL-MS^3 data-dependent acquisition. The predominant fragmentation pathway in CID MS/MS scan of the peptide is the loss of HNE from the precursor ion. The prominent neutral loss peak at *m/z* 826.02 obtained from CID-based fragmentation of the precursor ion *m/z* 903.98 (doubly charged LVLEVAQH*LGESTVR) was selected for an additional round of CID, as shown in Figure 2b. In this peptide, the site of HNE modification can be assigned to His by the NL-MS^3 method, because no other amino acids are known to be susceptible to HNE modification. ECD was triggered for the precursor ion *m/z* 904.0085 (m/z_{calc} 904.0198; 12.5 ppm error in mass accuracy). In the ECD spectrum, cleavage of 10 of 14 backbone amine linkages was observed (Figure 2c), and it was possible to assign the site of HNE modification on the basis of the fragmentation pattern. Upon ECD-based MS/MS, all fragment ions that contain the His residue exhibited a +156 Da mass shift relative to the unmodified peptide. The fragment ions c_8 (*m/z* 1063.6370) and z_8 (*m/z* 1038.5671) confirm the presence of a HNE residue at His-8 in this peptide. Thus, utilization of NL-ECD-MS/MS can undoubtedly show the HNE modification site, because ECD is capable of retaining the HNE

moiety on the peptide during fragmentation. Iavarone *et al*. have reported that fragmentation efficiency in ECD increases with increasing precursor charge state.[32] We also noted that ECD of the doubly charged precursor ion *m/z* 904.0085 produced a limited range of higher c (c_8, c_9, c_{10}, and c_{14}) and z (z_8-z_{13}) fragment ions.

Supporting Information Figure 1a and b shows the CID-based MS/MS and MS/MS/MS spectra of the HNE-modified aconitate hydratase peptide (IVYGH*LDDPANQEIER) obtained by NL-MS^3 data-dependent acquisition. The peak corresponding to neutral loss of HNE in the CID MS/MS spectra of the doubly charged precursor ion *m/z* 1013.02 during NL-MS^3 was not intense (Supporting Information Figure 1a), as compared to the former two peptides. Neutral loss of HNE corresponding to the ion at *m/z* 935.48 was nevertheless observed from the precursor ion, which therefore triggered MS^3 and ECD of the neutral loss fragment ion and precursor ion, respectively, upon using the NL-MS^3 and NL-ECD-MS/MS approaches (Supporting Information Figure 1b and 1c). For this peptide, the CID-MS/MS spectrum of the precursor ion itself contained abundant b and y fragment ions (9 out of 15 backbone amide bond cleavage) that distinctly localized the site of HNE addition to His-5; thus, NL-MS^3 and NL-ECD-MS/MS did not provide additional information that could not be obtained from CID-MS/MS alone. The cleavage of 8 of the 14 N-Cα bonds (without considering the N-terminal side of proline) in the peptide backbone of $(M + 2H)^{2+}$ ions showed a fragmentation efficiency of 53%. Only the fragment ions c_{14}-c_{15} and z_{10}-z_{15} were produced. The mass difference of 293 Da between z_{12} (*m/z* 1576.76) and z_{11} (*m/z* 1283.59) corresponds to the mass of HNE-modified His, which permits the localization of the HNE site at His-5 in the peptide IVYGHLDDPANQEIER. Although complete sequence coverage was not obtained, the observed fragments still allowed determination of the sites of modification. Nevertheless, NL-MS^3 and NL-ECD-MS/MS did yield complementary

information (b and y ions in the CID-based method, whereas several c and z ions upon employing ECD), and in general, all the methods (CID-MS/MS, NL-MS^3 and NL-ECD-MS/MS) together are necessary for the unambiguous localization of HNE-modification sites.

Effect of charge state on neutral loss and ECD fragmentation of HNE-modified peptides

DeGnore *et al*. have reported that the tendency of phosphopeptides to lose the phosphate moiety in CID-based fragmentation in an ion trap depends strongly on the charge state.[33] Unlike loss of H_3PO_4 from phosphopeptides, the tendency of HNE neutral loss is independent of the charge states of the peptides, at least for doubly or triply charged precursor ions. Supporting Information Figure 2a-d shows the CID MS/MS spectra of triply charged HNE-modified AGT I, AGT II, LVLEVAQHLGESTVR, and IVYGHLDDPANQEIER, respectively. The fragment ion from a neutral loss was observed in all but the MS/MS of the triply charged peptide IVYGH*LDDPANQEIER.

ECD fragmentation was found to be more efficient in triply charged peptides; hence, multiply charged precursors are generally preferred for this technique.[34] Supporting Information. Figure 3a-c shows ECD mass spectra of the HNE-modified triply charged peptides DRVYIHPFH*L, DRVYIH*PF, and LVLEVAQH*LGESTVR obtained by NL-ECD-MS/MS. Intensities of the HNE-neutral loss fragment ions during CID MS/MS of these peptides were high enough that the original precursor ions passed the defined selection criteria for another stage of mass spectrometric analysis; that is, ECD MS/MS. The ECD MS/MS spectra were of improved quality, as evident by the longer peptide sequence tags (consecutive cleavages) than CID MS/MS spectra. The peptide IVYGH*LDDPANQEIER did not show any neutral loss for the 3+ charge state; hence, the 3+ precursor ion of this peptide was not selected for ECD. It is

observed from the ECD spectrum that the $(M + 2H)^{2+}$ ion preferentially produces large c and z fragment ions, but ECD of 3+ charge states of same peptides produces both large and small fragment ions. This tendency to shift toward generation of lower mass fragment ions with ECD of peptides of increasing charge state has been observed.[32] It was also observed that the ECD spectra of 3+ precursor ions in the peptides DRVYIHPFH*L and DRVYIH*PF showed a neutral loss of HNE from charge-reduced species (*m/z* 648.84, 2+ and 1296.68, 1+ for DRVYIHPFH*L and *m/z* 523.76, 2+ and 1046.50, 1+ for DRVYIH*PF) and also from some fragment ions (e.g., c_7 *m/z* 898.46 and z_5 *m/z* 660.32, z_6 *m/z* 759.39 in DRVYIH*PF). Overall, it appears that the sequence of the peptide will determine its tendency toward neutral loss of HNE from the precursor ion, and until the correlation of primary structure with fragmentation behavior is well-characterized, both CID and ECD methods of dissociation for successful sequence identification and modification site elucidation will be necessary.

Enrichment of HNE-modified peptides by solid-phase hydrazide (SPH) strategy for NL-driven tandem mass spectrometry

The reduction of sample complexity prior to mass spectrometric analysis of PTMs is advantageous, since it increases the chance of detecting those modifications that are substoichiometric in nature or affecting low-abundance proteins. Taking this into consideration, we tested the efficiency of the NL-MS^3 and NL-ECD-MS/MS approach for the analysis of HNE-modified peptides that were spiked into and enriched from a complex protein digest by the SPH method described by Roe *et al*.[7] Three HNE-modified synthetic peptides (DRVYIH*PF, LVLEVAQH*LGESTVR, and IVYGH*LDDPANQEIER) were spiked into mouse brain tryptic digest, and the resulting mixture was subjected to SPH enrichment. Figure 3a shows the base

peak chromatogram of the brain protein tryptic digest spiked with standard peptides obtained by NL-MS^3 data-dependent acquisition, together with the full-scan FTMS corresponding to the elution time of peptide DRVYIH*PF. The complex full-scan FTMS shows that too many ions were concurrently presented to the mass spectrometer along with the doubly protonated peptide DRVYIH*PF (*m/z* 601.84, 2+) at the elution time of the latter. Figure 3b corresponds to the base peak chromatogram of the SPH-enriched HNE-modified peptides obtained by NL-MS^3 data-dependent acquisition and full-scan FTMS upon the elution of DRVYIH*PF. The spectrum clearly shows the efficiency of the SPH enrichment technique in selectively enriching the HNE-modified peptide DRVYIH*PF. The other two spiked HNE-modified peptides (LVLEVAQH*LGESTVR and IVYGH*LDDPANQEIER) were also successfully enriched by SPH beads from the complex matrix of brain protein digest (data not shown). MS/MS of *m/z* 601.84 (DRVYIH*PF, 2+) and MS^3 of the neutral loss ion (*m/z* 524.08) corresponding to the loss of HNE from the doubly charged peptide of *m/z* 601.84 was triggered in NL-MS^3 analysis of the peptide in the complex mixture before and after SPH enrichment. However, compared with the MS^3 spectra from the enriched fraction, the low quality of the MS^3 spectra of the peptide in a complex mixture can be observed (Supporting Information Figure 4a, b). This may be because enrichment techniques increase the number of ion counts for fragmentation because the MS/MS and MS^3 spectra of *m/z* 524.08 in the nonenriched fraction were triggered with an ion count of normalization level 14 900 and 210, respectively, whereas the ion count normalization level was 22 100 and 420 after SPH enrichment. The quality of the MS/MS spectrum of peptide LVLEVAQH*LGESTVR was somewhat compromised, and no neutral loss ion of significant intensity was visible because the peptide coeluted with DRVYIH*PF. The retention time (RT) of DRVYIH*PF was around 72 min, and the RT of LVLEVAQH*LGESTVR was 73.5 min. It is

noteworthy that performing NL-MS^3 data-dependent acquisition from brain protein digest spiked with HNE-modified peptides recorded approximately 310 MS^3 spectra, whereas MS^3 was triggered on only two ions, *m/z* 349.76 and 524.08, corresponding to neutral loss peaks from triply and doubly charged DRVYIH*PF, after SPH enrichment. Therefore, the enrichment technique also reduces the acquisition of false MS^3 spectra triggered due to isobaric fragment ions produced during CID. Modified peptides may also ionize less efficiently than unmodified peptides by electrospray and MALDI, depending on the chemical properties of the modification.[21] By reducing potential suppression effects through the removal of unmodified peptides, SPH-based enrichment of HNE-modified species could therefore increase the relative intensity of the precursor ion signal for efficient fragmentation by CID or ECD and for subsequent application of NL-driven tandem mass spectrometry.

CONCLUSIONS

The current report demonstrates the synergistic role of CID and ECD methods of fragmentation to detect and localize HNE modification in various peptide models. It was observed that a loss of 156 Da from the peptide precursor ion following CID indicates the presence of HNE but precludes localization of the site of modification, depending on the quality of the MS/MS spectrum. The benefits of implementation of ECD for the characterization of various posttranslational modifications are being realized gradually, and we have shown that the ECD method of fragmentation will facilitate unambiguous assignment of HNE adduct sites in peptides.[19] To this end, we have explored the benefit of NL-ECD-MS/MS in characterization of HNE modification because this technique was efficient in characterizing phosphorylated

peptides.[30]

This study has demonstrated that NL-ECD-MS/MS provides a useful tool to analyze HNE-modified peptides because ECD fragmentation will allow for the retention of the HNE moiety on the product ions and, in addition, generally produces more meaningful peptide fragmentation than CID-based MS/MS analysis. Since CID and ECD yield complementary fragment ions, the combination of the two increases the specificity of sequence information,[35] and hence, their combined use is beneficial.[11] Zubarev *et al*. have discussed the limitations associated with using CID or ECD alone, and the authors argue that the best would be to implement both techniques together for obtaining sequence information of peptides.[36] The inclusion of ECD can reduce the uncertainty associated with CID alone by providing additional sequence information. On the other hand, most search engines work best for CID mass spectra.[36] We have shown here that a NL-ECD-MS/MS approach utilizing both CID and ECD and synergistically combining them to enable enhanced MS/MS analyses also has benefits for the interrogation of posttranslational protein modifications. Since this method does not involve a long duty cycle normally associated with full ECD-based data-dependent acquisition, it is less likely that HNE-modified peptides will be overlooked with this method.

SPH enrichment of HNE-modified peptides[7] prior to data-dependent LC-MS/MS is expected to increase the chances of detecting low-abundance proteins that are susceptible to substoichiometric HNE modification during oxidative stress. We have also demonstrated the value of this selective enrichment methodology for subsequent NL-driven tandem mass spectrometric acquisitions.

ACKNOWLEDGEMENT

This research has been supported by Grant AG025384 from the National Institutes of Health. Laszlo Prokai is the Robert A. Welch Professor at the University of North Texas Health Science Center (endowment BK-0031).

REFERENCES

1. Esterbauer, H., Schaur, R. J., and Zollner, H. (1991) *Chemistry and biochemistry of 4-hydroxynonenal, malonaldehyde and related aldehydes.* Free Radic. Biol. Med. 11, 81-128

2. Aldini, G., Dalle-Donne, I., Facino, R. M., Milzani, A., and Carini, M. (2007) *Intervention strategies to inhibit protein carbonylation by lipoxidation-derived reactive carbonyls.* Med. Res. Rev. 27, 817-868

3. Uchida, K. (2003) *4-hydroxy-2-nonenal: A product and mediator of oxidative stress.* Prog. Lipid Res. 42, 318-343

4. Sayre, L. M., Lin, D., Yuan, Q., Zhu, X., and Tang, X. (2006) *Protein adducts generated from products of lipid oxidation: Focus on HNE and one.* Drug Metab. Rev. 38, 651-675

5. Carbone, D. L., Doorn, J. A., Kiebler, Z., Ickes, B. R., and Petersen, D. R. (2005) *Modification of heat shock protein 90 by 4-hydroxynonenal in a rat model of chronic alcoholic liver disease.* J. Pharmacol. Exp. Ther. 315, 8-15

6. Stevens, S. M.,Jr, Rauniyar, N., and Prokai, L. (2007) *Rapid characterization of covalent modifications to rat brain mitochondrial proteins after ex vivo exposure to 4-hydroxy-2-nonenal*

by liquid chromatography-tandem mass spectrometry using data-dependent and neutral loss-driven MS3 acquisition. J. Mass Spectrom. 42, 1599-1605

7. Roe, M. R., Xie, H., Bandhakavi, S., and Griffin, T. J. (2007) *Proteomic mapping of 4-hydroxynonenal protein modification sites by solid-phase hydrazide chemistry and mass spectrometry.* Anal. Chem. 79, 3747-3756

8. Guan, Z., Yates, N. A., and Bakhtiar, R. (2003) *Detection and characterization of methionine oxidation in peptides by collision-induced dissociation and electron capture dissociation.* J. Am. Soc. Mass Spectrom. 14, 605-613

9. Crabb, J. W., O'Neil, J., Miyagi, M., West, K., and Hoff, H. F. (2002) *Hydroxynonenal inactivates cathepsin B by forming michael adducts with active site residues.* Protein Sci. 11, 831-840

10. Zubarev, R. A., Kelleher, N. L., and McLafferty, F. W. (1998) *Electron capture dissociation of multiply charged protein cations. A nonergodic process*. J. A. Chem. Soc. 120, 3265-3266

11. Zubarev, R. A. (2004) *Electron-capture dissociation tandem mass spectrometry.* Curr. Opin. Biotechnol. 15, 12-16

12. Tsybin, Y. O., Ramstrom, M., Witt, M., Baykut, G., and Hakansson, P. (2004) *Peptide and protein characterization by high-rate electron capture dissociation fourier transform ion cyclotron resonance mass spectrometry.* J. Mass Spectrom. 39, 719-729

13. Syka, J. E., Coon, J. J., Schroeder, M. J., Shabanowitz, J., and Hunt, D. F. (2004) *Peptide and protein sequence analysis by electron transfer dissociation mass spectrometry.* Proc. Natl. Acad. Sci. U. S. A. 101, 9528-9533

14. Han, H., Xia, Y., Yang, M., and McLuckey, S. A. (2008) *Rapidly alternating transmission mode electron-transfer dissociation and collisional activation for the characterization of polypeptide ions.* Anal. Chem. 80, 3492-3497

15. Turecek, F. (2003) *N[bond]C(alpha) bond dissociation energies and kinetics in amide and peptide radicals. is the dissociation a non-ergodic process?* J. Am. Chem. Soc. 125, 5954-5963

16. Turecek, F., Syrstad, E. A., Seymour, J. L., Chen, X., and Yao, C. (2003) *Peptide cation-radicals. A computational study of the competition between peptide N-calpha bond cleavage and loss of the side chain in the [GlyPhe-NH2 + 2H]+. cation-radical.* J. Mass Spectrom. 38, 1093-1104

17. Jones, J. W., Sasaki, T., Goodlett, D. R., and Turecek, F. (2007) *Electron capture in spin-trap capped peptides. an experimental example of ergodic dissociation in peptide cation-radicals.* J. Am. Soc. Mass Spectrom. 18, 432-444

18. Bakhtiar, R. and Guan, Z. (2006) *Electron capture dissociation mass spectrometry in characterization of peptides and proteins.* Biotechnol. Lett. 28, 1047-1059

19. Rauniyar, N., Stevens, S. M.,Jr, and Prokai, L. (2007) *Fourier transform ion cyclotron resonance mass spectrometry of covalent adducts of proteins and 4-hydroxy-2-nonenal, a reactive end-product of lipid peroxidation.* Anal. Bioanal Chem. 389, 1421-1428

20. Zubarev, R. A., Haselmann, K. F., Bogdan, B., Kjeldsen, F. Jensen, F. (2002) *Towards an understanding of the mechanism of electron-capture dissociation: a historical perspective and modern ideas*. Eur. J. Mass. Spectrom. 8, 337-349

21. Stensballe, A., Jensen, O. N., Olsen, J. V., Haselmann, K. F., and Zubarev, R. A. (2000) *Electron capture dissociation of singly and multiply phosphorylated peptides.* Rapid Commun. Mass Spectrom. 14, 1793-1800

22. Shi, S. D., Hemling, M. E., Carr, S. A., Horn, D. M., Lindh, I., and McLafferty, F. W. (2001) *Phosphopeptide/phosphoprotein mapping by electron capture dissociation mass spectrometry.* Anal. Chem. 73, 19-22

23. Haselmann, K. F., Nielsen, P. F., and Zubarev, R. A. (2005) *Characterization of an N-acylated glucagon-like peptide-1 derivative by electron capture dissociation.* J. Am. Soc. Mass Spectrom. 16, 548-552

24. Mirgorodskaya, E., Roepstorff, P., and Zubarev, R. A. (1999) *Localization of O-glycosylation sites in peptides by electron capture dissociation in a fourier transform mass spectrometer.* Anal. Chem. 71, 4431-4436

25. Medzihradszky, K. F., Guan, S., Maltby, D. A., and Burlingame, A. L. (2007) *Sulfopeptide fragmentation in electron-capture and electron-transfer dissociation.* J. Am. Soc. Mass Spectrom. 18, 1617-1624

26. Ramstrom, M., Hagman, C., Tsybin, Y. O., Markides, K. E., Hakansson, P., Salehi, A., Lundquist, I., Hakanson, R., and Bergquist, J. (2003) *A novel mass spectrometric approach to the analysis of hormonal peptides in extracts of mouse pancreatic islets.* Eur. J. Biochem. 270, 3146-3152

27. Palmblad, M., Tsybin, Y. O., Ramstrom, M., Bergquist, J., and Hakansson, P. (2002) *Liquid chromatography and electron-capture dissociation in fourier transform ion cyclotron resonance mass spectrometry.* Rapid Commun. Mass Spectrom. 16, 988-992

28. Davidson, W. and Frego, L. (2002) *Micro-high-performance liquid chromatography/Fourier transform mass spectrometry with electron-capture dissociation for the analysis of protein enzymatic digests.* Rapid Commun. Mass Spectrom. 16, 993-998

29. Cooper, H. J., Akbarzadeh, S., Heath, J. K., and Zeller, M. (2005) *Data-dependent electron capture dissociation FT-ICR mass spectrometry for proteomic analyses.* J. Proteome Res. 4, 1538-1544

30. Sweet, S. M., Creese, A. J., and Cooper, H. J. (2006) *Strategy for the identification of sites of phosphorylation in proteins: Neutral loss triggered electron capture dissociation.* Anal. Chem. 78, 7563-7569

31. Cooper, H. J., Hudgins, R. R., Hakansson, K., and Marshall, A. G. (2002) *Characterization of amino acid side chain losses in electron capture dissociation.* J. Am. Soc. Mass Spectrom. 13, 241-249

32. Iavarone, A. T., Paech, K., and Williams, E. R. (2004) *Effects of charge state and cationizing agent on the electron capture dissociation of a peptide.* Anal. Chem. 76, 2231-2238

33. DeGnore, J. P. and Qin, J. (1998) *Fragmentation of phosphopeptides in an ion trap mass spectrometer.* J. Am. Soc. Mass Spectrom. 9, 1175-1188

34. Cooper, H. J., Hakansson, K., and Marshall, A. G. (2005) *The role of electron capture dissociation in biomolecular analysis.* Mass Spectrom. Rev. 24, 201-222

35. Nielsen, M. L., Savitski, M. M., and Zubarev, R. A. (2005) *Improving protein identification using complementary fragmentation techniques in fourier transform mass spectrometry.* Mol. Cell. Proteomics 4, 835-845

36. Zubarev, R. A., Zubarev, A. R., and Savitski, M. M. (2008) *Electron Capture/Transfer versus collisionally Activated/Induced dissociations: Solo or duet?* J. Am. Soc. Mass Spectrom. 19, 753-761

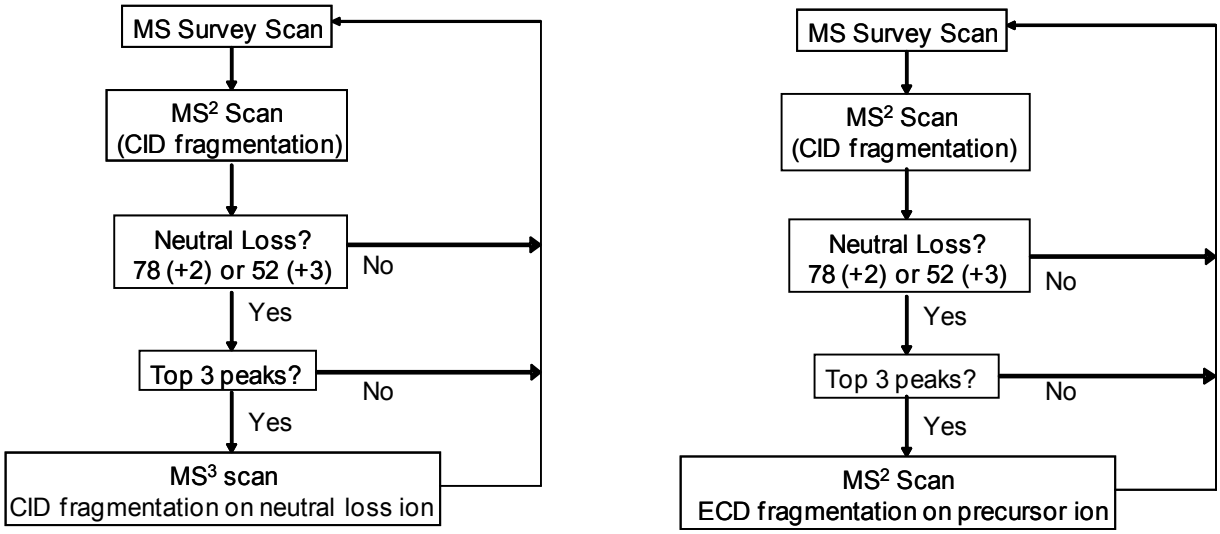

Scheme 1. Flow Charts of NL-MS^3 and NL-ECD-MS/MS Acquisitions

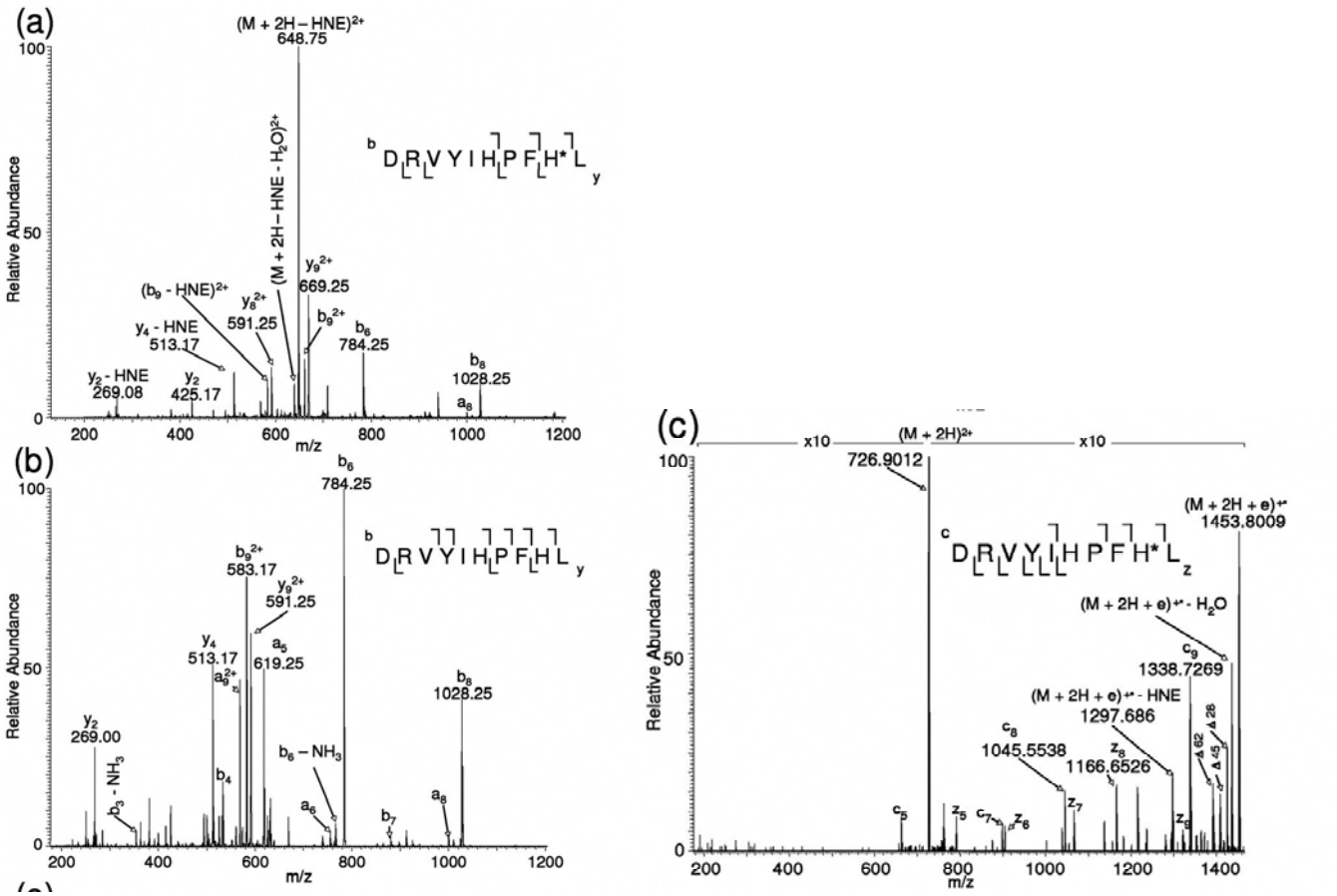

Figure 1. **(a)** ESI-MS/MS spectrum of the HNE-modified AGT I peptide, DRVYIHPFH*L, from its $(M + 2H)^{2+}$ precursor ion at *m/z* 726.91, obtained through direct infusion; **(b)** MS/MS/MS (MS^3) spectrum showing another round of CID performed manually on the neutral loss ion, *m/z* 648.75, observed in the MS/MS spectrum; **(c)** ECD-FTICR MS/MS spectrum of the $(M + 2H)^{2+}$ ion *m/z* 726.9012 of DRVYIHPFH*L. The mass difference between fragment ions c_8 (*m/z* 1045.5538) and c_9 (*m/z* 1338.7269) is 156 Da higher as compared to the ECD mass spectrum of the unmodified peptide (not shown). An asterisk after the one-letter code of an amino acid residue denotes its HNE modification.

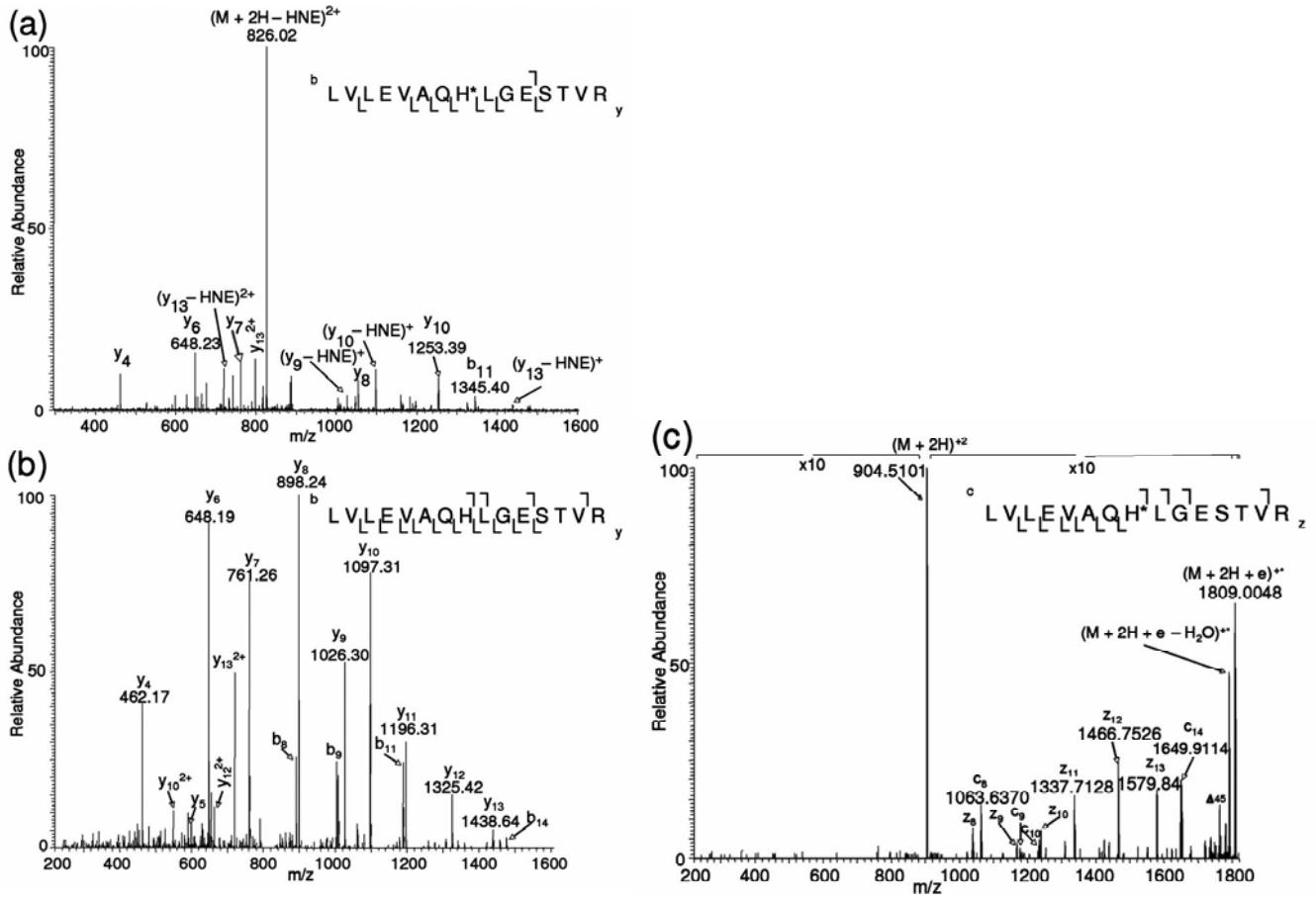

Figure 2. (a) CID-MS/MS spectrum of the ATP synthase subunit beta tryptic peptide, LVLEVAQH*LGESTVR, $(M + 2H)^{2+}$ at *m/z* 904.03 obtained from data-dependent acquisition. **(b)** MS/MS/MS spectrum of the neutral loss ion *m/z* 826.02 obtained by the NL-MS^3 method. **(c)** ECD MS/MS spectrum of the precursor ion $(M + 2H)^{2+}$, *m/z* 904.0085, obtained by NL-ECD-MS/MS. An asterisk after the one-letter code of an amino acid residue denotes its HNE modification.

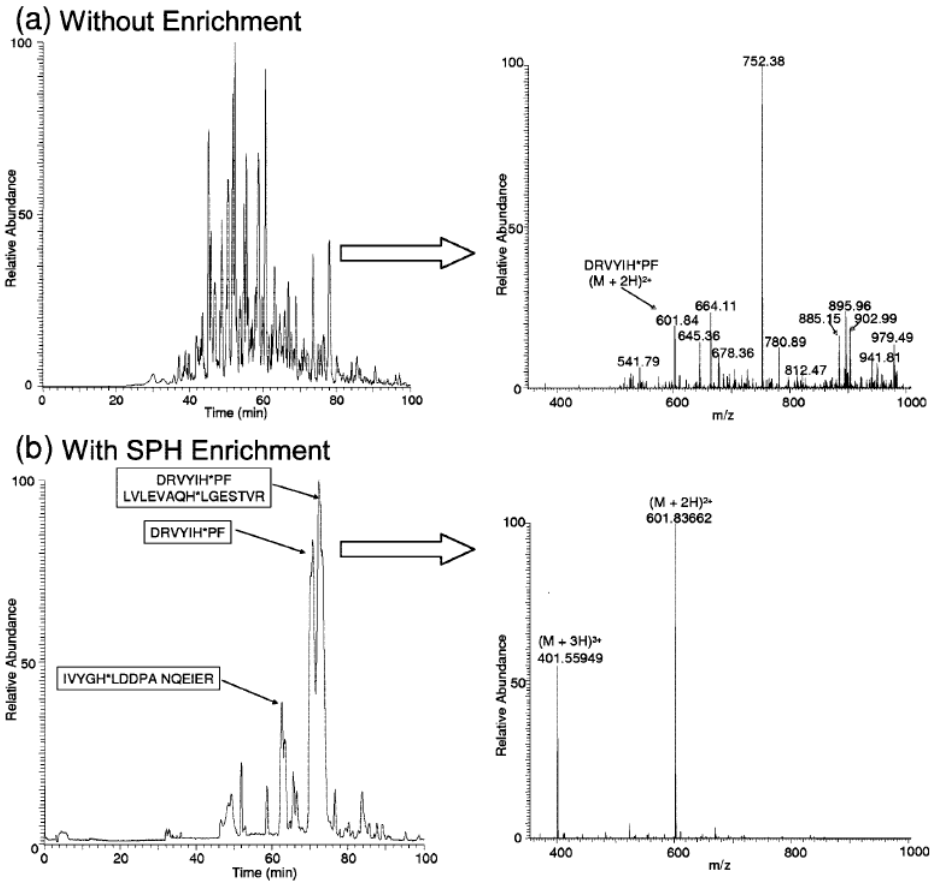

Figure 3. SPH enrichment of HNE-modified peptide standards, DRVYIH*PF, LVLEVAQH*LGESTVR, and IVYGH*LDDPANQEIER from a mouse brain tryptic digest. **(a)** Base peak chromatogram from NL-MS^3 data-dependent acquisition showing the complex mixture of mouse brain tryptic peptide spiked with the three standard peptides, together with the full-scan FTICR spectrum displaying the doubly protonated ion of DRVYIH*PF peptide at *m/z* 601.84, but other coeluting peptides present in the complex mixture of mouse brain tryptic digest, as well. **(b)** Base peak chromatogram showing the peptides enriched by solid-phase hydrazide beads (HNE-modified LVLEVAQH*LGESTVR coeluted with HNE-modified DRVYIH*PF), along with the full-scan FTICR spectrum revealing only peptide DRVYIH*PF after its release from the SPH beads by 10% formic acid.

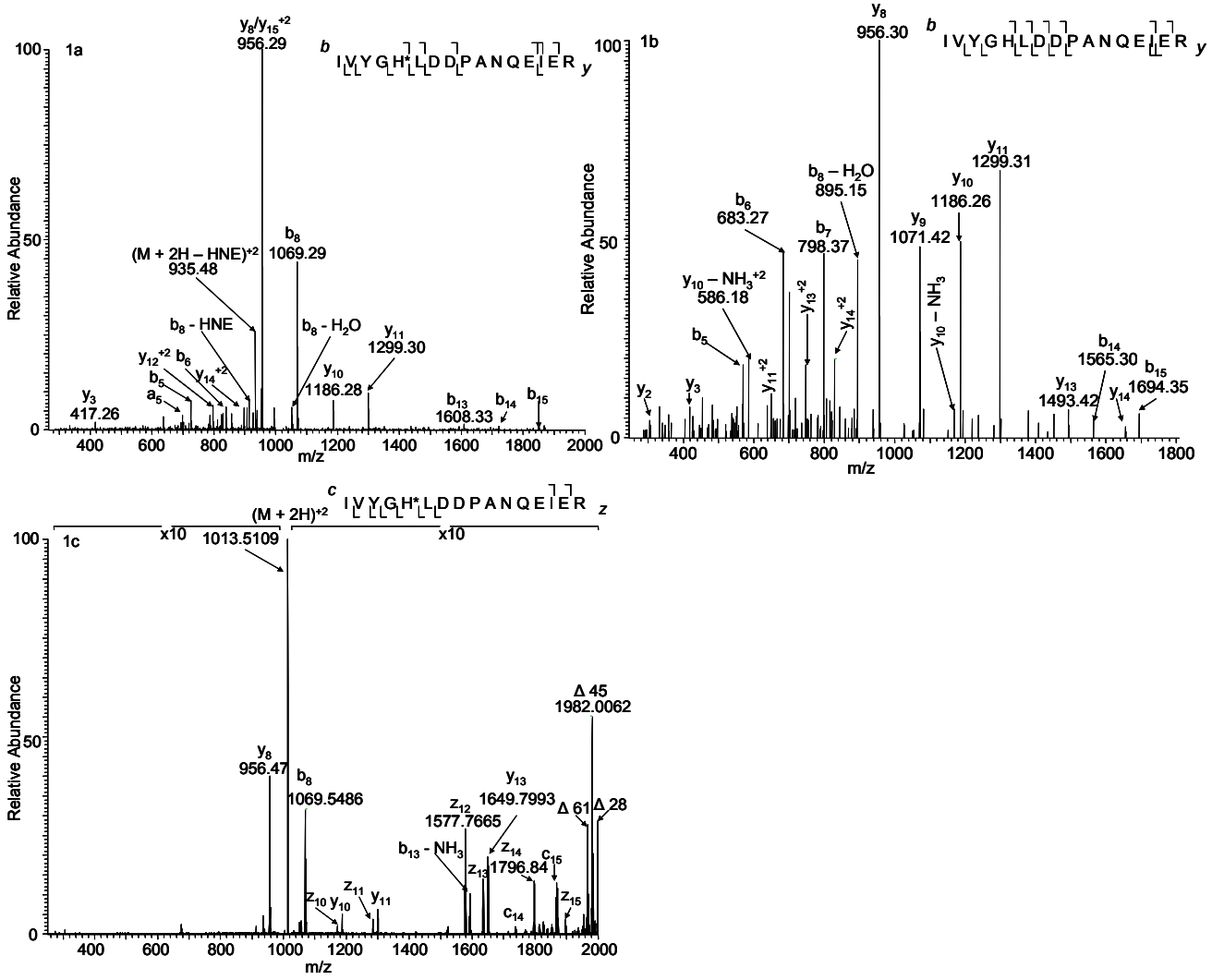

Supplementary Figure 1. (a) CID-MS/MS spectrum of the HNE-modified aconitate hydratase tryptic peptide, IVYGH*LDDPANQEIER, $(M+2H)^{2+}$ at *m/z* 1013.02 obtained from data-dependent acquisition. **(b**) MS/MS/MS (MS^3) spectrum of the neutral loss ion *m/z* 935.48 obtained by NL-MS^3 method. **(c)** ECD-MS/MS spectrum of the precursor ion $(M+2H)^{2+}$, *m/z* 1013.0093, obtained by NL-ECD-MS/MS. An asterisk after the one-letter code of the amino acid residue denotes its HNE modification. Loss of 28, 45, 61 Da from the charge reduced precursor ion, as reported in Ref. 30, are indicated by Δ28, Δ45 and Δ61, respectively.

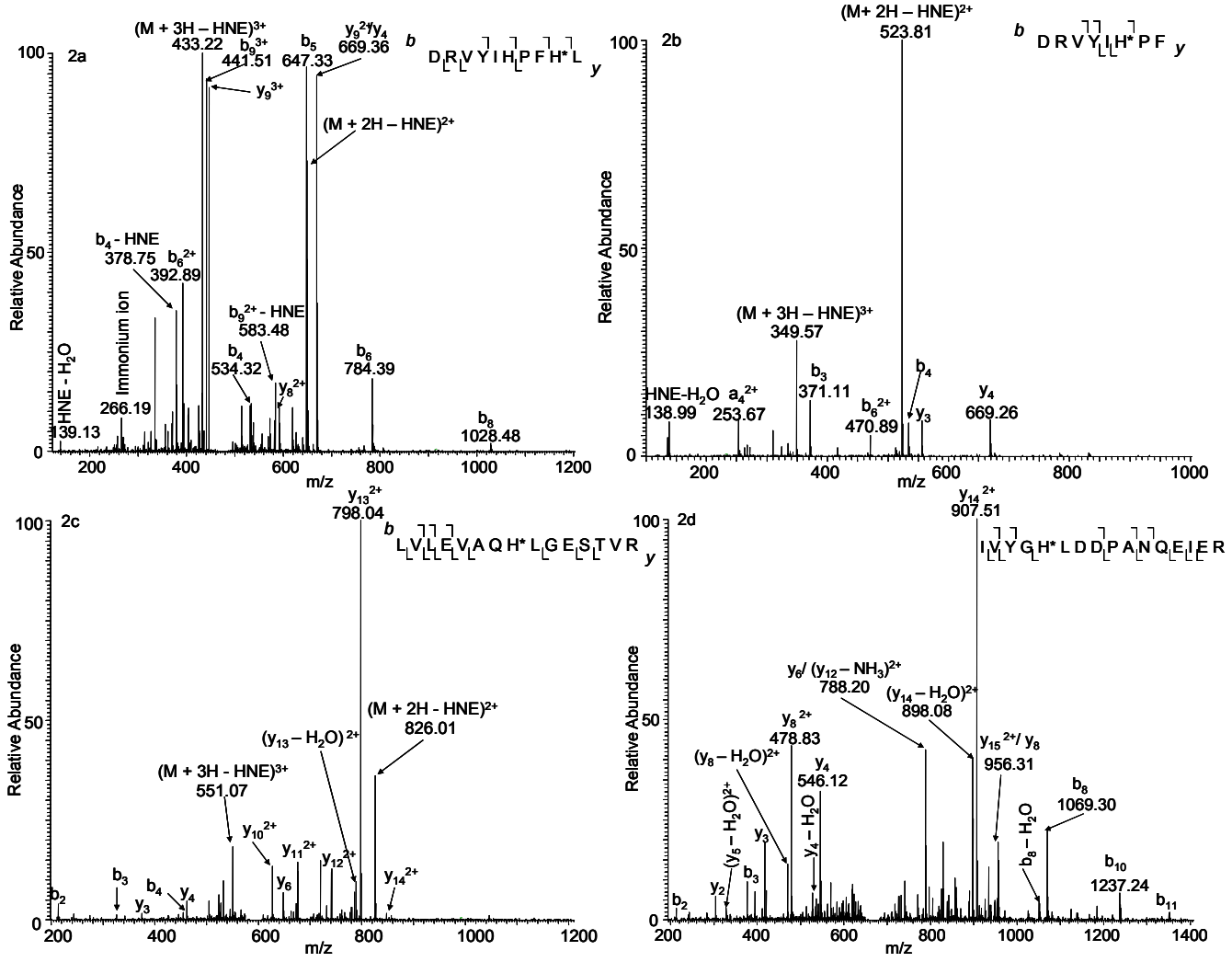

Supplementary Figure 2. CID-MS/MS spectra of triply protonated (3+) peptides **(a)** DRVYIHPFH*L, **(b)** DRVYIH*PF, **(c)** LVLEVAQH*LGESTVR and (**d**) IVYGH*LDDPANQEIER. An asterisk after the one-letter code of the amino acid residue denotes its HNE modification. HNE-modified His immonium ion at *m/z* 266 is observed in MS/MS spectrum of DRVYIHPFH*L, which serves as a fingerprint for the presence of HNE group on His residue (Michael adduct) in the peptide. Also observed is an *m/z* 139 ion from dehydrated HNE in the MS/MS of $(M + 3H)^{3+}$ for peptides DRVYIHPFH*L and DRVYIH*PF.

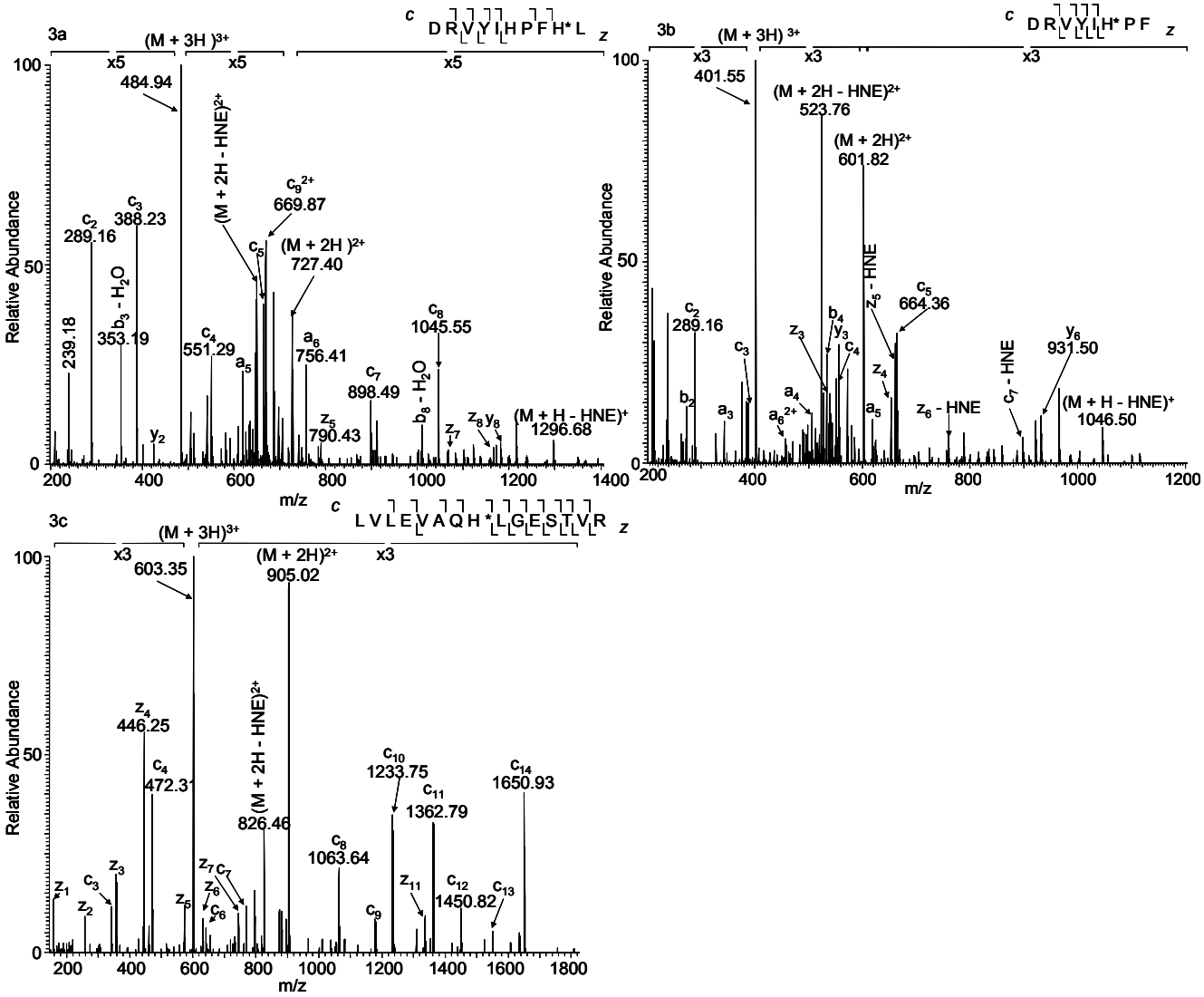

Supplementary Figure 3. ECD-FT-ICR mass spectra of $(M+3H)^{3+}$ ions of the HNE-modified peptides **(a)** DRVYIHPFH*L, **(b)** DRVYIH*PF and (**c**) LVLEVAQH*LGESTVR. An asterisk after the one letter code of the amino acid residue denotes its HNE modification.

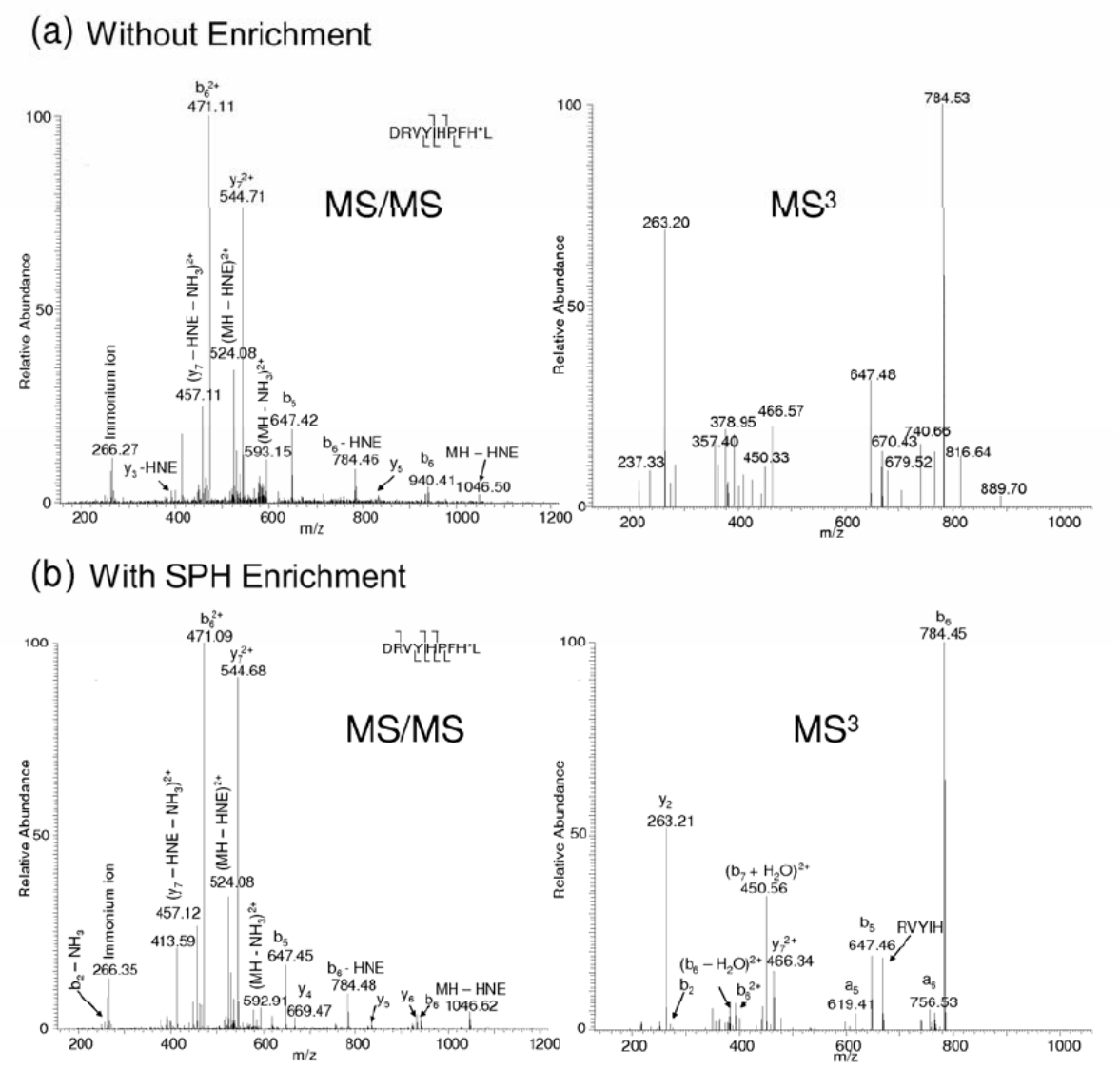

Supplementary Figure 4. **(a)** CID-MS/MS of *m/z* 601.84 obtained by NL-MS^3 data-dependent acquisition without prior enrichment of HNE modified peptides, along with MS/MS/MS (MS^3) of the neutral loss peak, *m/z* 524.08, showing a low quality spectrum, and **(b)** CID-MS/MS of *m/z* 601.84 obtained by NL-MS^3 data-dependent acquisition following SPH enriched method, along with MS/MS/MS (MS^3) of the neutral loss peak, *m/z* 524.08, observed in CID-MS/MS.

CHAPTER V

DETECTION AND IDENTFICATION OF 4-HYDROXY-2-NONENAL SCHIFF-BASE ADDUCTS ALONG WITH PRODUCTS OF MICHAEL ADDITION USING DATA-DEPENDENT NEUTRAL LOSS-DRIVEN MS^3 ACQUISITION: METHOD EVALUATION THROUGH AN IN VITRO STUDY ON CYTOCHROME C OXIDASE MODIFICATIONS

Navin Rauniyar, Laszlo Prokai

Department of Molecular Biology & Immunology,

University of North Texas Health Science Center,

Fort Worth, TX-76107

Published in: *Proteomics* 2009, 9, 5188-5193

ABSTRACT

We report a data-dependent neutral-loss-driven MS^3 acquisition to enhance, in addition to abundant Michael adducts, the detection of Schiff-base adducts of proteins and 4-hydroxy-2-nonenal, a reactive end product of lipid peroxidation. In vitro modification of cytochrome c oxidase, a mitochondrial protein complex, was used as a model to evaluate the method. The technique allowed for a confident validation of modification sites and also identified a Schiff-base adduct in subunit Vb of the protein complex.

Keywords:

4-Hydroxy-2-nonenal • Michael addition • Neutral loss-driven MS^3 • Protein adducts • Schiff base • Technology

INTRODUCTION

4-Hydroxy-2-nonenal (HNE) exerts a potentially detrimental effect to proteins by forming covalent adducts, resulting in diminished protein function, altered physicochemical properties[1] and induction of antigenicity[2]. The modification can take place by the 1,4-addition (Michael addition) of the nucleophilic groups in cysteine (Cys), histidine (His) or lysine (Lys) residues of the protein, respectively, onto the electrophilic double bond of HNE, giving an increase in the protein's molecular mass by 156 Da with each molecule of HNE being added. Alternatively, Schiff bases are formed with ε-NH_2 groups of Lys residues, which yield an increase of 138 Da in molecular weight as the reaction involves the loss of a water molecule (Fig. 1). Michael adducts generally represent >99% of HNE protein modifications, whereas Schiff-base adduct formation is less prevalent even in the presence of excess HNE.[3,4] As Schiff-base formation is a reversible process, it is difficult to characterize such modification in proteins. In addition to being a short-lived species, the MS/MS spectra of Schiff-base adducts may have neutral loss (NL) ions that can preclude their identification as NL limits further fragmentation that would provide sequence information to facilitate the identification of the modified peptide. An NL-driven MS^3 (NL-MS^3) technique that exploits the NL feature of CID and performs fragmentation on the NL ion exhibiting a difference of 156 Da from the precursor ion (corresponding to Michael addition of HNE) has been reported by our group[5] and Roe *et al*.[6] Here, the loss of HNE observed upon MS/MS of HNE-modified peptides will trigger MS^3 analysis of the NL product ion to reveal the sequence of the peptide.

To our knowledge, the implementation of an NL-MS^3 method for characterizing Schiff-base adducts of HNE modification has not been reported. In this article, we describe the

application of this technique to facilitate the identification of Schiff-base modification site(s) in tryptic peptides of HNE-modified proteins. Cytochrome c oxidase (Complex IV, COX) was used for this study, as Chen *et al*.[7] have shown that HNE generated during oxidative stress induced by tert-butylhydroperoxide is inhibitory to COX activity in a concentration-dependent manner. In a separate study, they have also shown that ethanol administration to rats enhanced the formation of HNE in liver mitochondria which, in turn, decreased the activity of COX by forming adducts with the enzyme complex.[8] Furthermore, myocardial reperfusion following short-term ischemia in rats was found to cause enhanced formation of HNE adducts with COX subunits, in particular subunit IV, resulting in significant decrease in the enzyme activity.[9] HNE treatment was also found to inhibit the activities of COX and aconitase in PC12 cells and thus inducing apoptosis.[10] COX subunits susceptible for HNE-modifications in vitro by Michael addition have been identified.[11] However, modification sites other than His-36 of subunit VIII have not been localized, and Schiff-base adducts have not been reported.

COX is the terminal component of the mitochondrial respiratory chain and catalyzes transfer of electrons from cytochrome c to molecular oxygen, generating a proton gradient required for ATP synthesis. COX is an integral inner membrane protein of mitochondria and its dimeric assembly is necessary for H1 pumping. Each monomeric mammalian COX consists of 13 protein subunits of which ten subunits (IV, Va, Vb, VIa, VIb, VIc, VIIa, VIIb, VIIc and VIII) are encoded by nuclear DNA, and the remaining three largest subunits I, II and III that comprise the catalytic core of the enzyme are mitochondrial in origin. The subunits are associated at a ratio of 1:1 stoichiometry except subunit VIIIb, which is present in two copies.[12]

As an integral membrane-protein complex, in addition to being surrounded by other phospholipids, COX contains tightly bound cardiolipin which is also required for full electron

transport activity.[13] Eighty percent or more of the fatty acids of cardiolipin constitutes of linoleate that are vulnerable to damage by reactive oxygen species generated upon ‘‘leakage’’ of electrons during coupling of electron transfer to oxidative phosphorylation.[14] Consequently, reactive lipid products including α,β-unsaturated aldehydes such as HNE and 4-hydroxy-2-hexenal are produced as end products. These aldehydes act as toxic second messengers of oxidative stress and can endanger the integrity of enzyme complexes.[15]

EXPERIMENTAL

To characterize the structural modification of COX by HNE, crude preparation of COX from bovine heart mitochondria was purchased from Worthington Biochemical (Lakewood, NJ, USA) and used without further enrichment. COX was modified in vitro with HNE (Cayman Chemical, Ann Arbor, MI, USA). One hundred microliters of COX (60 U/mL) was incubated in 100 mL of 20 mM Tris-sulfate plus 2 mM dodecyl maltoside or 8 M Urea buffer and 2 mM HNE at 37°C for 5 h and then washed three times with ethyl acetate (100 mL aliquots) to remove the excess HNE. The remaining proteins in the aqueous phase were then reduced with 30 mM DTT at 60°C for 30 min and alkylated with 55 mM iodoacetamide at room temperature in dark for 30 min. After acetone precipitation to remove the excess DTT and iodoacetamide, the proteins were resuspended in 100 mM ammonium bicarbonate and subsequently digested with 3 mg of trypsin (TPCK treated, Applied Biosystems, Foster City, CA, USA) for 18 h at 37°C. The digestion was terminated by adding formic acid (1% of total volume), and the peptide solution was lyophilized using a FreeZone freeze dry systems (Labconco, Kansas City, MO, USA).

Mass Spectrometry

HNE-modified COX tryptic digests were then used for RP HPLC-MS/MS analysis employing the NL-MS^3 technique described previously[5] and modified to detect, in addition to the Michael adducts, Schiff bases also. Online RP-HPLC-MS/MS analysis was performed on a hybrid linear ion trap (LTQ)-7-Tesla FT-ICR mass spectrometer (LTQ-FT, ThermoFinnigan, San Jose, CA, USA) equipped with a nanoelectrospray ionization source and operated with the Xcalibur (version 2.2) data acquisition software. Five microliters of COX protein digest were loaded onto a ProteopepTM II C18 capillary trap (New Objective, Woburn, MA, USA) and desalted with an aqueous washing phase containing 3% v/v ACN and 1% v/v acetic acid for 5 min prior to injection onto a 15 cm × 75 μm PepMap C18 column (LC Packings, Sunnyvale, CA, USA). Following peptide desalting and injection onto the analytical column, elution by a linear gradient was carried out by raising ACN to 40% v/v in 90 min at 250 nL/min flow rate using an Eksigent nanoLC-2D system (Dublin, CA, USA). The mobile phase was mixed from solvent A (0.1% acetic acid and 99.9% water, v/v) and B (0.1% acetic acid and 99.9% ACN, v/v). First, conventional data-dependent mode of acquisition was utilized in which an interim accurate *m/z* survey scan (giving resolving power of 12,500 about 0.1 s after the start of recording) performed in the FTICR cell was used to trigger consecutive MS/MS analyses of the top most five intense precursor ions in the LTQ (i.e. MS/MS spectra were recorded at low-mass resolving power, <1000). FT-ICR full-scan mass spectra were acquired at 100,000 mass resolving power (*m/z* 400) from *m/z* 350 to 1500 using the automatic gain control mode of ion trapping (106 target ion count). CID in the LTQ was performed using a 3.0 Th isolation width and 35% normalized collision energy with helium as the collision gas. During CID, the dissociation of the precursor ion was induced using an activation time window of 30 ms. Charge state rejection was enabled to

exclude data-dependent MS/MS scans of precursor ions with a single charge. For NL-MS^3 data-dependent acquisitions, isolation and subsequent fragmentation of ions exhibiting an *m/z* 69 or 46 difference (representing NL of HNE from doubly or triply charged precursor ions, respectively) from the precursor ion were conducted to detect Schiff-base adducts, if the NL fragment ions passed specified selection criteria (i.e. they were among the three most intense ions in the MS/MS spectra, which were determined empirically considering the employed separation speed and our instrument's acquisition rate) as shown in Fig. 2. In addition, MS^3 of precursor ions exhibiting a difference of *m/z* 78 or 52 corresponding to doubly or triply charged precursor ion species was used to enable the detection of Michael adducts (+156 Da).[5]

MS/MS data generated by conventional and NL-MS^3 data-dependent acquisition via the LTQ-FT were extracted by BioWorks version 3.3 and were not combined for the subsequent database search that relied on the IPI bovine (version 3.21, 32,872 entries) protein sequence database and the MASCOT version 2.2 (Matrix Science, Boston, MA, USA) search algorithm. MASCOT was searched with parent-ion and fragment-ion mass tolerances of 10.0 ppm and 0.80 Da, respectively, and specifying trypsin as digestion enzyme. For NL-MS^3 experiments, a parent-ion tolerance of 1.5 Da was utilized since the measurement of the NL fragment ion *m/z* occurred in the LTQ. Carbamidomethylation of Cys, oxidation of methionine, carbamylation of Lys and the N-terminal amino acid residue, HNE-Schiff-base adducts on Lys, as well as HNE–Michael adduct formation on Cys, His and Lys were specified as variable modifications among the MASCOT options. In general, probability-based MOWSE scores corresponding to a significance threshold of $p<0.05$ were considered for peptide identification.

Scaffold (version_Scaffold_2_00_06, Proteome Software, Portland, OR, USA) was used to validate MS/MS-based peptide and protein identifications. Peptide identifications were

accepted if they could be established at greater than 20.0% probability as specified by the Peptide Prophet algorithm.[16] Manual validation of MS/MS data of each HNE-modified peptide was performed to discard false positives and accept false negatives, if any. Protein identifications, where protein probabilities were assigned by the Protein Prophet algorithm[17], were accepted if they could be established at greater than 99.0% probability and contained at least two identified peptides.

RESULTS AND DISCUSSION

MS analysis of HNE-modified COX tryptic digests allowed for the detection of all subunits except VIc and VIII of the enzyme complex. In vitro incubation of COX with HNE resulted in the modification of several sites occurring in different subunits. Figure 2 shows the schematic representation of the NL-MS^3 method for the analysis of Schiff-base and Michael adducts. In this figure, the NL ion showing the designated difference (*m/z* 46 or 69 for Schiff base and *m/z* 52 or 78 for Michael adducts) is selected for an additional round of fragmentation giving MS^3 spectra. The NL ion present in MS/MS spectra provides a signature tag of modification type (Schiff base or Michael addition), whereas the extensive fragment ions observed in MS^3 spectra facilitate correct identification of the peptide sequence.

The results in Fig. 3 obtained by data-dependent acquisition and NL-MS^3 technique show that the implementation of the latter technique improved the detection and identification of a Schiff-base-modified site in the tryptic peptide KGQDPYNILAPK of COX subunit Vb. Figure 3A shows the MS/MS spectrum of $[M+2H]^{2+}$ ion at *m/z* 672.4 of the unmodified peptide KGQDPYNILAPK. The MASCOT ion score and identity score were 48.5 and 34.3,

respectively, corresponding to a 95% peptide identification probability in Scaffold software. Figure 3B shows the MS/MS spectrum of $[M+2H]^{2+}$ ion at *m/z* 741.4 of the HNE-modified peptide KGQDPYNILAPK. The MASCOT ion score and identity score were 10.0 and 34.0, respectively, corresponding to an 88% peptide identification probability with the site of modification localized at the N-terminal lysine. In the MS/ MS spectrum, the peak at *m/z* 672.47 was falsely labeled as an internal fragment (PYNILA) instead of an NL ion by the Scaffold program, which was apparently the reason for the lower MASCOT ion score. However, the NL ion at *m/z* 672.47 indicated the presence of a Schiff-base adduct, as the mass difference between the NL ion and precursor ion was 138 Da (Fig. 3B). Implementation of the NL-MS^3 technique allowed for an additional round of CID-based fragmentation on the NL ion at *m/z* 672.47, yielding enough fragment ions (Fig. 3C) to improve the search algorithm score to an acceptable probability threshold for correct peptide identification. The MASCOT ion score of the MS^3 spectrum was 49.2 with the MASCOT identity score being 47.2 corresponding to a 95% peptide identification probability. Although there was no direct evidence for the site of modification in the MS/MS and MS^3 spectra, the side-chain amino group of the N-terminal Lys was the only plausible site for HNE attachment in this tryptic peptide according to the chemistry of HNE modifications in proteins (Fig. 1) and considering the trypsin-based bottom-up methodology. Localization of a Schiff-base on the C-terminal residue had not been an acceptable alternative in this regard, because trypsin would have been unable to cleave after a modified Lys. On the other hand, the N-terminal Lys in KGQDPYNILAPK is preceded by arginine (Arg, R) in the COX subunit Vb; therefore, the observed cleavage between Arg and the Schiff-base modified Lys complied with the selectivity of the proteolytic enzyme employed.

We observed only a single site of a Schiff-base HNE adduct in the COX enzyme

complex. However, the reaction of COX with HNE is dominated by Michael addition products (+156 Da) corroborating the prevalence of the latter type of adducts observed previously.[3] Thirteen sites of Michael addition were identified in eight different COX subunits (II, IV, Va, Vb, VIa, VIb, VIIa and VIIc; Table 1) after our in vitro experiment. MS/MS and/or MS^3 spectra for the corresponding modified peptides were provided in the Supporting Information. HNE modification of subunits II, IV, Vb, VIIa and VIIc by Michael addition was in agreement with a previous report.[11] We were not able to detect subunit VIII (modified or unmodified) by our method. The 4962-Da COX subunit VIII has been reported to undergo HNE modification at its His-36 residue, which is associated with the loss of activity for COX.[11] However, the assignment was made by off-line ‘‘top-down’’ technique after extensive effort to isolate the HNE-modified protein. On the other hand, our ‘‘bottom-up’’ shotgun approach involving online LC-MS/MS has identified, along with 12 additional sites for covalent attachment of the lipid peroxidation product, site-specific modification in subunit VIIc (His-2 of the mature protein[18] based on identifying the HNE-modified tryptic peptide SH*AYEEGPGK, Table 1) also shown to contribute to the significant loss of COX activity upon exposure to HNE.[11]

Michael addition of HNE mostly targeted His residues of COX proteins, except for subunit Va where modifications occurred at Lys and Cys residues, respectively, based on our identification of WVTYFNK*APDIDAWELR and SLC*APISWVSTWDDR among the modified tryptic peptides. From the MS characterization of HNE modification sites in COX, nearly all modified peptides produced NLs and, hence, the NL-MS^3 technique was helpful in increasing the search algorithm scores to acceptable probability thresholds for correct peptide identification.

Some HNE-modified peptides could be identified based only on the MS^3 spectra, whereas

others were identified by MS/MS spectra in addition to the corresponding MS^3 spectra, ultimately increasing the identity score assigned by the MASCOT search algorithm. Two HNE-modified peptide fragments from subunit Va of COX, WVTYFNKPDIDAWELR and SHGSHETDEEFDAR@ (Table 1), were identified solely by the NL-MS^3-based technique. However, the major limitation of the NL-MS^3 technique is that HNE provides no diagnostic mass difference upon NL that may result in ambiguity when more than one possible candidate sites are present within the peptide. In the tryptic peptide WVTYFNK*APDIDAWELR, the HNE modification site can be assigned to Lys, as this is the only probable site of modification. However, the MS^3 spectrum does not identify which His is modified in the tryptic peptide SHGSHETDEEFDAR. Electron capture dissociation (ECD) that provides complementary fragmentation information and retains labile modifications during fragmentation could potentially overcome this limitation through NL-triggered ECD-MS/MS (NL-ECD-MS/MS).[19] In this technique, CID would provide sequence information for unmodified peptides and, in the case of HNE-modified peptides that exhibit a HNE-NL, ECD is initiated which in turn facilitates the identification of the exact site containing the HNE group. Nevertheless, the Schiff-base adduct in the tryptic peptide K*AGQDPYNILAPK of subunit Vb is a novel HNE modification site identified by our NL-MS^3 technique reported here.

CONCLUSION

In conclusion, our results show that the NL-MS^3 data-dependent acquisition technique can be a valuable tool in ‘‘bottom-up’’ characterization of even low-abundance Schiff-base adducts of HNE to proteins, in addition to the predominant Michael addition products. The

method can possibly be equally effective in identifying these type of adducts involving other reactive carbonyl compounds such as 4-hydroxy-2-hexenal or 4-oxo-2-nonenal. Modified peptides of low abundance could apparently be missed by the reported data-dependent acquisition strategy, albeit the functional significance of the corresponding modifications would probably be diminished. Beyond proving the applicability of NL-MS^3 to detect Schiff-base adducts, we propose that our approach may also add an important control to the experiments probing posttranslational protein modifications by HNE or related lipid peroxidation end products. Specifically, the identification of low-prevalence Schiff-base adducts[3,4] among the modified peptides could indicate that the majority of the abundant modification sites bearing potential impact on function are found for the proteins and sequences covered by the employed shotgun analysis.

ACKNOWLEDGEMENTS

This research has been supported by grants (AG025384 and AA015982) from the National Institutes of Health. Laszlo Prokai is the Robert A. Welch Professor at the University of North Texas Health Science Center (endowment BK-0031). Dr. Marianna E. Jung is acknowledged for providing the crude bovine heart COX preparation. The authors thank Dr. Stanley M. Stevens, Jr., for his help in the method development and for comments on the manuscript.

REFERENCES

1. Dalle-Donne, I., Aldini, G., Carini, M., Colombo, R., Rossi, R., and Milzani, A. (2006) *Protein carbonylation, cellular dysfunction, and disease progression.* J. Cell. Mol. Med. 10, 389-406

2. Scofield, R. H., Kurien, B. T., Ganick, S., McClain, M. T., Pye, Q., James, J. A., Schneider, R. I., Broyles, R. H., Bachmann, M., and Hensley, K. (2005) *Modification of lupus-associated 60-kDa ro protein with the lipid oxidation product 4-hydroxy-2-nonenal increases antigenicity and facilitates epitope spreading.* Free Radic. Biol. Med. 38, 719-728

3. Bruenner, B. A., Jones, A. D., and German, J. B. (1995) *Direct characterization of protein adducts of the lipid peroxidation product 4-hydroxy-2-nonenal using electrospray mass spectrometry.* Chem. Res. Toxicol. 8, 552-559

4. Uchida, K. and Stadtman, E. R. (1992) *Modification of histidine residues in proteins by reaction with 4-hydroxynonenal.* Proc. Natl. Acad. Sci. U. S. A. 89, 4544-4548

5. Stevens, S. M., Jr., Rauniyar, N., and Prokai, L. (2007) R*apid characterization of covalent modifications to rat brain mitochondrial proteins after ex vivo exposure to 4-hydroxy-2-nonenal by liquid chromatography-tandem mass spectrometry using data-dependent and neutral loss-driven MS^3 acquisition.* J. Mass Spectrom. 42, 1599-1605

6. Roe, M. R., Xie, H., Bandhakavi, S., and Griffin, T. J., *Proteomic Mapping of 4-Hydroxynonenal Protein Modification Sites by Solid-Phase Hydrazide Chemistry and Mass Spectrometry.* Anal. Chem. 79, 3747-3756

7. Chen, J., Schenker, S., Frosto, T. A., and Henderson, G. I. (1998) *Inhibition of cytochrome c oxidase activity by 4-hydroxynonenal (HNE). role of HNE adduct formation with the enzyme subunits.* Biochim. Biophys. Acta 1380, 336-344

8. Chen, J., Robinson, N. C., Schenker, S., Frosto, T. A., and Henderson, G. I. (1999) *Formation of 4-hydroxynonenal adducts with cytochrome c oxidase in rats following short-term ethanol intake.* Hepatology 29, 1792-1798

9. Chen, J., Henderson, G. I., and Freeman, G. L. (2001) *Role of 4-hydroxynonenal in modification of cytochrome c oxidase in ischemia/reperfused rat heart.* J. Mol. Cell. Cardiol. 33, 1919-1927

10. Raza, H., John, A., Brown, E. M., Benedict, S., and Kambal, A. (2008) *Alterations in mitochondrial respiratory functions, redox metabolism and apoptosis by oxidant 4-hydroxynonenal and antioxidants curcumin and melatonin in PC12 cells.* Toxicol. Appl. Pharmacol. 226, 161-168

11. Musatov, A., Carroll, C. A., Liu, Y. C., Henderson, G. I., Weintraub, S. T., and Robinson, N. C. (2002) *Identification of bovine heart cytochrome c oxidase subunits modified by the lipid peroxidation product 4-hydroxy-2-nonenal.* Biochemistry 41, 8212-8220

12. Malatesta, F., Antonini, G., Sarti, P., and Brunori, M. (1995) *Structure and function of a molecular machine: Cytochrome c oxidase.* Biophys. Chem. 54, 1-33

13. Robinson, N. C. (1993) *Functional binding of cardiolipin to cytochrome c oxidase.* J. Bioenerg. Biomembr. 25, 153-163

14. Shigenaga, M. K., Hagen, T. M., and Ames, B. N. (1994) *Oxidative damage and mitochondrial decay in aging.* Proc. Natl. Acad. Sci. U. S. A. 91, 10771-10778

15. Esterbauer, H., Schaur, R. J., and Zollner, H. (1991) *Chemistry and biochemistry of 4-hydroxynonenal, malonaldehyde and related aldehydes.* Free Radic. Biol. Med. 11, 81-128

16. Keller, A., Nesvizhskii, A. I., Kolker, E., and Aebersold, R. (2002) *Empirical statistical model to estimate the accuracy of peptide identifications made by MS/MS and database search.* Anal. Chem. 74, 5383-5392

17. Nesvizhskii, A. I., Keller, A., Kolker, E., and Aebersold, R. (2003) *A statistical model for identifying proteins by tandem mass spectrometry.* Anal. Chem. 75, 4646-4658

18. Aqua, M. S., Lomax, M. I., Schon, E. A., and Grossman, L. I. (1989) *Nucleotide sequence of a cDNA for bovine cytochrome c oxidase subunit VIIc*. Nucleic Acids Res. 17, 8376

19. Rauniyar, N., Stevens, S. M., Prokai-Tatrai, K., and Prokai, L. (2009) *Characterization of 4-hydroxy-2-nonenal-modified peptides by liquid chromatography-tandem mass spectrometry using data-dependent acquisition: Neutral loss-driven MS3 versus neutral loss-driven electron capture dissociation.* Anal. Chem. 81, 782-789

Table 1. HNE-modified cytochrome c oxidase tryptic peptides derived from bovine heart mitochondria and identified by online RP-HPLC combined with conventional data-dependent and NL-driven MS^3 acquisition on a hybrid LTQ-FT mass spectrometer

IPI accession number	COX subunits	HNE-modified peptide sequence[a)]	Method of identification[b)]	Mechanism of reaction[c)]
IPI00708779	II	MLVSSEDVLH*SWAVPSLGLK	++	MA
IPI00714240	IV	AH*GSVVK	+	MA
		DYPLPDVAH*VK	++	MA
IPI00691338	Va	WVTYFNK*PDIDAWELR	+++	MA
		SHGSHETDEEFDAR@	+++	MA
IPI00694849	Vb	LVPH*QLAH	++	MA
		($_{alk}$C)PS($_{alk}$C)GTH*YK	++	MA
		K*GQDPYNILAPK	++	SB
IPI00689990	VIa	GDH*GGTGAR	+	MA
		ERPAFIPYH*HLR	++	MA
IPI00709627	VIb	N($_{alk}$C)WQNYLDFHR	++	MA
		SLC*PISWVSTWDDR	++	MA
IPI00717407	VIIa	LFQEDNGLPVH*LK	++	MA
IPI00694475	VIIc	SH*YEEGPGK	++	MA

a) *, Site of HNE-modification and @, MS^3 spectra were unable to identify which His was modified.

b) +, HNE-modified peptide identified only by data dependent acquisition, ++, HNE-modified peptide identified both by data-dependent and NL-driven MS^3 acquisition method and +++, HNE-modified peptide identified only by NL-driven MS^3 method.

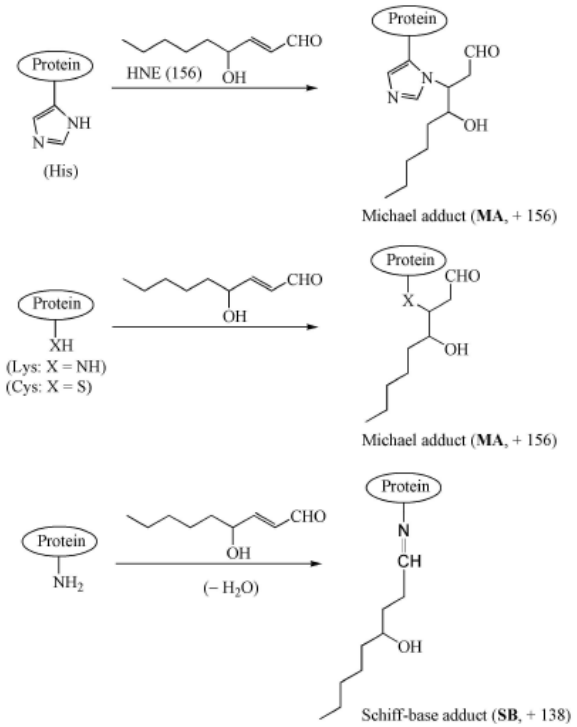

Figure 1. Primary reaction chemistry observed for 4-hydroxy-2-nonenal (4-HNE) modification of proteins

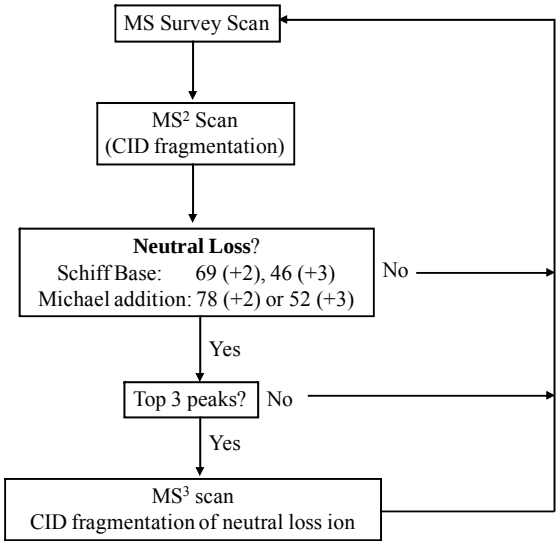

Figure 2. Schematic representation of the NL-MS^3 method for the MS analysis of Schiff-base and Michael adducts.

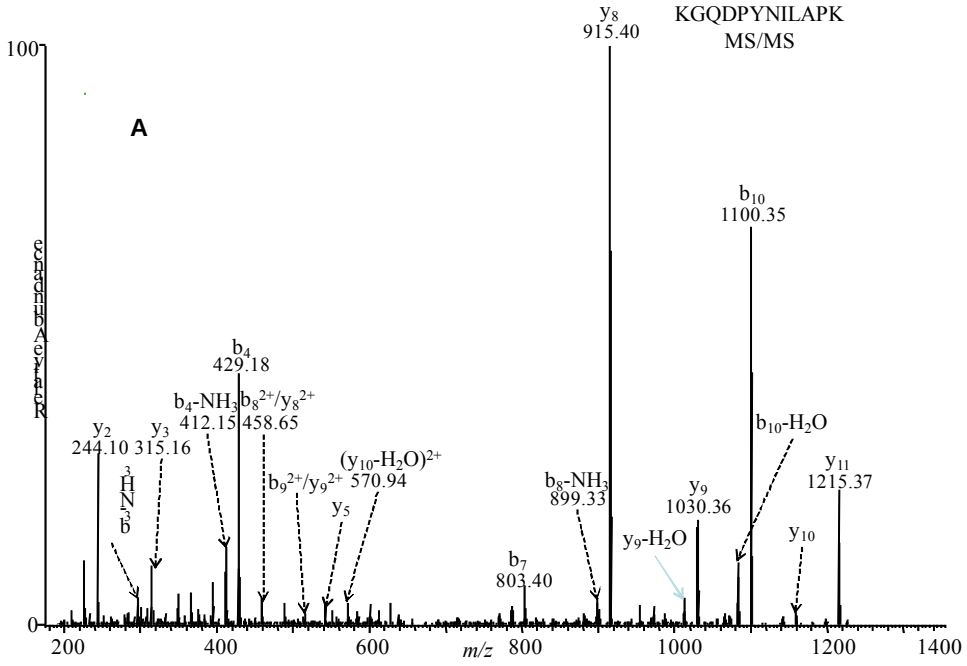
A
KGQDPYNILAPK
MS/MS
y8
915.40
b10
1100.35
b4
429.18
b4-NH3
412.15
b8 2+/y8 2+
458.65
y2
244.10
y3
315.16
b10-H2O
y11
1215.37
(y10-H2O)2+
b9 2+/y9 2+ 570.94
y5
b8-NH3
899.33
y9
1030.36
y9-H2O
y10
b7
803.40
100
0
200
400
600
m/z
800
1000
1200
1400

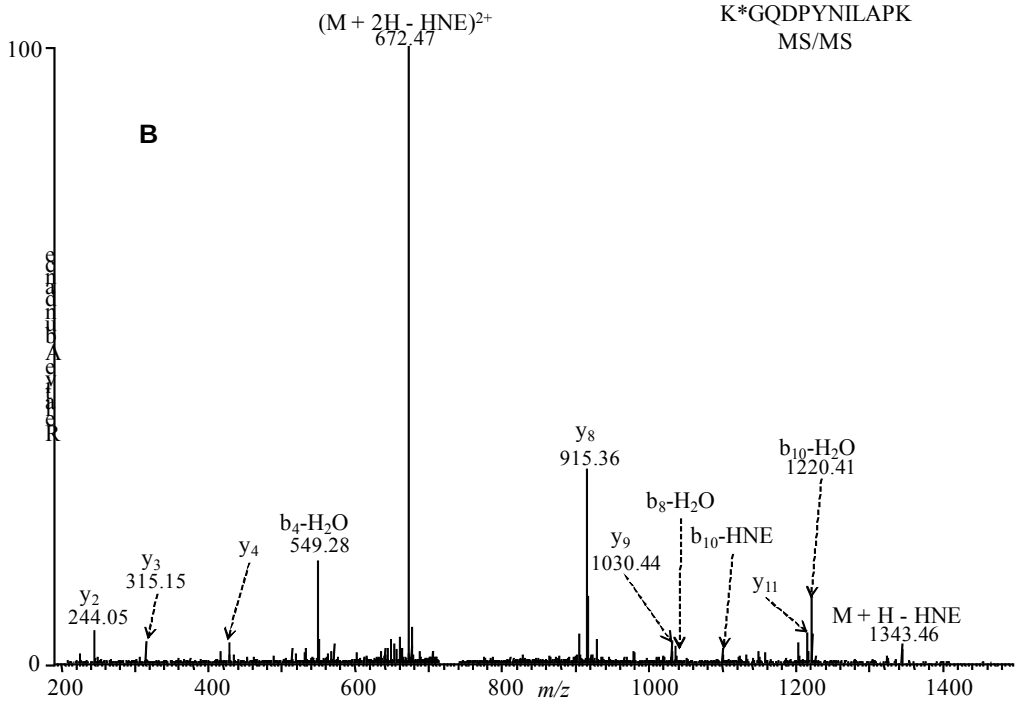
B
(M + 2H - HNE)2+
672.47
K*GQDPYNILAPK
MS/MS
y8
915.36
b10-H2O
1220.41
b8-H2O
b4-H2O
549.28
y4
y9
1030.44
b10-HNE
y3
315.15
y11
y2
244.05
M + H - HNE
1343.46
100
0
200
400
600
800
m/z
1000
1200
1400

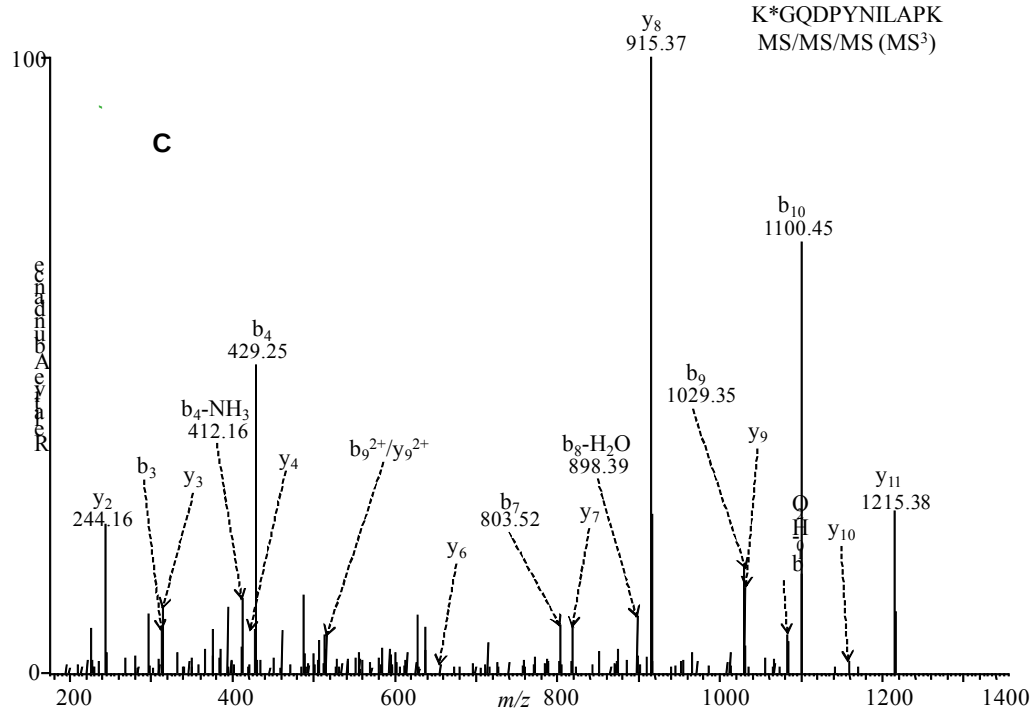

Figure 3. (A) MS/MS product-ion spectrum of $[M + 2H]^{2+}$ ion (*m/z* 672.4) of unmodified COX Vb subunit tryptic peptide, KGQDPYNILAPK. **(B)** MS/MS product-ion spectrum of $[M + 2H]^{2+}$ ion (*m/z* 741.4) of the HNE-modified peptide. The Schiff-base adduct (M_{SB}) produces a predominant NL peak from the doubly charged molecule at *m/z* 672.47 in the MS/MS spectra. **(C)** CID product-ion mass spectrum (MS^3) of the NL ion (*m/z* 672.5), observed in MS/MS spectra of the HNE-modified peptide (chart b).

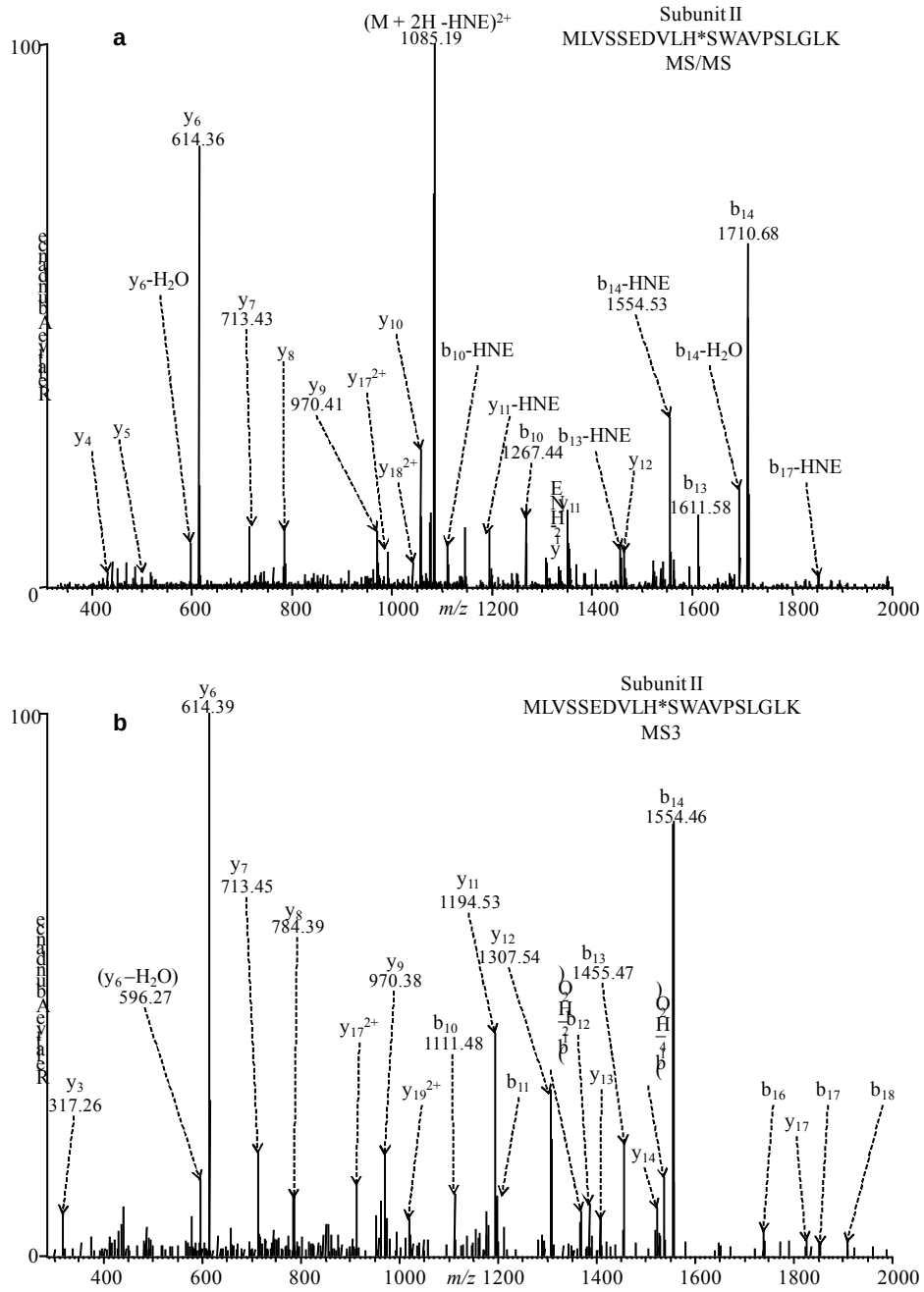

Figure S1. (a) MS/MS product-ion spectrum of $[M + 2H]^{2+}$ ion of the HNE-modified COX II subunit tryptic peptide, MLVSSEDVLH*SWAVPSLGLK. **(b)** CID product-ion mass spectrum (MS^3) of the neutral loss ion (*m/z* 1085.19), observed in MS/MS spectra of the HNE-modified peptide.

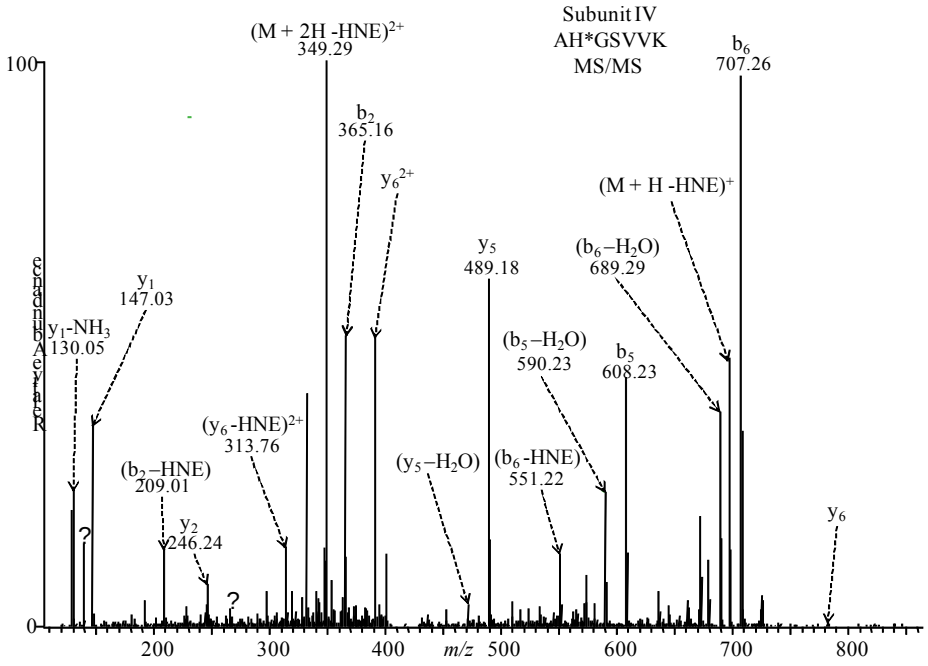

Figure S2. MS/MS product-ion spectrum of $[M + 2H]^{2+}$ ion of the HNE-modified COX IV subunit tryptic peptide, AH*GSVVK. The symbol (●) corresponds to the HNE moiety dehydration fragment ion at *m/z* 139 and (♦) denotes HNE-modified histidine immonium ion peak at *m/z* 266.

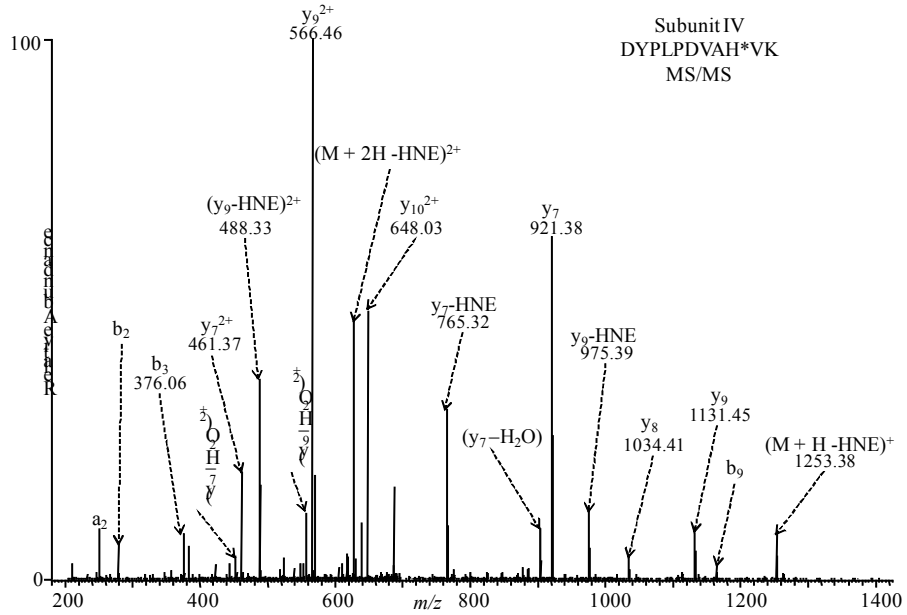

Figure S3. MS/MS product-ion spectrum of $[M + 2H]^{2+}$ ion of the HNE-modified COX IV subunit tryptic peptide, DYPLPDVAH*VK.

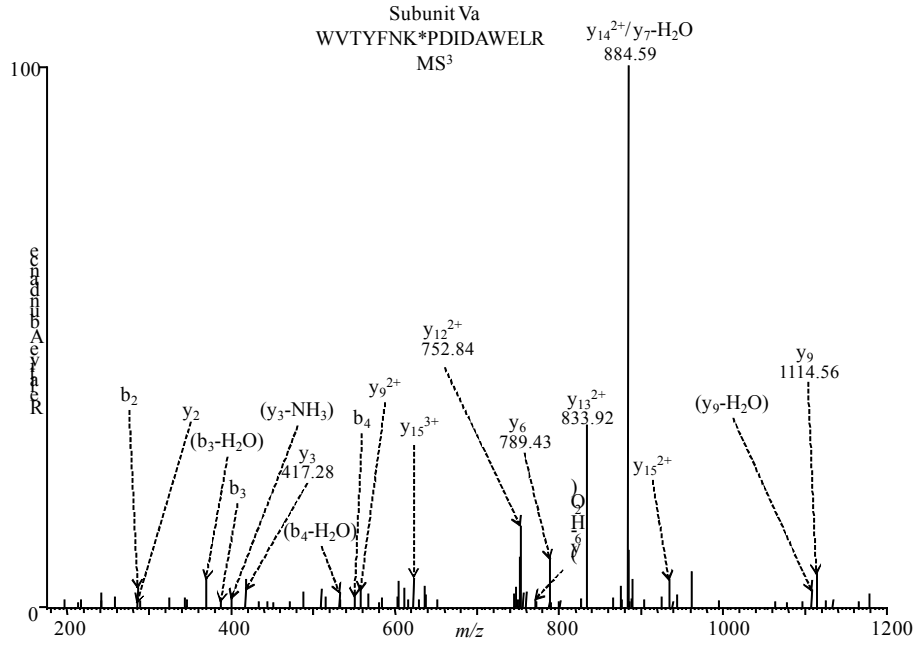

Figure S4. CID product-ion mass spectrum (MS^3) of the HNE-modified COX Va subunit tryptic peptide, WVTYFNK*PDIDAWELR.

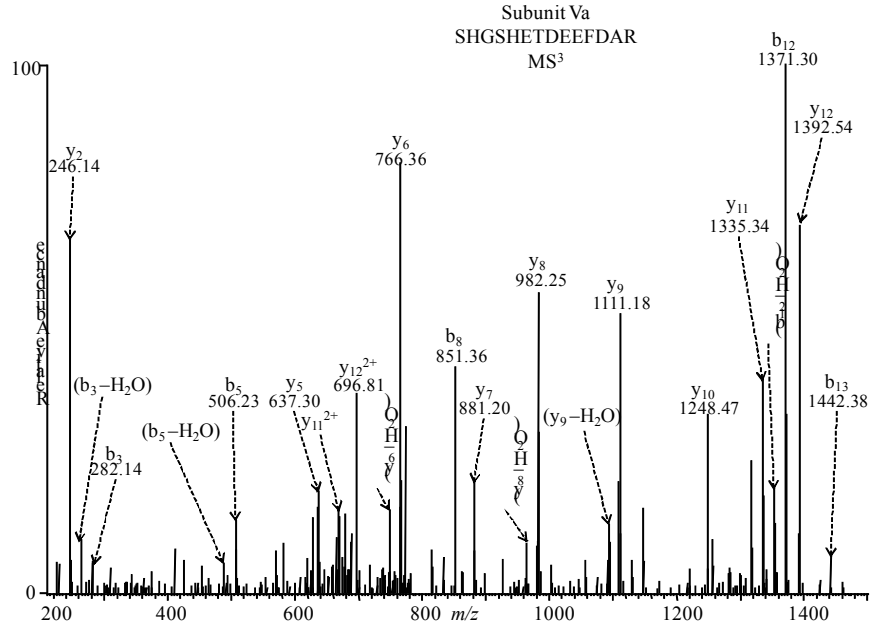

Figure S5. CID product-ion mass spectrum (MS^3) of the HNE-modified COX Va subunit tryptic peptide, SHGSHETDEEFDAR. The presence of more than one histidine results in ambiguity in correct assignment of site of modification by MS^3 spectra.

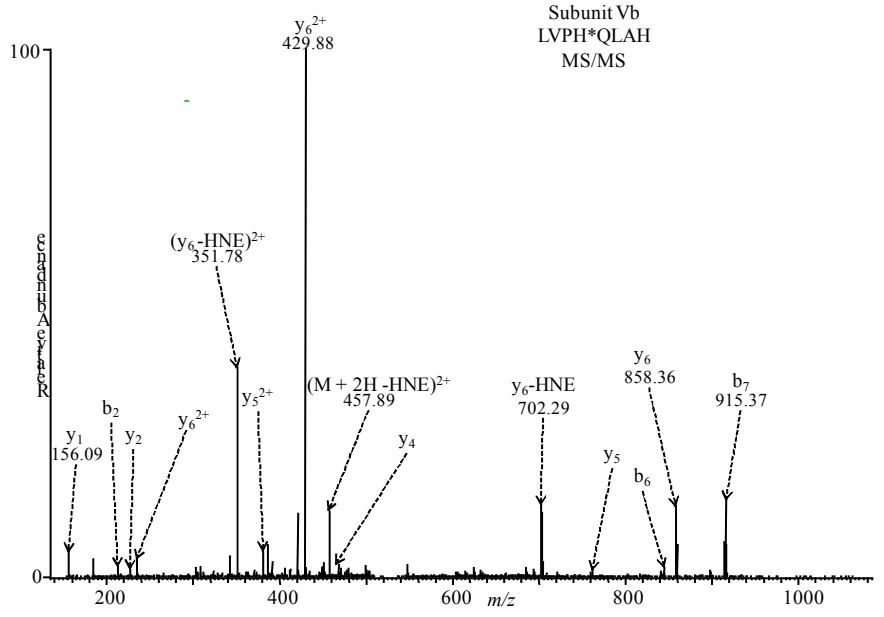

Figure S6. MS/MS product-ion spectrum of $[M + 2H]^{2+}$ ion of the HNE-modified COX Vb subunit C-terminal peptide, LVPH*QLAH.

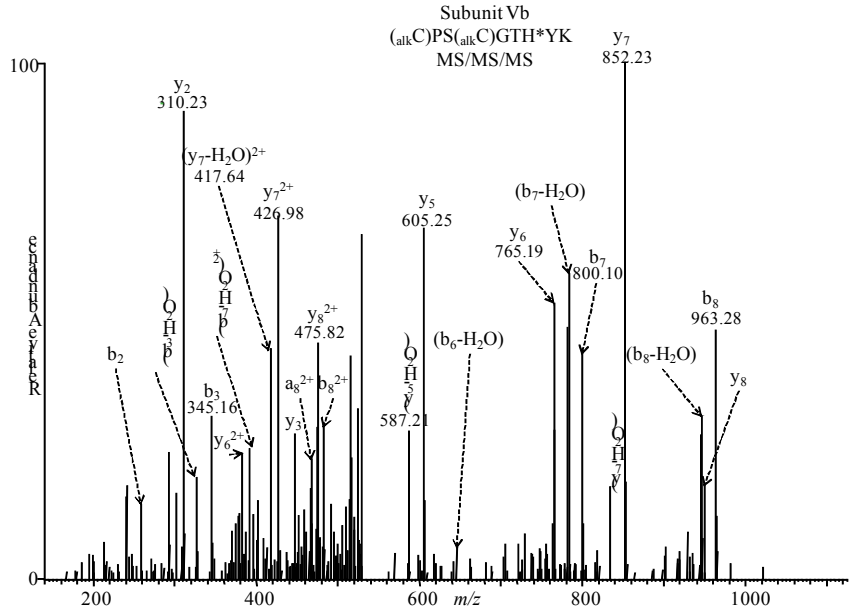

Figure S7. CID product-ion mass spectrum (MS^3) of the HNE-modified COX Vb subunit tryptic peptide, ($_{alk}$C)PS($_{alk}$C)GTH*YK.

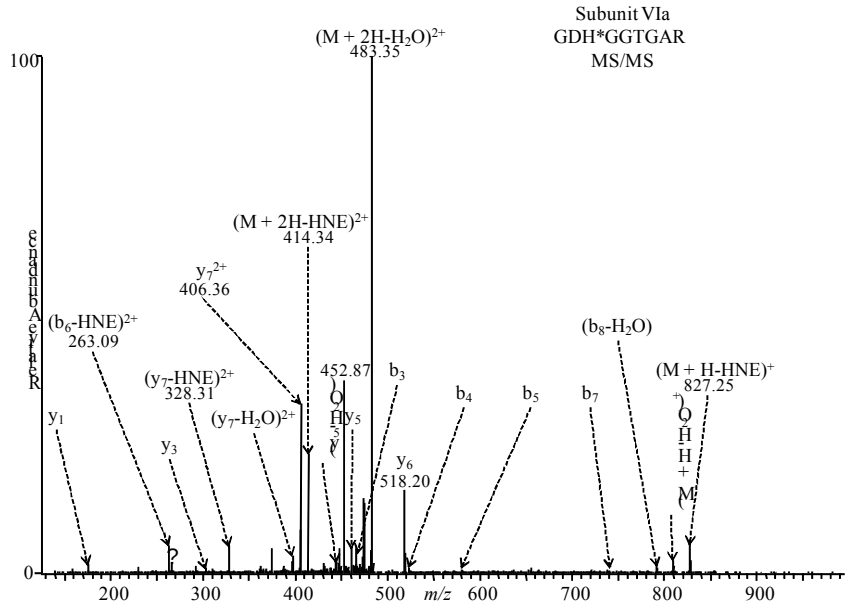

Figure S8. MS/MS product-ion spectrum of $[M + 2H]^{2+}$ ion of the HNE-modified COX VIa subunit tryptic peptide, GDH*GGTGAR. The symbol (♦) denotes HNE-modified histidine immonium ion peak at *m/z* 266.

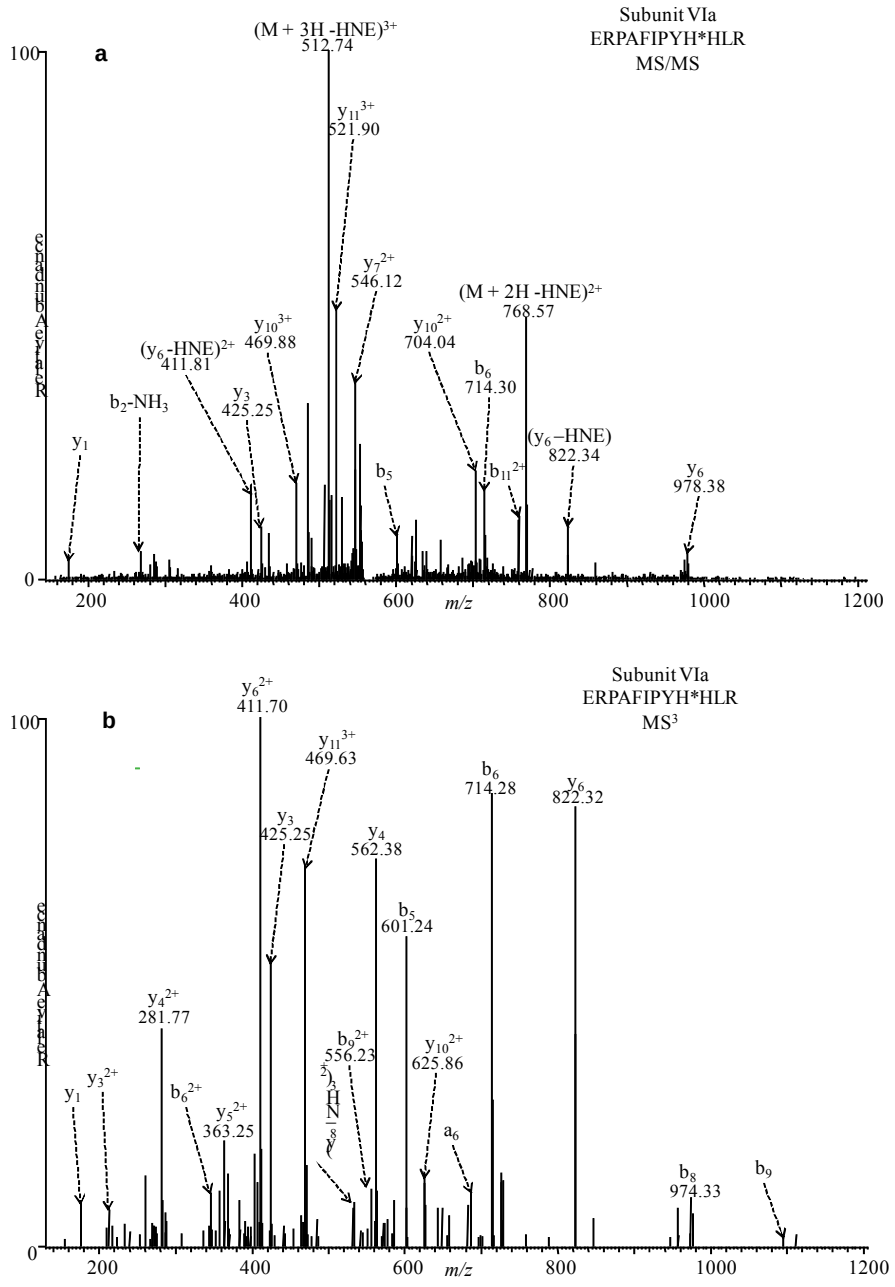

Figure S9. (a) MS/MS product-ion spectrum of $[M + 3H]^{3+}$ ion of the HNE-modified COX VIa subunit tryptic peptide, ERPAFIPYH*HLR. **(b)** CID product-ion mass spectrum (MS^3) of the neutral loss ion (*m/z* 512.74), observed in MS/MS spectra of the HNE-modified peptide.

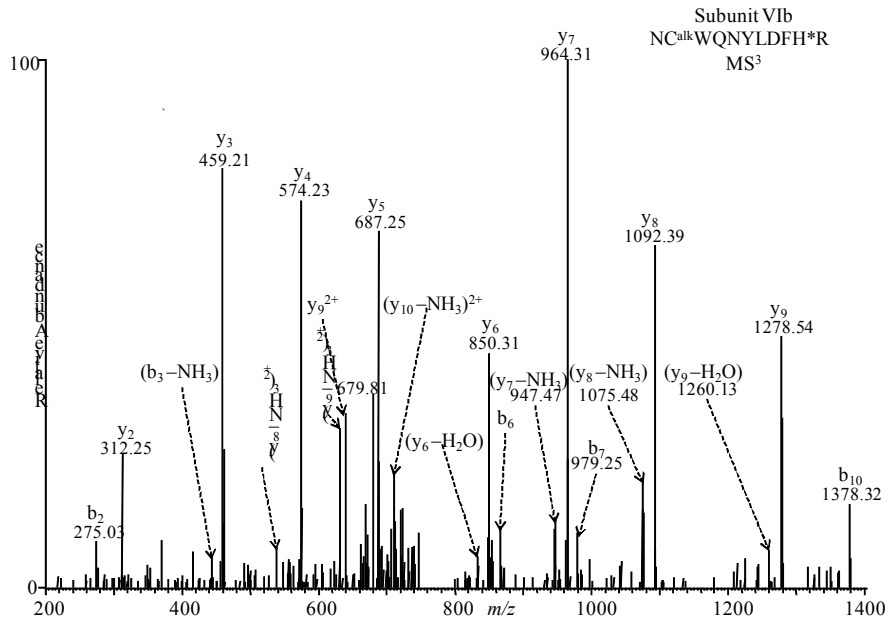

Figure S10. CID product-ion mass spectrum (MS^3) of the HNE-modified COX VIb subunit tryptic peptide, $NC^{alk}WQNYLDFH*R$.

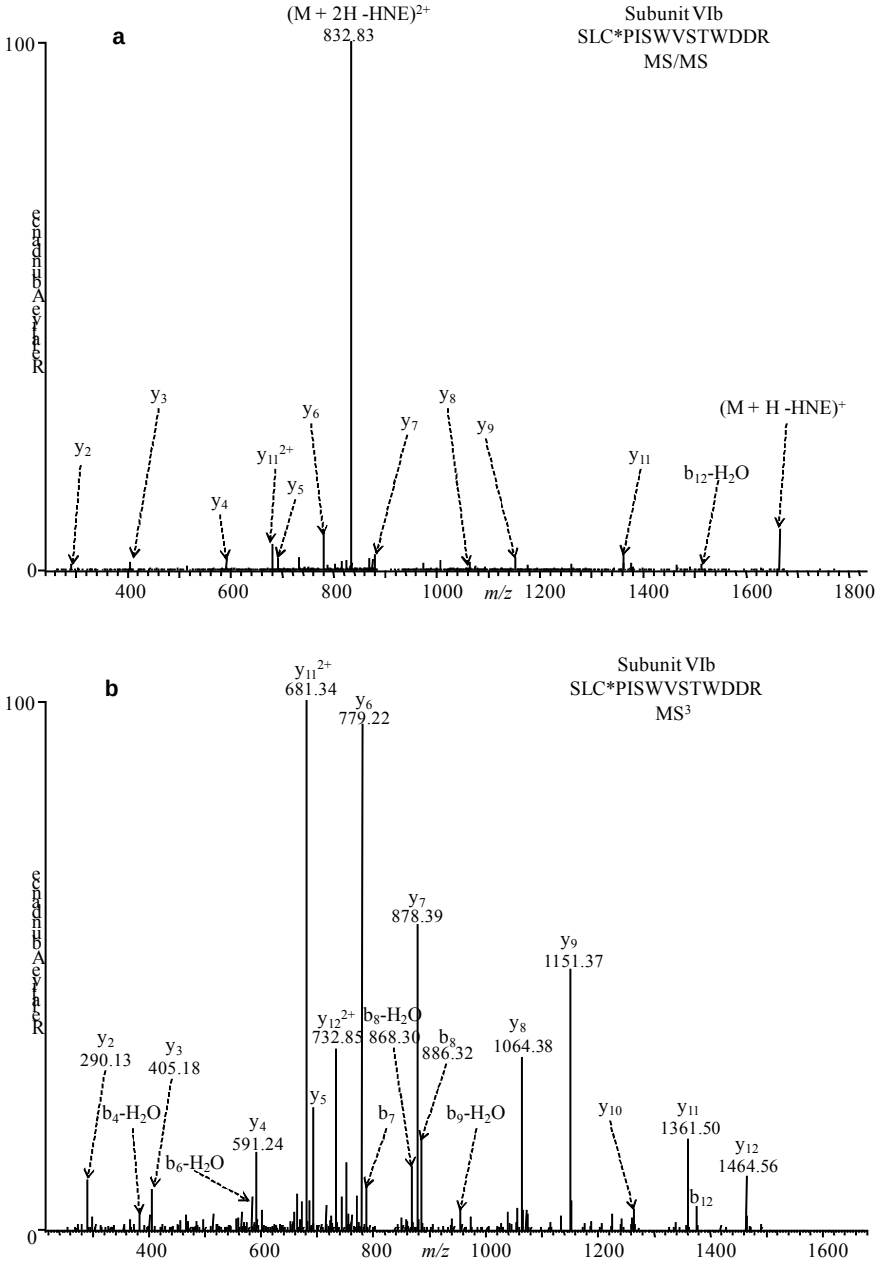

Figure S11. (a) MS/MS product-ion spectrum of $[M + 2H]^{2+}$ ion of the HNE-modified COX VIb subunit tryptic peptide, SLC*PISWVSTWDDR. **(b)** CID product-ion mass spectrum (MS^3) of the neutral loss ion (*m/z* 832.83), observed in MS/MS spectra of the HNE-modified peptide.

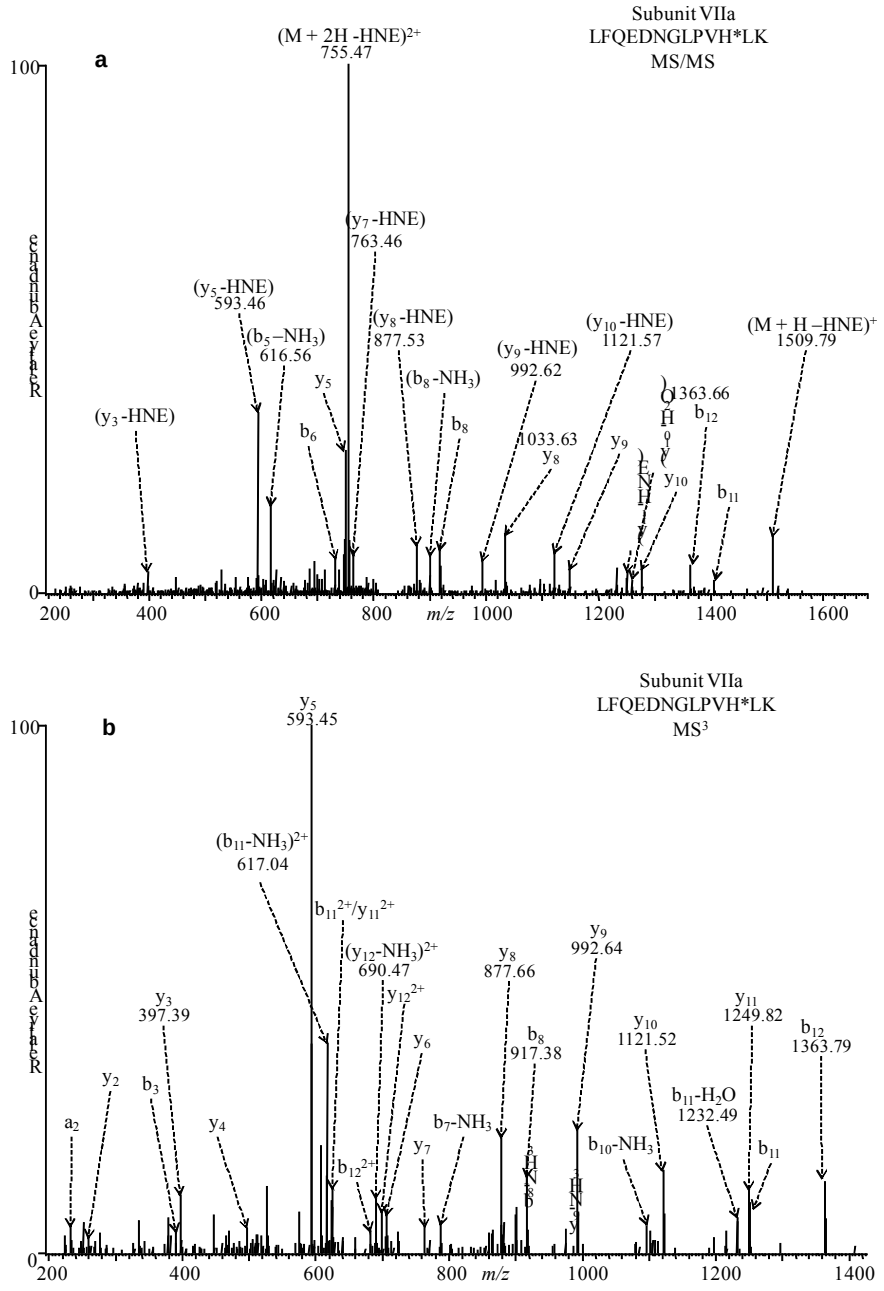

Figure S12. (a) MS/MS product-ion spectrum of $[M + 2H]^{2+}$ ion of the HNE-modified COX VIIa subunit tryptic peptide, LFQEDNGLPVH*LK. **(b)** CID product-ion mass spectrum (MS^3) of the neutral loss ion (*m/z* 755.47), observed in MS/MS spectra of the HNE-modified peptide.

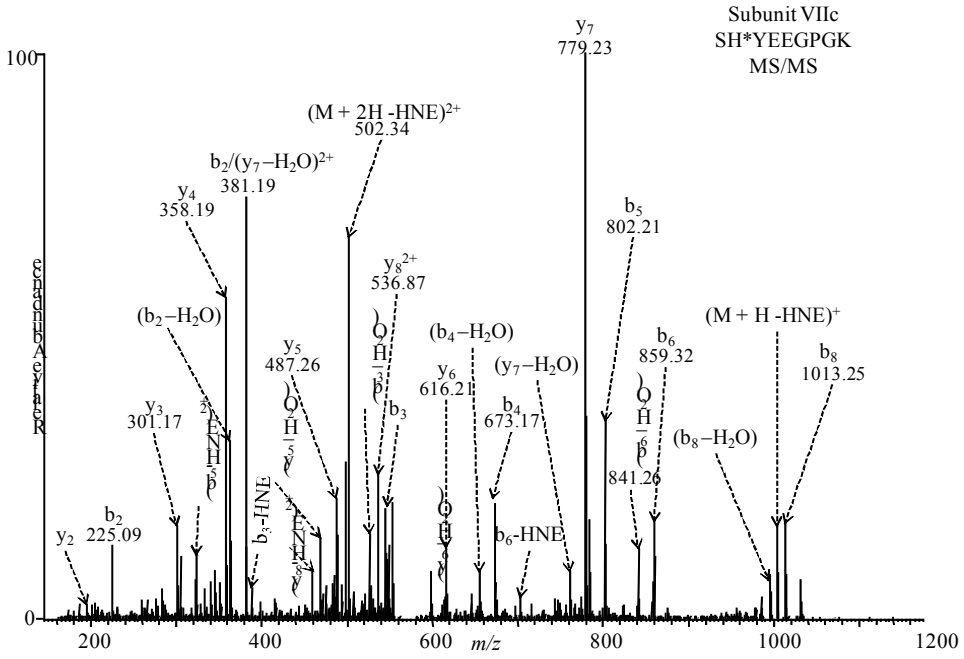

Figure S13. MS/MS product-ion spectrum of $[M + 2H]^{2+}$ ion of the HNE-modified COX VIIc subunit tryptic peptide, SH*YEEGPGK.

CHAPTER VI

SUMMARY AND DISCUSSION

Mass spectrometry has established itself as an important analytical tool with many functions. In addition to its role in protein identification, it is the only technique available to detect and discover new modifications. The objective of this study was to develop mass spectrometric-based methods to identify posttranslational 4-hydroxy-2-nonenal (HNE) modification of peptides and proteins. The localization of carbonylation sites in proteins is fundamental to understand cellular signaling by this lipid peroxidation end-product and the mechanisms of HNE-induced cytotoxicity at the molecular level. However, the neutral loss of HNE during CID-dissociation of peptides poses difficulty in characterization of actual sites of HNE adduction to the peptide and this difficulty is intensified by the fact that no consensus sequence for the chemical selectivity of HNE modification has been observed. This dissertation develops and evaluates several mass spectrometry-based methods to identify HNE modification to peptides and proteins.

In chapter 2, the characterization of the extent of HNE-modification to a model protein, apomyoglobin, was performed by a direct infusion method using nanoelectrospray ionization in a Fourier transform-ion cyclotron resonance (FT-ICR) mass spectrometer. The high mass resolving power and mass measurement accuracy of the instrument clearly showed the pattern of adduct formation and component molecular weights without the need for deconvolution and

additional data manipulation. Three to nine HNE groups per protein were detected to modify apomyoglobin preferentially via Michael-type addition as the mass of the protein increased sequentially by 156 Da. Interestingly, Schiff base modification of HNE to apomyoglobin was also detected and this finding was verified by performing theoretical simulation of each HNE adduct within a particular *m/z* range.

Additionally, the drawback of a conventional CID method of peptide fragmentation and the value of the ECD-based fragmentation technique in determination of HNE adducts was shown using oxidized insulin B chain as a peptide model. The CID tandem mass spectrum of HNE-modified oxidized insulin B chain was complicated by neutral-loss product ions rendering it difficult to assign the exact sites of modification. Since the ECD method of peptide dissociation has the benefit of fragmenting peptide backbones exclusively without cleaving the labile HNE bond, the HNE modification in oxidized insulin B chain was easily localized to His-5 and His-10 in the sequence. Since CID and ECD yield complementary fragment ions, the combination of these two methods of peptide fragmentation increases the specificity of sequence information and, hence, the use of both methods of peptide fragmentation is recommended for precise determination of HNE adduction in peptides and proteins. This is mainly because the neutral loss of HNE observed in CID fragmentation spectra could serve as a signature tag for the presence of the adduct in the peptide, and ECD can then be utilized to provide enhanced information regarding peptide sequence and site(s) of modification. The significance of implementing both dissociation methods to determine HNE modification is discussed in chapter 3 and 4.

In chapter 3, a bottom-up approach, which involves proteolytic digestion of proteins and then separation of the generated peptide mixtures prior to mass spectrometry, was used to

determine relative sites of HNE modification on apomyoglobin. The HNE-modified peptides, derived from tryptic digest of the modified protein, were selectively enriched by solid-phase hydrazide (SPH) beads and then subsequently analyzed by liquid chromatography–nanoelectrospray ionization tandem mass spectrometry using both CID and ECD (LC–CID-MS/MS and LC–ECD-MS/MS) methods of peptide fragmentation. The employed SPH reagent captures only Michael adducts of HNE-carbonylated peptides by immobilizing them to the glass beads as hydrazones. The interfering unmodified peptides were removed and the peptide carbonyls were recovered by acid-catalyzed hydrolysis of the hydrazone linkage. The SPH reagent successfully enriched HNE-modified peptides, overcoming the issue of ion suppression of the modified peptides by the native peptides. During LC–CID-MS/MS, the neutral loss of HNE in CID served as a signature tag for the modified peptides. The ECD-induced fragmentation of the enriched peptides upon LC–ECD-MS/MS analysis aided the elucidation of primary structural information and assignment of exact carbonylation sites in the protein by generating nearly complete fragment ion series due to efficient peptide backbone cleavage (in most cases over 75%) and the retention of the labile HNE moiety in the peptide. The data-dependent LC–ECD-MS/MS enabled identification of eight HNE-modified tryptic peptides whereas data-dependent LC–CID-MS/MS was able to detect peptides that were missed by data-dependent LC–ECD-MS/MS. ECD readily allowed identification of mono-, bis- and tris-carbonylated isomers of peptides, some of which were not apparent by CID-MS/MS technique because of the poor peptide fragmentation and, hence, lack of ions discerning the isomers. Nevertheless, by the use of a high mass accuracy mass spectrometer and a front-end enrichment of modified peptides prior to separation by reversed-phase liquid chromatography, 10 out of the 11 HNE Michael adducts in His residues on apomyoglobin (His-24, His-36, His-64, His-81, His-

82, His-93, His-97, His-113, His-116 and His-119) were identified by combined use of data-dependent acquisition LC–CID-MS/MS and LC–ECD-MS/MS. Thus, this study showed that prior enrichment of HNE-modified peptides and the implementation of both CID- and ECD-MS/MS were advantageous in the in-depth interrogation and unequivocal localization of HNE-induced carbonylation of apomyoglobin that occurs via Michael addition to its His residues. Also, by reducing the potential suppression effects through the removal of unmodified peptides, SPH-based enrichment of HNE-modified species could increase the relative intensity of the precursor ion signal for efficient fragmentation by CID or ECD and for subsequent application of NL-driven tandem mass spectrometry as discussed in chapter 4.

Since a number of HNE-modified peptides produced a predominant HNE neutral loss fragment-ion signal (156 Da; 78 or 52 Da for doubly or triply charged peptides) upon CID, a comparison of NL-driven MS^3 and a NL-driven ECD data-dependent acquisition methods in determination of HNE modification is presented in chapter 4. In NL-driven MS^3 strategy, the neutral loss of HNE observed upon MS/MS of HNE-modified peptides triggers MS^3 analysis of the neutral-loss product ion to reveal the sequence of the peptide. However, the limitation associated with the NL-driven MS^3 method is the ambiguity in correct assignment of the HNE modification site when more than one candidate site is present as MS^3 is triggered on the neutral loss ion. In the NL-driven ECD method, ECD is triggered on precursor ions of peptides showing the neutral loss of 156 Da (78 or 52 Th depending on the charge state of the peptide 2+ or 3+) corresponding to an HNE molecule in the pre-scan acquired via CID-MS/MS in the linear ion trap, thereby reducing the duty cycle associated with full data-dependent ECD analysis. As mentioned previously, the tendency of ECD to retain the HNE group during MS/MS of the precursor ion facilitated the correct localization of the modification site.

In this study, it was also shown that, unlike the loss of a phosphate (H_3PO_4) group from the phosphopeptides, predisposition of a peptide molecular ion to lose HNE during CID is independent of the charge state (2+ or 3+) of the peptide. Also, it was observed that the sequence of the HNE-modified peptide determined its tendency towards the neutral loss of HNE from the precursor ion and, until the correlation of the primary structure with fragmentation behavior is well-characterized, both CID and ECD methods of dissociation would be necessary for successful sequence identification and modification site elucidation. Additionally, it was also shown that coupling of solid-phase enrichment of HNE-modified peptides facilitated enhanced quality of MS^3 spectrum by increasing the number of ion counts for fragmentation. Moreover, the enrichment technique also reduced the acquisition of false MS^3 spectra triggered due to isobaric fragment ions produced during CID.

Schiff bases of HNE are formed with ε-NH_2 groups of Lys residues in proteins, which yield an increase of 138 Da in molecular weight as the reaction involves the loss of a water molecule. However, Schiff-base formation is a reversible process and hence it is difficult to characterize such modifications in proteins. In chapter 5, the efficiency of the NL-driven MS^3 method in detection of Schiff-base HNE adducts (in addition to that of Michael adducts) that occurs in low abundance to cytochrome c oxidase (COX) was demonstrated. COX was used for this study, because it is an important component of the mitochondrial respiratory chain and various studies have shown that this enzyme complex is a target of HNE attack generated during oxidative stress. The susceptibility of COX to HNE may be due to the presence of cardiolipin at its vicinity in the membrane. Eighty percent or more of the fatty acids of cardiolipin constitutes of linoleate, an unsaturated omega-6 fatty acid, which are vulnerable to damage by reactive oxygen species.

For NL-driven MS^3 data-dependent acquisitions of Schiff bases, isolation and subsequent fragmentation of the fragment ion exhibiting an *m/z* of 69 or 46 lower (representing the neutral loss of HNE Schiff base adducts from doubly- or triply-charged precursor ions, respectively) compared to the precursor ion in the MS/MS spectrum were conducted to detect them. For this additional round of fragmentation of the neutral-loss fragment ions, the ions should pass specified selection criteria (i.e., they were among the three most intense ions in the MS/MS spectra, which were determined empirically considering the employed separation speed and our instrument's acquisition rate). In addition, MS^3 of precursor ions exhibiting a difference of *m/z* 78 or 52 corresponding to doubly or triply charged precursor ion species was used to enable the detection of Michael adducts (+156 Da). The technique allowed for the identification of a Schiff-base adduct in subunit Vb of the protein complex. Thirteen sites of Michael addition were identified in eight different COX subunits (II, IV, Va, Vb, VIa, VIb, VIIa and VIIc). Michael addition of HNE mostly targeted His residues of COX proteins, except for subunit Va, where modifications occurred at Lys and Cys residues, respectively.

FUTURE DIRECTIONS

We have performed an extensive study on mass spectrometry-based approaches for the characterization of HNE modification to proteins and peptides. The main foci of the current studies were to develop various methods for the precise determination of the position of Michael and Schiff-base adducts of HNE to nucleophilic residues in HNE-modified synthetic peptides and model proteins obtained upon exposing them to HNE. The developed methods can now be implemented to investigate HNE modifications in various proteins in tissues or body fluids under oxidative stress conditions.

The proposed study in continuation of the current project is to profile HNE-modified proteins in brain mitochondria from young and old animals (e.g., rats/mice). Brain mitochondria will be used for further studies because ROS are produced by a variety of pathways during normal metabolism in an aerobic environment and are also generated during mitochondrial oxidative phosphorylation pathways.[1] Brain tissue is particularly vulnerable to oxidative stress-induced lipid peroxidation due to its high metabolic rate, abundant redox transition metals and high content of polyunsaturated fatty acids.[2-4] Studies have shown that ROS production is increased with age in all regions of the rat brain,[5] and neuronal cells might be particularly affected because they are postmitotic; hence, they suffer more damage compared to other organs during oxidative stress. Under normal conditions, moderately oxidized proteins are degraded by the proteasome. However, oxidative stress can cause decline in proteasomal activity, preventing appropriate turnover and can potentially lead to proteinaceous aggregates.[6,7] HNE-modified proteins are poor substrates for the proteasome and tend to inhibit the turnover of other proteins by inhibiting the proteasome.[7] Loss of proteasomal activity by specific modification of its subunits by HNE during cardiac ischemia-reperfusion has been demonstrated.[8]

The cataloging of HNE targets of brain mitochondrial proteins will further help in building hypotheses and assessing the effects the modification of specific amino acid residues may have on the protein function and activity, as well as determining its effect on downstream targets or other interacting proteins. The identification of affected signaling pathways based on specific protein damage due to HNE modification can provide information on the disease process. Ultimately, the identification and understanding of target proteins of HNE and sites of modifications *in vivo* may offer new efficacious avenues of pharmacological defense.

Additionally, the developed methods can be implemented to determine the target proteins of HNE carbonylation by *in vitro* incubation of mitochondrial protein preparations. HNE modifications to certain proteins may be difficult to discern from *in vivo* tissues as the protein would be targeted for degradation, if the covalent modification results in significant changes of protein conformation or result in exposure of hydrophobic domains from the protein core. In such cases, *in vitro* studies can provide the evidence of such modifications. The *in vitro* paradigm is expected to contribute to our understanding of the oxidatively induced brain-protein carbonylation. The study involving HNE-induced carbonylation of specific brain proteins *in vitro* yields the identities of the protein subset that could be oxidative stress-related target for this posttranslational modification. Thus, this study will provide an "inclusion-list" that can be used to trigger sequential CID-MS/MS scans during subsequent analysis by a targeted shotgun approach for the identification of HNE-modified peptides. This allows testing whether such "listed" modifications have an impact on protein function, or they are merely "innocent bystanders" of HNE-driven chemical reactions. Several follow-up studies based on *in vitro* modification experiments have shown that sequence-specific modifications by electrophiles lead to functional changes in proteins and alteration in enzyme activities.[9]

Alternatively, the HNE-modified peptides identified in *in vitro* studies can be used for targeted quantitation of protein carbonylation in *in vivo* studies by selected reaction monitoring (SRM) using a triple-quadrupole mass spectrometer. SRM allows highly sensitive and quantitation of unique peptides from proteins of interest and is based on the specific combination of precursor- and fragment-ion masses. Several studies have shown that during diseased states, change in protein carbonylation occurs without any concomitant variation in the protein expression levels. Since HNE attachment may not necessarily cause change in protein

abundance, modification-focused quantification of protein carbonylation will help in the characterization of accompanied changes in protein function and, also, will be able to provide important insights into molecular signaling mechanisms by this lipid peroxidation end-product and a better understanding of its role in many cellular processes.

REFERENCES

1. Kokoszka, J. E., Coskun, P., Esposito, L. A., and Wallace, D. C. (2001) *Increased mitochondrial oxidative stress in the Sod2 (+/-) mouse results in the age-related decline of mitochondrial function culminating in increased apoptosis.* Proc. Natl. Acad. Sci. U. S. A. 98, 2278-2283

2. Yamane, M., Abe, A., and Nakajima, M. (1994) *High-performance liquid chromatograpy-thermospray mass spectrometry of omega-hydroxy polyunsaturated fatty acids from rat brain homogenate.* J. Chromatogr. B. Biomed. Appl. 662, 91-96

3. Pamplona, R., Dalfo, E., Ayala, V., Bellmunt, M. J., Prat, J., Ferrer, I., and Portero-Otin, M. (2005) *Proteins in human brain cortex are modified by oxidation, glycoxidation, and lipoxidation. effects of alzheimer disease and identification of lipoxidation targets.* J. Biol. Chem. 280, 21522-21530

4. Reed, T., Perluigi, M., Sultana, R., Pierce, W. M., Klein, J. B., Turner, D. M., Coccia, R., Markesbery, W. R., and Butterfield, D. A. (2008) *Redox proteomic identification of 4-hydroxy-2-nonenal-modified brain proteins in amnestic mild cognitive impairment: Insight into the role of lipid peroxidation in the progression and pathogenesis of alzheimer's disease.* Neurobiol. Dis. 30, 107-120

5. Tsay, H. J., Wang, P., Wang, S. L., and Ku, H. H. (2000) *Age-associated changes of superoxide dismutase and catalase activities in the rat brain.* J. Biomed. Sci. 7, 466-474

6. Friguet, B. (2006) *Oxidized protein degradation and repair in ageing and oxidative stress.* FEBS Lett. 580, 2910-2916

7. Grune, T. and Davies, K. J. (2003) *The proteasomal system and HNE-modified proteins.* Mol. Aspects Med. 24, 195-204

8. Bulteau, A. L., Lundberg, K. C., Humphries, K. M., Sadek, H. A., Szweda, P. A., Friguet, B., and Szweda, L. I. (2001) *Oxidative modification and inactivation of the proteasome during coronary occlusion/reperfusion.* J. Biol. Chem. 276, 30057-30063

9. Liebler, D. C. (2008) *Protein damage by reactive electrophiles: Targets and consequences.* Chem. Res. Toxicol. 21, 117-128